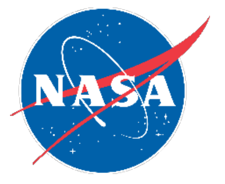

NASA Electronic Parts and Packaging (NEPP) Program

NEPP Task: Guidelines for Selection of Ceramic Capacitors for Space Applications

Cracking Problems in Low-Voltage Chip Ceramic Capacitors

Alexander Teverovsky

ASRC Federal Space and Defense
Alexander.A.Teverovsky@nasa.gov

Worked performed at NASA Goddard Space Flight Center

2018

Cracking Problems in Low-Voltage Chip Ceramic Capacitors

Abstract

Cracking remains the major reason of failures in multilayer ceramic capacitors (MLCCs) used in space electronics. Due to a tight quality control of space-grade components, the probability that as manufactured capacitors have cracks is relatively low, and cracking is often occurs during assembly, handling and the following testing of the systems. Majority of capacitors with cracks are revealed during the integration and testing period, but although extremely rarely, defective parts remain undetected and result in failures during the mission. Manual soldering and rework that are often used during low volume production of circuit boards for space aggravate this situation. Although failures of MLCCs are often attributed to the post-manufacturing stresses, in many cases they are due to a combination of certain deviations in the manufacturing processes that result in hidden defects in the parts and excessive stresses during assembly and use. This report gives an overview of design, manufacturing and testing processes of MLCCs focusing on elements related to cracking problems. The existing and new screening and qualification procedures and techniques are briefly described and assessed by their effectiveness in revealing cracks. The capability of different test methods to simulate stresses resulting in cracking, mechanisms of failures in capacitors with cracks, and possible methods of selecting capacitors the most robust to manual soldering stresses are discussed.

Contents

1. INTRODUCTION 5

2. MANUFACTURING PROCESSES AND TYPES OF MLCCS 8

2.1. DIELECTRIC MATERIALS 10
2.2. ELECTRODE MATERIALS 11
2.3. TERMINATION MATERIALS 12
- *Flexible terminations 14*

2.4. DESIGN 15
- *Laser marking 18*

3. TESTING AND QUALITY ASSURANCE 19

3.1. COMPARATIVE ANALYSIS OF SPECIFICATIONS 19
- *Military specifications 20*
- *NASA/GSFC specifications 22*
- *ESA and JAXA specifications 24*
- *Automotive industry specifications 25*

3.2. QUALIFICATION PROCEDURES AND CRACKING PROBLEMS IN MLCCS 25
- *Thermal shock 26*
- *Life testing 27*
- *Humidity testing 27*
- *Resistance to soldering heat 28*
- *Flex testing 30*
- *Sample size 31*

4. CHARACTERISTICS OF MLCCS 32

- *Rated voltage 32*

4.1. CAPACITANCE AND DISSIPATION FACTOR 32
4.2. INSULATION RESISTANCE AND LEAKAGE CURRENTS 34
- *Specified IR values 35*
- *Absorption and intrinsic leakage currents 36*
- *Effect of cracking on IR 38*

4.3. BREAKDOWN VOLTAGE 39
4.4. MECHANICAL CHARACTERISTICS 40
- *Flexural strength 41*
- *Vickers hardness 43*
- *Indentation fracture toughness 43*

5. FAILURE MECHANISMS IN MLCCS WITH CRACKS 44

5.1. DEGRADATION OF PME AND BME CAPACITORS IN THE PRESENCE OF MOISTURE 45
5.2. DEGRADATION IN DRY ENVIRONMENTS 51

6. SPECIAL CASES OF MLCC CRACKING DURING MANUFACTURING, ASSEMBLY, AND TESTING 52

6.1. HYDROGEN-RELATED CRACKING 53
6.2. EFFECT OF PICK AND PLACE MACHINE 55
6.3. ELECTRO-MECHANICAL RESONANCE 55

7. REVEALING CRACKS 57

7.1. OPTICAL EXAMINATIONS 57
- *Vicinal illumination 57*
- *Revealing delamination by discoloration of ceramic layers. 58*

7.2. ELECTRICAL MEASUREMENTS 58
- *Methanol test 59*
- *Temperature dependence of capacitance 59*
- *Time Domain Reflectometry (TDR) 59*
- *Absorption voltage 59*

7.3. ELECTRO-MECHANICAL EFFECTS 60
- *Variations of the electro-mechanical resonance spectrum 60*
- *Resonant ultrasound spectroscopy (RUS) 60*
- *Tone-burst excitation 61*
- *Acoustic emission 61*
- *Laser interferometry 61*

8. CRACKING CAUSED BY MANUAL SOLDERING 62

8.1. WORKMANSHIP RECOMMENDATIONS FOR MANUAL SOLDERING 63
- *Effect of touch-up 64*

8.2. SELECTING CAPACITORS ROBUST TO MANUAL SOLDERING 65
- *Terminal solder dip testing 65*
- *Assessment of the susceptibility to cracking 66*

9. CONCLUSION 67

10. REFERENCES 68

1. Introduction

Multilayer ceramic capacitors (MLCCs) constitute the majority of components used in electronic assemblies, mostly as filtering, bypass or decoupling devices. Since 2010 more than a trillion of MLCCs is manufactured every year in the world and consumed mostly by smart phones, PCs, TVs, and automotive industry [1, 2]. This makes MLCCs the most widely used passive component. Early generations of mobile phones used several dozens of MLCCs but modern smartphones have more than 600. A significant growth in consumption of electronics occurs within the automotive sector. Many vehicles today use more than 300 MLCCs in both 'under the hood' (engine management) applications and in the 'passenger compartment'. However, the latest Tesla models of electric cars have over 10,000 MLCCs per vehicle. Most commercial applications require cheaper and smaller size MLCCs. In 2018 almost 50% of the market share were size 0402 devices, but their production is declining and size 0201 capacitors are growing much faster. It is expected that in the near future the predominance of the 0201 case size will decline in favor of the size 01005, which already has 10% market share. Further, the designers should consider the 008004, a device that is taking off rapidly and is already outselling the 1206 size capacitors. Advancement of small size, high CV value, low-voltage MLCCs in commercial systems raised concerns regarding insulation resistance, IR, degradation and parametric failures in capacitors related to migration of oxygen vacancies [3, 4].

Compared to commercial, hi-rel and especially space systems are using a more conservative approach for selection of components and a substantial proportion of MLCCs used in high-level space projects has size 1206 and larger. However, the trend for using smaller size, high volumetric efficiency capacitors exists, and the use of advanced technology capacitors in newly design space instruments and systems is increasing.

Considering the amount of MLCCs used, the overall probability of their failures is extremely low. Still, because they are failing typically in a short circuit mode, failures might cause catastrophic consequences to the whole system, cease some system functions, or result in intermittent failures that can be misgauged as a software problem. Capacitors are typically responsible for up to 30% of the field failures in commercial systems, and until recently, approximately half of these failures were due to cracking in the parts [5].

The proportion of MLCCs in space instruments is similar to commercial assemblies and varies from 10 to 20% of all electronic components. According to Paumanok Publications [6] the cost of capacitors procured by aerospace industry is 73% of the whole cost of passive components. The major vendors that produce 57% of all capacitors procured by aerospace companies are AVX Corporation, Vishay Intertechnology, and Kemet Electronics (see Fig.1.1). Japanese vendors who dominate commercial market (TDK Corporation, Murata Manufacturing, Matsushita, Rubycon) do not sell directly to the global defense markets; however, capacitors produced in Japan find their way into defense electronics through distribution.

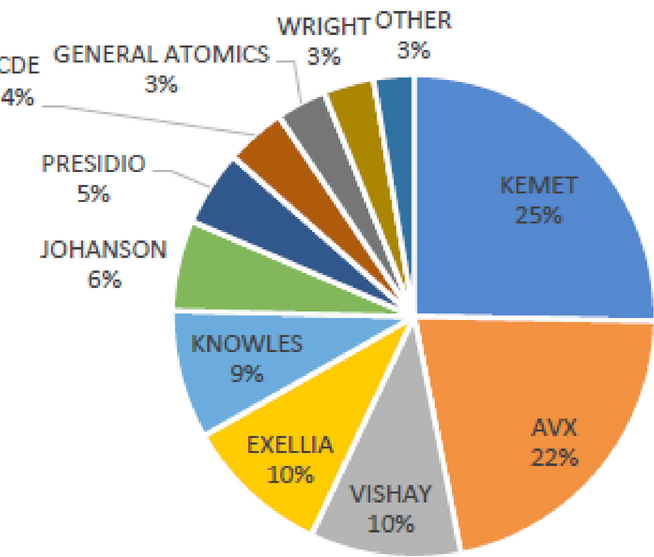

Figure 1.1. Top manufacturers of capacitors for defense and aerospace electronics in 2017 [6]

Cracks and delamination in MLCCs might originate from manufacturing processes or be introduced during assembly or the following handling and testing of the boards (flex cracks or thermal shock cracks). Examples of different types of cracks are shown in Fig. 1.2.

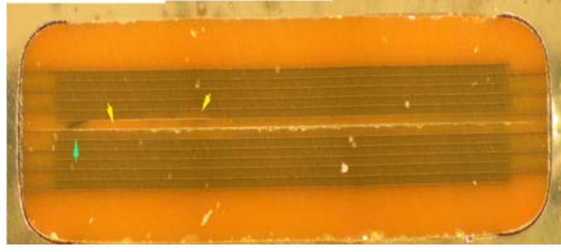

a) Manufacturing defect: CDR 0.1 μF 100 V capacitor that failed due to delamination at ~1.5 kohm during board-level testing

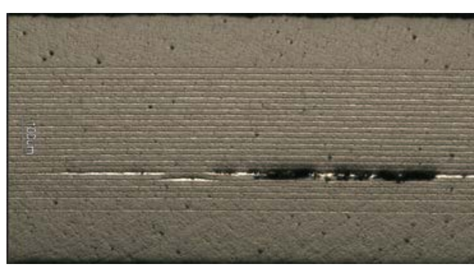

b) Manufacturing defect: voids and delaminations (knit line cracks).

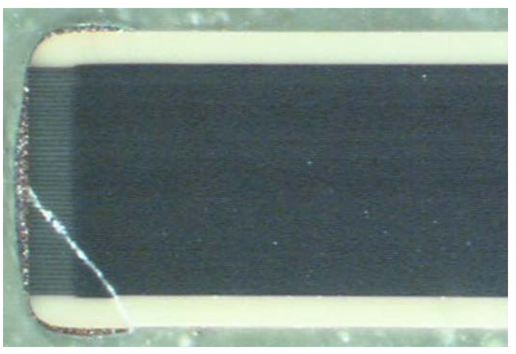

c) Assembly-related defect: flex crack.

d) Assembly-related defect: thermal shock cracking.

e) Cracking caused by manual soldering.

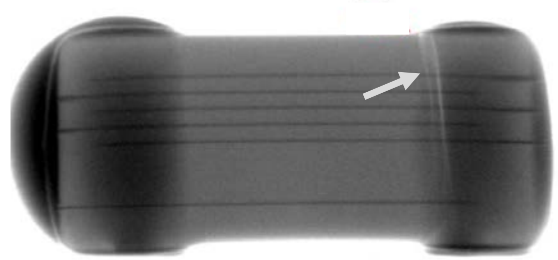

f) Cracking caused by touch-up after reflow soldering.

Figure 1.2. Different types of cracks in MLCCs.

A brief description of different causes of cracking is given below.

1. Manufacturing defects.

Note that some defects might not result in formation of visual cracks, but rather weaken the part and make them more susceptible to cracking during assembly and applications. For example, thermal cracks caused by soldering might initiate at the internal flaws such as voids and delaminations.

- 1.1. Rapid cooling of the laminates can cause so-called firing cracks that typically propagate perpendicular to the plane at the terminals.
- 1.2. Insufficient binding strength and/or the presence of foreign materials might result in knit-line cracks that typically extend parallel to the electrodes.
- 1.3. Delaminations and knit line defects were a rather common defects in early ceramic capacitors, but are rare in contemporary MLCCs, especially those manufactured to military specification. Formation of the electrode-ceramic delaminations during manufacturing can be attributed to variety of reasons. C. Hodgkins [7] identified nine principal causes for interlayer ceramic-metal separation that include outgassing of the solvent binder

(removal of the vaporized binder during pre-sintering processes that occurs along the ceramic/metal electrode interfaces), trapped air during lamination, and surface contamination. Another possible reason for delaminations of PME capacitors is oxidation of palladium electrodes in air that is accompanied with volume expansion.

2. Assembly.
   2.1. Pick-and-place machines can damage parts by excessive stresses created by centering jaws or vacuum picks.
   2.2. Thermal shock cracks are due to a sharp temperature increase during soldering. These stresses might form large, visible U-shaped cracks on the surface of capacitors.
   2.3. Thermal shock cracks might also occur when liquid cleaners are applied to a board that has not sufficiently cooled after soldering reflow. The effect is due to a much higher sensitivity of MLCCs to the cold (from hot to cold) compared to hot (from hot to cold) thermal shocks [8]. To prevent this type of cracking the boards should be cooled slowly, preferably by natural cooling, or at a rate not exceeding 2 ºC to 3 ºC/sec., to temperatures below 60 ºC.
   2.4. Tensile stresses and cracking might develop in MLCCs after soldering them onto alumina boards, which is due to the differences in CTEs between the ceramic material and substrate, with the latter having lower CTEs. These stresses were responsible for many observed failures in the first ceramic chip capacitors mounted on alumina substrates in hybrids [9].

3. Board-level handling.
   Due to the lack of stress relief in mounted chip capacitors, deformation and flexing of the PWB might create significant tensile stresses resulting in so-called flex cracking. These cracks mostly originate at the bottom surface near the edge of the termination margin and propagate inside at angles close to 45º [10]. Typical sources of the flex cracking are de-paneling, test probing, handling during visual examinations, attachment of standoff elements and connectors, etc.

4 Application.
   4.1. Deformation of the board caused by temperature cycling, vibration or mechanical shocks that occur during the ground phase testing and integration or launch of the spacecraft might cause flexing of the board sufficient for cracking of MLCCs. Multiple guidelines for design and board layout have been developed to reduce the probability of this type of failures [11].
   4.2. Due to electrostriction in ceramic materials, voltage cycling might create mechanical stresses that would further develop preexisting microcracks, resulting in failures. This mechanism might be especially important for high-voltage ceramic capacitors [12, 13].
   4.3. Electro-mechanical resonances in class II dielectric capacitors due to the reverse piezoelectric effect in ceramics (see section 6.3).

Although soldering-induced damage might not lead to immediate failures and damaged capacitors may endure weeks or months of service use, it can cause degradation of characteristics with time resulting eventually in field failures. In this regard, microcracks in capacitors generated during assembly can be considered as a “time bomb” [14] that causes increased leakage currents, shorts, opens, or intermittent contacts as degradation develops or cracks propagate with time during application.

Cracking in ceramic capacitors is an old problem. It appeared in the 1970s when first surface mount technology (SMT) chip capacitors were introduced to the market and their employment in NASA applications begun [9, 15]. According to J. Maxwell [11] this problem will continue to be with us in the foreseeable future. Two main factors contribute to the problem: brittleness of ceramic materials and thermal and mechanical stresses associated with the assembly process and/or post assembly handling and testing. Both factors are intrinsic to chip ceramic capacitors and explain the persistence of the problem.

Due to a relatively large size of military and space-grade capacitors used in space systems and use of manual soldering, a substantial proportion of MLCC cracking failures is attributed to the assembly process. Experience shows that the propensity to cracking is lot-related, which means that cracking is often due to a combination of the weakness in the part caused by flaws introduced during manufacturing and assembly-related stresses. A proper screening or qualification testing could have revealed lots with defects and reduced the probability of failures.

Historically, majority of defects in MLCCs were due to the manufacturing processes, and the screening and qualification (S&Q) system used in military specifications was focused on revealing and removing this type of defects. Currently, the proportion of manufacturing defects have been reduced substantially, and most problems with MLCCs are due to the post-manufacturing stresses. However, the requirements in military specifications remain mostly unchanged and do not address sufficiently post-manufacturing stresses.

One of the most powerful means used by hi-rel OEMs to improve reliability of components is derating that limits the level of stress (typically, voltage and temperature) compared to the operating conditions specified for the part. However, due to the low-voltage failure phenomena in MLCCs (see section 5.1) derating might be not effective in reducing risks associated with cracking in the parts.

In this report, we will first give an overview of manufacturing processes and types of MLCCs and consider to what degree the existing S&Q system assures safe assembly and reliable operation of the part. Techniques used to reveal capacitors with cracks, failure modes and mechanisms related to cracking will be reviewed and possible risk mitigating measures to reduce failures associated with manual soldering discussed.

2. Manufacturing processes and types of MLCCs

All MLCCs are manufactured using a ceramic slurry (a mixture of ceramic powder, dispersant, solvent, and organic binder) and a paste for metal electrodes (see Fig.2.1). The dielectric layers are formed by the casting process and then electrodes are formed by applying the paste by screen printing. Dry or wet stacking processes are used depending on conditions of the layers used for lamination. During the wet process, the next layer of the ceramic slurry and electrode paste are laid down on the top of the previous layer and then the stack is dried out to remove the binder (at ~ 400 ºC). During the dry process the layers are casted on a Mylar or stainless steel belt, then dried out, removed from the belt, stacked, and laminated at elevated temperature under pressure. It is considered that the wet process that is typically used to manufacture precious metal electrode (PME) capacitors allows for a better interlayer bonding that results in less delamination.

The dry process that is mostly used for the base metal electrode (BME) technology allows for thinner dielectric layers and larger number of electrodes. Maximum number of layers for dry technology is ~1000 layers with the thickness of the dielectric down to submicrometers, whereas for the wet technology the number of layers typically is less than 200 and the thickness is more than ~5 μm. However, experience shows that the type of the process is not a significant factor affecting the probability of cracking in MLCCs and both methods, when optimized, are capable of producing high-quality, defect free microstructure of MLCCs.

After cutting and presintering, the parts go through the tumbling process (not shown in Fig.2.1) to smooth and round the corners and help to obtain good coverage of the termination ink and subsequent barrier layer plating. The tumbling occurs in rotating barrels filled with water and zirconium balls. Tumbling also minimizes mechanical stresses at the corners of the part and reduces breakages during pick and place operations [16].

After tumbling and drying, the parts are sintered/fired in kilns at high (typically above 1000 ºC) and tightly controlled temperatures. The following processes include application of the base termination to make contacts to the internal electrodes, electroplating and finishing.

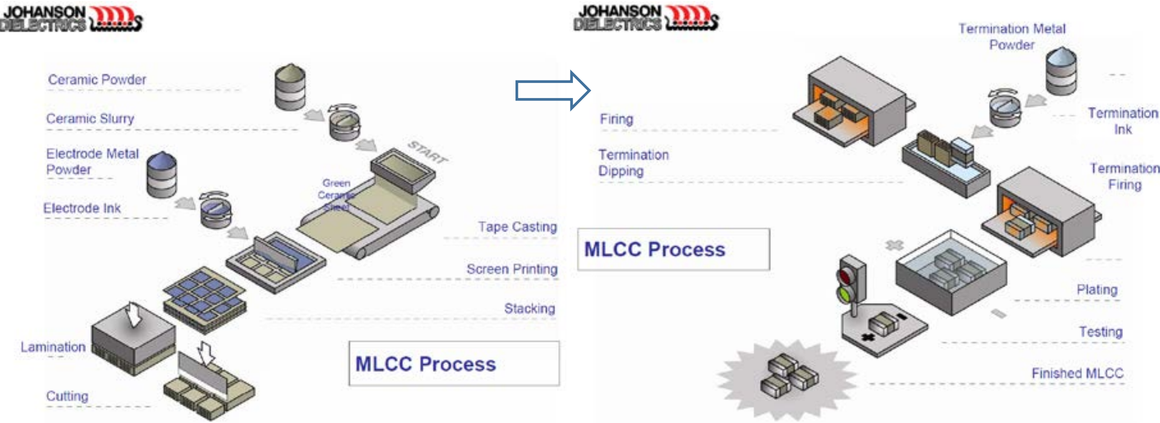

Figure 2.1. Schematic of the processes of MLCCs manufacturing [17].

Fig.2.2 shows a typical construction of a low-voltage (below 200 V) MLCC. The major elements of the part are ceramic dielectric, metal electrodes, and terminations. Respectively, the type of capacitors depends on materials used in these elements (see Table 2.1). Different types of ceramic materials can be used with different types of metal electrodes and terminations resulting in a large variety of types of MLCCs. This variety further increases considering different sizes and outlines of the parts. Standard design low-voltage MLCCs have two terminals, but for some applications, in particular, for decoupling in microcircuits (e.g. FPGA), a design is changed to reduce inductance of the parts.

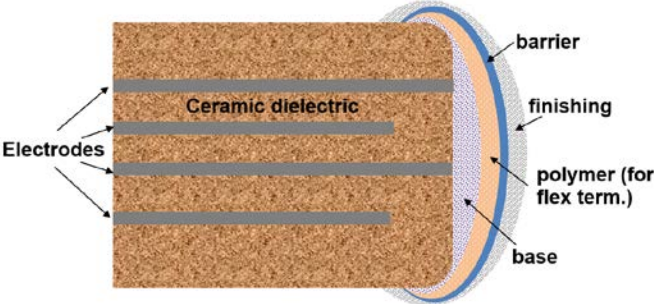

Figure 2.2. Schematic of a low-voltage MLCC.

Table 2.1. Classification of low-voltage MLCCs

Ceramic dielectric	Electrode	Termination	Design (size and olutline)
• Class I (C0G, NP0, BP, BG) High stability, low loss • Class II (e.g. X7R, BX) High volumetric efficiency with variations of cap. ±15% in temp. range from -55ºC to +125ºC. • Class III (e.g. Y5V) Higher volumetric efficiency than class II, but less stable.	• Ag/Pd (PME) • Ni (BME)	• Base termination: o silver glass frit (for PME) o copper glass frit (for BME) • Barrier layer: o Ni o Cu (non-magnetic) • Polymer (flex term. only) o Silver epoxy • Finish plating o Sn/Pb o Ag-Pd (non-magnetic) o Au (wire bond attachment) o Sn (ROHS compliant)	• Standard, two terminals. • Low inductance.

2.1. Dielectric materials

Materials used in MLCCs have polycrystalline structure that is based on barium titanate (BaTiO3) ceramics with different doping for different areas of application and a few percent of glass to interconnect crystal grains. Based on temperature stability of the dielectric constant, *K*, capacitors are divided into three classes of materials (see Table 2.2). Per EIA-198 [18] classification, the level of temperature stability is characterized by a three-character alphanumeric code (see Table 2.3) indicating the minimal low temperature, maximum high temperature, and maximum capacitance change over the temperature range.

Table 2.2. Characteristics of dielectric materials in MLCCs per EIA 198

EIA class dielectric*	Dielectric class	Low Temp. rating, ºC	High Temp rating, ºC	Maximum Temp shift	Maximum loss of C, % per decade hour **
C0G	I	-55	125	± 30 ppm/ºC	0
X7R	II	-55	125	± 15%	2.5
Y5V	III	-30	85	+22% -82%	7

Characteristics of class III ceramic capacitors vary substantially with temperature, voltage and time under bias or duration of storage. Due to a limited temperature range of class III capacitors, they cannot be tested and stressed to the level that is typically used for high-reliability parts and are not recommended for space applications.

Class I ceramic capacitors are the most temperature stable, have minimal dielectric losses and are typically used in RF systems. Thermal stability codes for this type of dielectrics are described in EIA-198, but the most commonly used is C0G type that is also known as NP0-type or BP/BG in MIL specifications. These materials are paraelectrics and have a relatively low dielectric constant ($K < 100$) that does not vary with voltage. Class I ceramic capacitors have a relatively small concentration of barium titanate, below 50%, and are composed of a mixture of finely ground materials such as Titanium dioxide (rutile, TiO2) or CaTiO3 modified by different additives (Zn, Zr, Nb, Mg, Ta, at al.). KEMET is using calcium zirconate (CaZrO3) ceramics with $K \sim 32$ for class I dielectrics that allows for expanding capacitance values in U2J type BME capacitors into the range previously available only in Class II dielectric materials such as X5R and X7R.

Table 2.3. Temperature characteristic codes for class II and III dielectrics

Low Temp., ºC	Symbol	High Temp., ºC	Symbol	Max. capacitance change over temp range, %	Symbol
+10	Z	+45	2	±1	A
-30	Y	+65	4	±1.5	B
-55	X	+85	5	±2.2	C
		+105	6	±3.3	D
		+125	7	±4.7	E
		+150	8	±7.5	F
		+200	9	±10	P
				±15	R
				±22	S
				+22 to -33	T
				+22 to -56	U
				+22 to -82	V

Examples. X7R: X=> -55C, 7=> +125C, R=> ±15%.
Z5U: Z=> +10C, 5=> +85C, U=> +22% to -56%

Class II and III dielectrics are based on ceramics with barium titanate concentration exceeding 90% that is doped with different elements (e.g. rare earth elements La, Nd, Sm, Gd, Dy, Ho, Er, Yt, Mg, Va) and behave as ferroelectrics at temperatures below ~ 125 ºC (Curie point) and as paraelectrics at higher temperatures. Their dielectric constant is high, in the range from 200 to more than 10,000 for class II and more than 10,000 for class III capacitors, but the value

of K is temperature dependent and varies substantially with applied voltage. Comparative temperature dependencies of dielectric constant for different types of dielectrics are shown in Fig. 2.3.

Polycrystals in barium titanate ceramics are comprised of micrometer size grains that have glassy grain boundaries and a crystalline core-shell structure that determines performance and reliability of capacitors [19]. A high-resistive shell doped with rare elements is formed around the grain of the barium titanate ceramic during sintering. At temperatures below the Curie point, the grains are divided into randomly oriented domains that have the same spontaneous polarization (see Fig. 2.4). AC electric field changes the direction of polarization resulting in high values of the dielectric constants. Under DC bias the reversal of polarization caused by AC signal is limited that is reflected in a reduction of the dielectric constant with DC voltage in class II and III dielectrics.

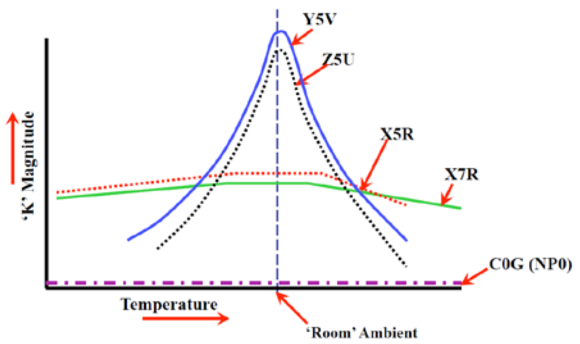

Figure 2.3. Comparative temperature dependencies of dielectric constant in different types of materials J. Prymak, KEMET tutorial [20].

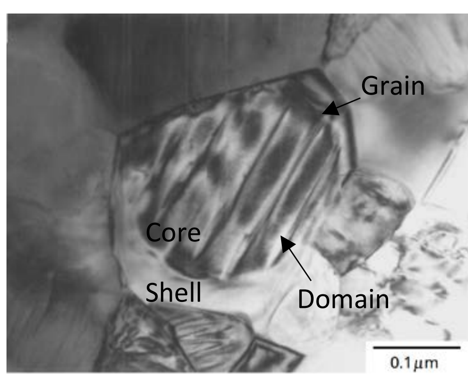

Figure 2.4. TEM image of a BaTiO3 ceramic showing core-sell structure of a grain [21].

Low-voltage PME MLCCs manufactured to military specifications have typically a relatively thick dielectric layers, in the range from 20 to 30 µm, and the number of layers below 100. Stacking of large size MLCCs is used to produce large, microfarad range capacitors. Similar values of capacitance in BME MLCCs are reached in a smaller size parts by reducing the thickness of the dielectric layers and increasing their number. Contemporary BME capacitors can have dielectric thickness as low as 0.5 - 0.7 µm and have up to 400 layers in case size 0402. Production of this type of capacitors require a very small grain size that is getting closer to the dimensional limit [22]. Reduction of the grain size below a certain optimum (~1 µm) decreases room temperature dielectric constant and temperature stability of capacitors. Until recently, maximum operation temperature of capacitors was 150 ºC (X8R, X8S, and X8T types), which is likely a limit for barium titanate ceramics. Development of new types of materials, e.g. tungsten-bronze type ferroelectrics, allows increasing further operating temperatures and development of X9R BME capacitors that can operate in the range from -55 ºC to +200 ºC.

2.2. Electrode materials

Historically, MLCCs used in space application had electrodes made of precious metals, typically silver/palladium alloys (PME capacitors), but starting 2017 capacitors with nickel electrodes, or base metal electrode (BME) capacitors manufactured per MIL-PRF-32535 are qualified for space applications. BME capacitors have been widely employed in commercial and automotive industry applications since mid-90th mostly due to a lower price of materials. Table 2.4 shows characteristics of different types of metals used to form electrodes in MLCCs including the atmosphere for the metal paste firing.

Table 2.4. Physical properties and price ratio of electrode materials [21]

Metal	Melting point, ºC	Resistivity, mohm	Firing atmosphere	Price ratio
Ag	961	1.62	Air	3
Cu	1080	1.72	Reducing	1
Ni	1453	6.9	Reducing	1
Pd	1552	10.4	Air	80

The paste that is typically used for PME capacitors has relatively large particle sizes, from 900 to 1000 nm, whereas BME technology uses pasts with smaller particles, from 300 to 500 nm. This allows formation of relatively thin nickel electrode layers. Typically, a composition of 70% Ag and 30% Pd is used for PME capacitors; however, depending on design, manufacturing process, and type of ceramic, the Ag/Pd ratio can vary substantially.

Silver/palladium alloys do not react with ceramic and do not oxidize significantly, which allows for sintering in air atmosphere. Although PME technology has been used for decades, some challenges during firing of capacitors with Ag/Pd electrodes still exist [2]. These challenges include catalyzation of the binder burn-out that might accelerate gas generation and cause delaminations and volumetric changes in the electrodes that can also facilitate delaminations. Volumetric changes are due to increasing Pd volume up to 68% when it is oxidized at ~500 °C and reduces back at ~800 °C. A low melting temperature glassy components should be used to limit the firing temperature for 70Ag/30Pd alloy to ~1,100°C, which results in reduction of the dielectric constant of ceramics. Silver evaporation during firing requires using special measures to increase Ag vapor pressure during sintering. Diffusion of silver into ceramic (mostly along the grain boundaries) limits the minimal thickness of the dielectric layers resulting in decreasing of volumetric efficiency of capacitors.

The major challenge for the BME technology is nickel oxidation in air during sintering that results in a substantial increase of resistance of electrodes. To reduce oxidation, high temperature operations (at ~1200 °C) are carried out in reduced atmospheres. This results in generation of positively charged oxygen vacancies in the ceramic, increases conductivity of the dielectric and causes IR degradation in capacitors with time of operation. To avoid the effects of reducing environments and stabilize ceramic, a special dopants e.g. rare earth oxides Y2O3, Dy2O3, Ho2O3, and Er2O3, are used. The dopans reduce concentration of oxygen vacancies and improve stability of capacitors during life testing [2]. In addition, stability of BME MLCCs is improved by re-oxidation at temperatures below sintering (~1000 °C) after firing of the parts. It is assumed that reoxidation of BME MLCCs is controlled by oxygen diffusion along the Ni inner electrodes [23].

Diffusion and migration of Ag into dielectric layers from inner Ag or Ag/Pd electrodes might pose a problem for long-term reliability. Silver is a material that is most susceptible to electromigration in the presence of moisture, and for this reason, cracking of PME capacitors creates a higher risk of electrical failures compared to BME capacitors (see section 5 of this report).

2.3. Termination materials

After sintering, the end of a capacitor with exposed electrodes is dipped in a metal glass frit (thick film ink) consisting of metal particles or flakes and doped borosilicate glass. This ink is then dried and sintered/fired to the ceramic body allowing glass particles to fuse along contacts creating a sponge like structure and diffusing into ceramic to assure adhesion between ceramic body and terminal metallization [24]. If manufacturing process is not optimized, the interface boundary amorphous layer might crack during capacitors' manufacturing or assembly thus increasing the risk of failure. If termination firing temperature is below the optimal, not all internal electrodes form good metallurgical contacts with terminations. Under environmental stresses during application, this might cause intermittent electrical contacts resulting in sporadic changes in the value of capacitance and malfunctions of the electronic system. The type and optimal amount of glass frit used in termination depends on the type of ceramic and design of the capacitor.

The thickness and material of the glass frit affect the probability of cracking caused by thermal stresses associated with soldering and/or temperature cycling [25]. Insufficient thickness of the base termination might increase the proportion of MLCCs' failures during wave soldering by several times. Experience shows that optimization of the base terminal materials and processes improves substantially the robustness of capacitors and reduces risks of failures during high humidity operations. The type of paste used might also affect the probability of IR failures in COG BME capacitors after storage at normal conditions [26].

A silver-based frit is used for PME and a copper-based (sometimes nickel-based) frit is used for BME technology. The copper-based frit is fired in oxygen-free atmosphere to avoid oxidation. Fig. 2.5 shows typical cross-sections of terminations in PME and BME capacitors.

After the termination has been sintered it is electroplated with a nickel layer to form a barrier and minimize dissolution of electrodes and base metallization during soldering. A final step in forming terminations is plating with a tin/lead solder for military or tin layer for commercial capacitors to assure solderability of the part.

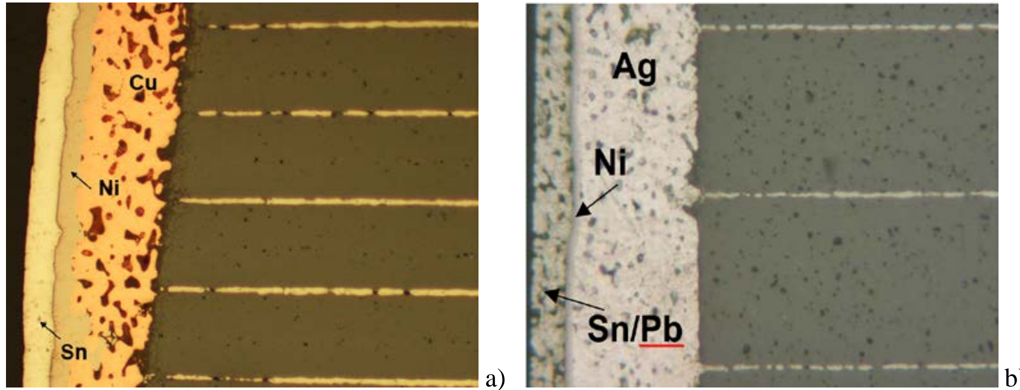

Figure 2.5. Terminations in BME (a) and PME (b) 50 V capacitors.

The porosity of the base termination and the presence of pinholes allow penetration of moisture through the terminals of the part [24]. This can cause corrosion of copper or degradation of insulation resistance of the capacitor in the presence of cracks that might create a path for moisture to short opposite electrodes. This degradation process might accelerate in the presence of defects in the termination such as terminal-ceramic delamination or pinholes shown in Fig. 2.6. Note, that MIL-PRF-123 considers acceptable pinholes of less than 130 µm and MIL-PRF-32535 reduces these requirements to 80 µm for capacitors with sizes smaller than 0805. These pinholes not only transparent for moisture, but can also trap contaminations and moisture for a long time thus enhancing the risk of corrosion.

Calculations have shown that the size of terminations affects the maximum principal stress in MLCCs [27]. Mechanical stresses in capacitors also depend on the thickness of nickel plating and process conditions [28]. Considering that CTE of nickel (13.4 ppm/K) is greater than that of ceramics (~9.6 ppm/K) and for both materials the Young's modulus is rather large, from ~ 100 GPa to 200 GPa, substantial tensile stresses might develop during soldering conditions, thus enhancing metal/ceramic separation close to terminals. In some cases, failures of MLCCs during temperature cycling have been attributed to increased stresses caused by nickel plating. The optimal thickness of Ni barrier layers at the terminations is considered to be in the range from 2 to 6 µm. Thicker layers might increase risks of cracking and delaminations and seal moisture and contaminations that could have penetrated inside the part during initial stages of the plating process. Termination materials and geometry are important elements of capacitors' design that affects the probability of cracking and failures [29]. The susceptibility to thermal shock failures is greater for terminations with Ni barrier compared to Pd/Ag terminated chips.

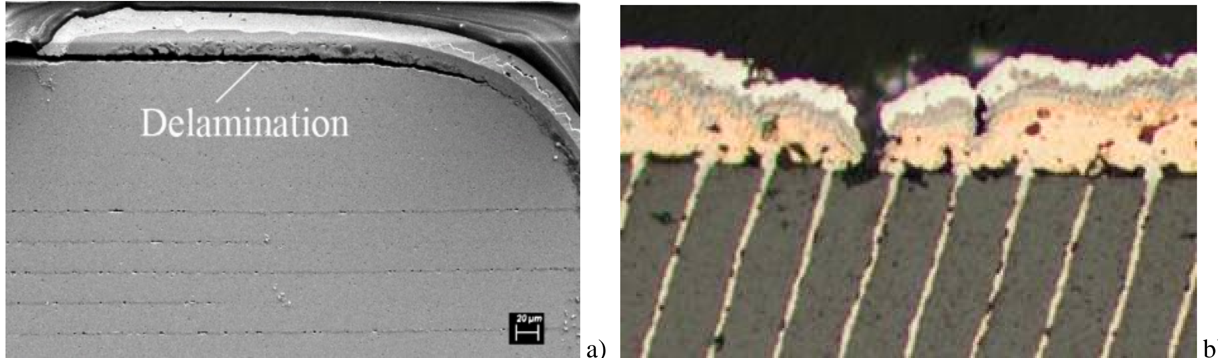

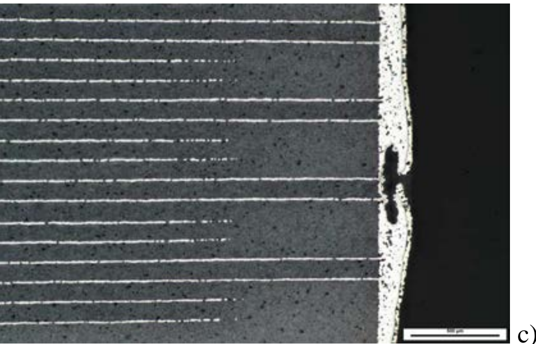 c)

Figure 2.6. Example of termination defects. a) delamination in a PME capacitor and pinholes in BME (b) and PME (c) capacitors.

For non-magnetic capacitors that are often required by medical or special RF applications, nickel cannot be used as the barrier layer and terminations are manufactured using Ag/Pd finishing. Capacitors with this type of terminations are not recommended for soldering due to the leaching of silver into molten solder and should be attached by silver epoxy. Also, a Cu barrier can be used instead of Ni on the top of Ag or Ag/Pd glass for the non-magnetic devices.

MLCCs with gold finishing are assembled using wire bonding at terminals. Gold electroplating might result in excessive hydrogen generation, and reactions of hydrogen with palladium in PME MLCCs might cause delaminations and cracking. The risk of hydrogen related delaminations is greater for PME compared to BME capacitors. A detailed description of different types of terminations and acceptable methods of assembly can be found in manufacturers' recommendations, e.g. [30, 31].

Commercial capacitors are typically compliant with the Restriction of Hazardous Substances (ROHS) regulations and their terminations are manufactured using lead-free metals (typically pure tin) that are susceptible to growing whiskers. For military and space applications, termination finishing with a Sn/Pb alloy having 3% lead minimum is required. Replacement of pure tin with Sn/Pb finishing in commercial MLCCs can be achieved either by solder dipping into Pb containing solder or by plating Sn/Pb layer on the top of the existing finishing and the following fusion (e.g., AEM Inc. refinishing process). The latter process is less risky because avoids thermal shock stresses to the parts.

- Flexible terminations

Flexible terminations that are formed by addition of a conductive polymer layer between the base and Ni barrier (see Fig.2.2) have been used for electronic boards' assembly for more than a decade. What started as a commercial technology to reduce failures related to flex cracking of MLCCs, is currently used for the advanced military and space grade capacitors manufactured per MIL-PRF-55681 and MIL-PRF-32535. The major reason for popularity of this technology is that flexible terminations reduce the stress that is transferred from the board to the ceramic body, and possible cracks instead of propagating to the active area of capacitors are contained within the polymer [32]. Experience and testing show that introduction of flex terminations decreases substantially cracking of MLCCs during soldering, handling, and field operations. Manufacturing experience shows that introduction of flexible terminations practically eliminated field returns caused by flex cracking.

Temperature cycling tests of capacitors with flex terminations in comparison with regular termination parts soldered onto PWBs showed a substantial improvement in reliability. Regular termination MLCCs started failing after 1000 cycles, whereas there was no failures detected in the flexterm capacitors after 3000 cycles.

Using conductive polymers in terminations improves substantially results of the drop testing. TDK data [33] show that capacitors with soft terminations had no cracking failures after 10,000 drops (dropping from 1 m at a frequency of 16 times per min), whereas a regular product had 30% failures after 2000 drops. In addition, after the drop testing the parts passed humidity load test (1000 hours at 85 °C and 85% RH under rated voltage) thus indicating absence of hidden cracks.

In BME capacitors with flex terminations operating in humid environments silver dendrites can grow along the surface of ceramics (see Fig. 2.7). Although the risk of increased metal migration along the cracks and failures caused by the growth of dendrites associated with silver-epoxy terminations exists, the benefits of reducing the probability of

cracking apparently prevail. As a result, the overall quality and reliability of BME capacitors with soft terminations is increased and field failures reduced.

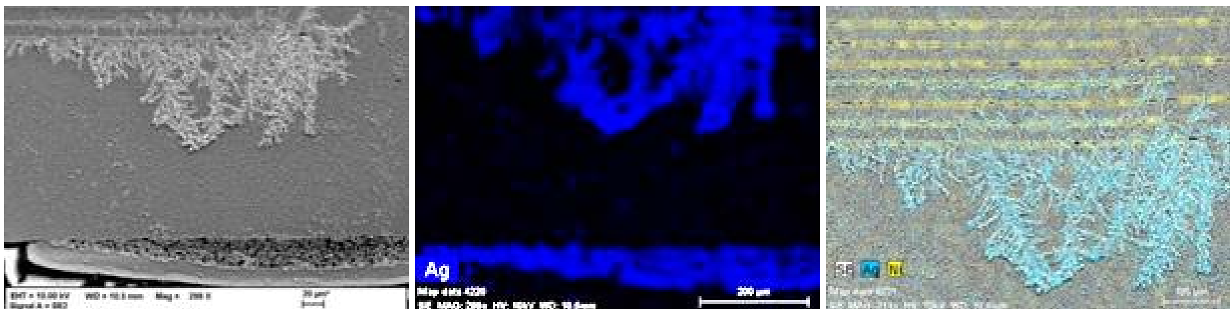

Figure 2.7. Silver dendrites on the surface of a cross-sectioned BME flex-termination capacitor after low-voltage humidity testing at 1.5 V (HSSLV).

2.4. Design

Most cracks in MLCCs caused by deformation of PWBs during assembly, handling or testing are initiated at the surface close to the terminal areas of capacitors (see Fig.2.8). These cracks might affect reliability of the parts if they are reaching active area of capacitors and cross opposite electrodes. For these reasons, parts with thicker cover plates and larger end margins are more resilient to cracking-related failures [34].

Existing requirements for margins in military specifications are similar to EIA-469 DPA standard [35] that has different margin and cover plate thickness limits for different groups of capacitors. The EIA-469 requirements for the margins are designed to provide sufficient electrical insulation, address mostly quality of the as-manufactured parts and do not consider cracking-related issues.

Thin dielectric MIL-PRF-32535 follows EIA-469 and specifies different limits for parts with VR above 50 V, below 6.3 V, 16 V and 25 V. For example, the thickness of cover plates should exceed 0.003" (75 μm) for capacitors rated to more than 50 V and can be as low as 0.001" (25 μm) for capacitors with VR ≤ 6.3 V. However, for capacitors intended for automotive industry, manufacturers have stricter requirements for the margins. A minimal size for margins and cover plates for commercial MLCCs manufactured by AVX is 75 μm, it is 100 to 125 μm for automotive grade capacitors and 110 to170 μm for space application [36, 37].

To mitigate risks of cracking-related failures, special designs of MLCCs have been developed. For low capacitance values, KEMET, similar to other manufacturers, offers the Floating Electrode (FE-CAP) capacitors (see Fig. 2.8.d). This design is also known as a Serial Cap design [38]. For mid capacitance values, the Open Mode solution that has enlarged end margins that create safe zones on both ends of the capacitor (see Fig.2.8.e). Other manufacturers, e.g. TDK [33], are using similar design approaches to reduce failures caused by cracking (see Fig. 2.9).

Various designs of MLCCs that have been suggested by manufacturers to decrease the probability of flex cracking can be summarize as following:

- Flexible termination.
  Application of relatively soft and/or tear-away termination layers made of conductive polymers (see Fig. 2.2) reduces the stress in ceramic and restricts flex cracks within a safe zone away from the body of the MLCC.
- Fail open design (Fig.2.8.e).
  End margins are widened, so if a crack occurs, it does not cross electrodes with opposite polarity, and thus prevents short-circuit failures.
- Floating electrodes (Fig. 2.8.d).
  Two capacitors connected in series within an individual case size, so the probability of shorting cracks is reduced substantially.
- Clip-on lead frame.
  Attachment of J-shaped leads see Fig. 2.9) mechanically decouples the MLCC from the PWB and allows for some stress relief.

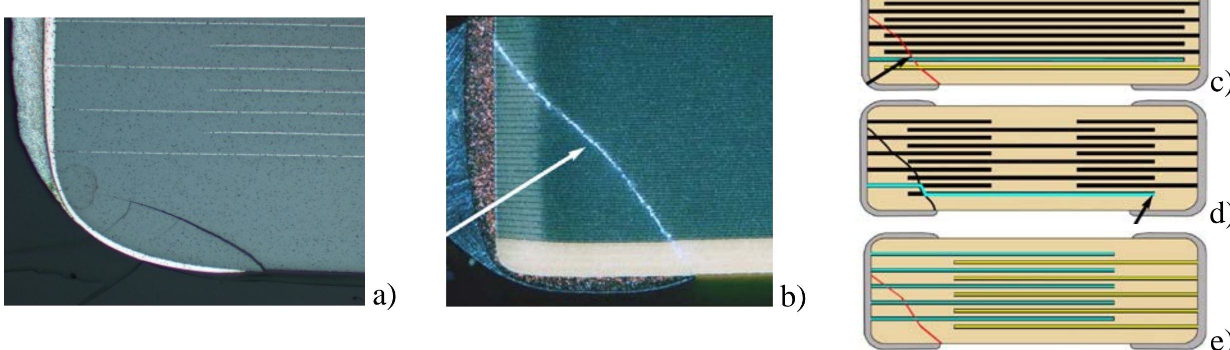

Figure 2.8. Soldering related cracks in MLCCs and schematics of a standard part (c), floating electrode capacitor (d), and Open Mode design (e) [38]. Yellow and blue lines in (c-e) represent electrodes with different polarity.

	image	Flex stress	Large capacity	Cost	Applications
1) MEGACAP		★★★	★★★	★	Circuits requiring especially high reliability and large capacitance
2) Soft termination		★★	★★	★★	Circuits in which flex stress or thermal shock can become an issue
3) Serial design, the CEU series (resin electrode s+ safety structure)		★★	★	★★	Circuits in which flex stress or thermal shock can become an issue and a serial connection of capacitors is considered
4) Open mode		★★	★	★★★	Circuits that do no require very big capacitance but flex stress can be an issue

Figure 2.9. MLCC designs with flex crack countermeasures used by TDK [33].

A combination of floating electrode and flex termination design (e.g. a TDK Dual-Fail-Safe, Mega Cap design [39]) allows to reduce the risk of failures even further. This design has been proven highly reliable, and no cracks developed in the parts after 3000 thermal shock cycles.

Obviously, the cost of improved reliability of MLCCs with increased margins or floating electrodes is a lesser volumetric efficiency. For this reason, flex termination is likely the most efficient cracking mitigating measure.

Typically, capacitors having maximum capacitance values for a given case size and rated voltage have smaller margins and hence, pose a higher risk of failures. For this reason, for a given rated voltage and case size, the use of parts with maximum available value of capacitance is not recommended.

Since operating frequencies of contemporary microcircuits have increased substantially, new designs of MLCCs that are used in a close proximity to the microcircuits to improve their performance, suppress noise, and stabilize operation, have been developed. Fig. 2.10. shows an example of low-inductance capacitors used in a package of XILINX FPGA.

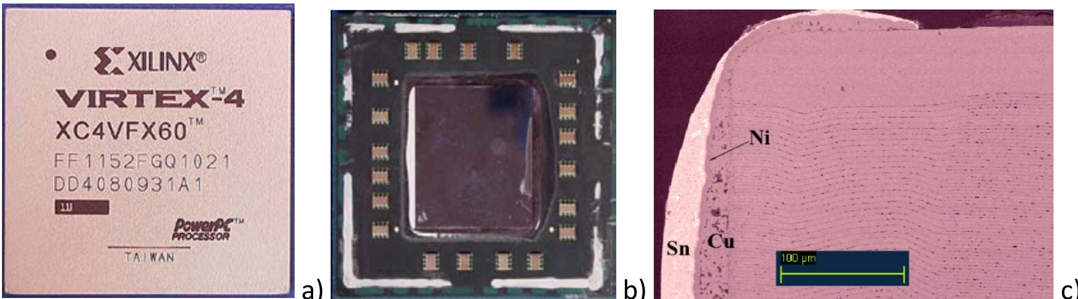

Figure 2.10. Overall external (a) and internal, after lid removal, (b) views of a XILINX VIRTEX-4 FPCA showing IDC-type ceramic capacitors mounted inside the package. Figure c) shows a cross-section of the termination area of IDC capacitors with dielectric thickness of ~2 µm.

The equivalent series inductance, ESL, is an important parameter of capacitors that determines their efficiency during operation at high frequencies. Fig.2.11.a shows an equivalent circuit of MLCCs operating in the RF range. The idea of low ESL designs of MLCCs is in reduction of the length of the effective AC current flow path (see. Fig. 2.11.b).

ESL values can be decreased several times simply by reversing the width and length of capacitors. This change in the design might potentially increase the susceptibility of the parts to cracking, first, by creating of a more rigid solder connections, and second, because ceramic areas close to terminals have a higher level of internal mechanical stresses and the larger this area is, the greater the probability of having a crack.

A more drastic reduction of ESL, to the picohenry levels is achieved by IDC and ball grid array vertical electrode designs. Figure 2.11.c shows examples of designs of low-ESL MLCCs. The effect of design changes on the susceptibility to cracking requires additional analysis; however, some part types, and in particular, IDC capacitors, have passed extensive testing by XILINX and has been successfully used for more than a decade in FPGAs.

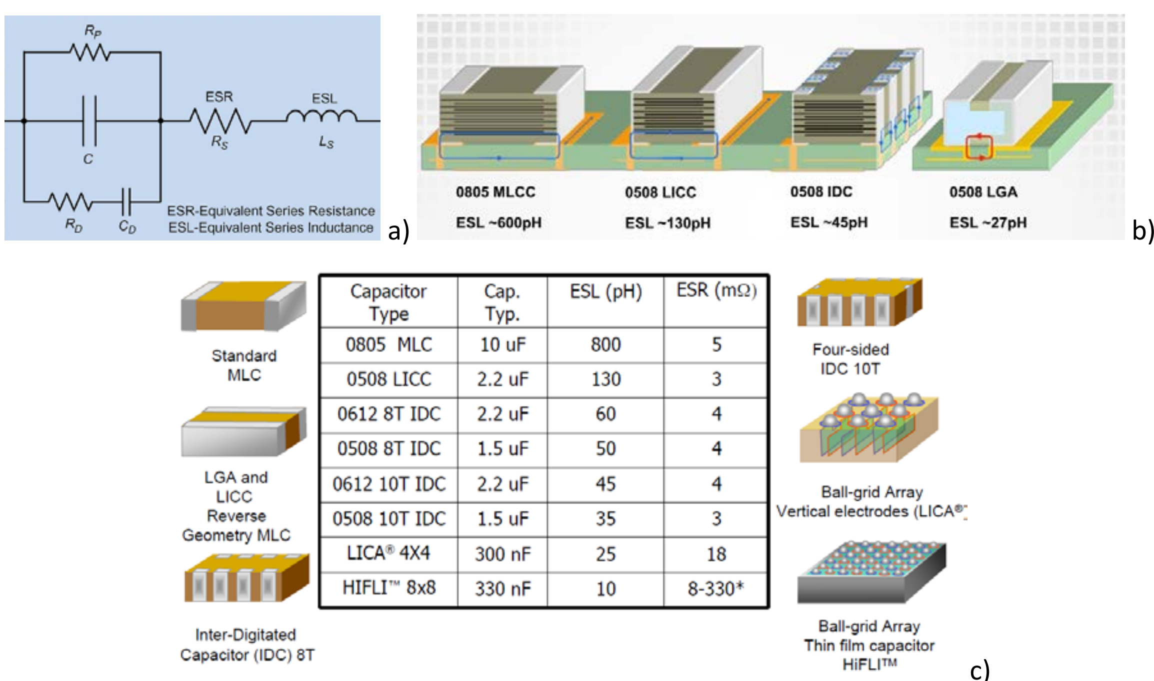

Capacitor Type	Cap. Typ.	ESL (pH)	ESR (mΩ)
0805 MLC	10 uF	800	5
0508 LICC	2.2 uF	130	3
0612 8T IDC	2.2 uF	60	4
0508 8T IDC	1.5 uF	50	4
0612 10T IDC	2.2 uF	45	4
0508 10T IDC	1.5 uF	35	3
LICA® 4X4	300 nF	25	18
HIFLI™ 8x8	330 nF	10	8-330*

Figure 2.11. Equivalent circuit of a capacitor at high frequency(a) a schematic of the AC current flow in capacitors (b), J.Marshall [37], and types of low inductance MLCCs, R.Demko (c), [20].

Stacked capacitors are manufactured by attaching leads to several MLCCs connected in parallel and arranged vertically one on the top of other (see for example Fig. 2.12a). This design allows for a substantial increase of capacitance at the same footprint and reduces the size of the circuit board. The lead-frame decouples mechanically capacitors from the board thus reducing microphonic noise and destructive effects of board flexing. Although the

lead-frame is attached using a high-temperature solder, the process is thoroughly controlled by the manufacturers that reduces the risk of cracking. However, shallow cracks under the terminations that are typical for most MLCCs occur also in stacked capacitors (Fig. 2.12b and c) and when the thickness of the cover plate is not sufficient, these cracks can cause life test failures as shown in Fig. 2.12d. When moisture and contaminations penetrate inside the crack, the electric field between the tip of the crack and top electrode is increased, and with time, this might cause failures according to the time dependent dielectric breakdown (TDDB) mechanism (see Fig. 12.2e).

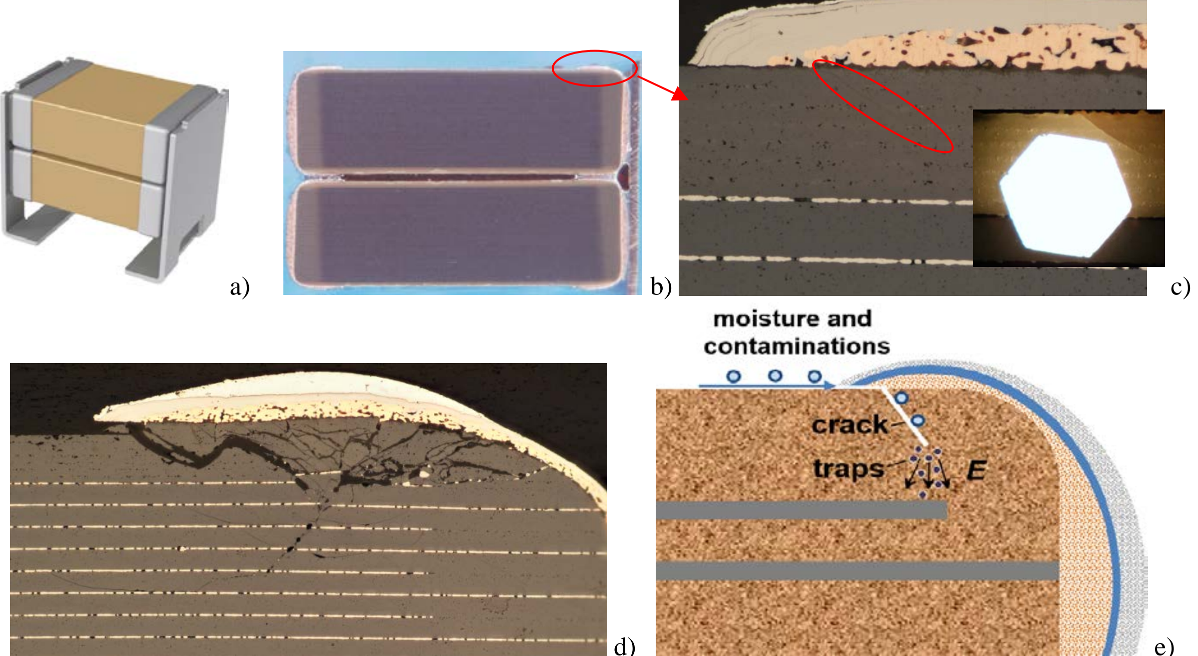

Figure 2.12. An overall view of a stacked capacitor (a), cross-sectioning showing a thin cover plate (b) and a shallow crack under the termination (c). Fig. d shows cross-sectioning of a capacitor that failed during life testing and (e) is a schematic of the TDDB mechanism of failure.

- Laser marking

Due to a small size, MLCCs are usually unmarked. However, some customers, prefer marked capacitors, so that they can have assurance that the correct component has been used [40]. A laser marking that is often used for plastic parts might cause damage to a ceramic capacitor in case the laser power level is above optimal (see Fig. 2.13.). Different types of capacitors use different materials and have different thickness of the cover layers and require different levels of the power setting to avoid cracking.

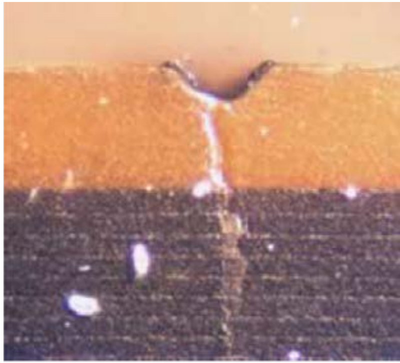

Figure 2.13. A capacitor damaged due to excessive power of laser marking machine.

3. Testing and quality assurance

All MLCCs are manufactured using similar technological processes and materials and the difference between commercial and military or space grade capacitors is mostly in the design rules, the level of consistency of used materials and processes, and in the approach to quality assurance (QA) or amount of testing. For example, the thickness of the dielectric layers is typically much greater for military capacitors, and types of materials that are fixed for military can be changed for commercial capacitors. Stability of design and materials is important to assure consistency of characteristics and reliability of the parts, but retards innovations and improvements of performance.

Approaches for quality assurance of commercial and military capacitors are substantially different. Quality assurance of mass production commercial capacitors is based on the build-in-design approach and extensive use of the Statistical Process Control (SPC) system [41, 42]. SPC is a data-driven methodology for quality analysis and improvement that is essentially a preventive activity performed in real-time during the manufacturing process. Military specifications also require SPC system to be used, but it is not considered a major element of QA, and inability to make in-process improvements reduces substantially its efficiency. Instead, QA for military capacitors is based on extensive inspections and testing of the parts. As stated by Dan Friedlander [42] "SPC targets failures prevention, burn-in (testing) targets failures detection".

The first military specifications had been developed before the mass production era that was driven by commercial electronics market, and historically played an important role in improving quality of electronic components. Obviously, statistics was not effective without automotive process control and for low production volumes, so QA in military specifications relied heavily on testing and inspection.

Historically, majority of MLCCs used in space applications by NASA have been manufactured and tested according to MIL-PRF-123 (CKS-style) and MIL-PRF-55681 (CDR-style). In 2017 a specification for thin dielectric ceramic capacitors that includes BME-type capacitors, MIL-PRF-32535 (M32535-style) has been developed. In addition, USA, EU, and Japan space agencies have developed their own specifications (source control drawing, SCD) that extended the range of capacitors suitable for space applications: S-311-P-828, S-311-P-838 by NASA/GSFC [43, 44], ESCC-3009 by ESA [45], and QTS-2040 by JAXA [46, 47].

Capacitors developed for automotive industry are used sometimes in low-level space projects because these parts are manufactured to a higher quality standards compared to a general use commercial capacitors. Quality of these parts should be in compliance with AEC-Q200 requirements [48]. However, this document describes only general specifications for passive components, and the parts that are actually used by car manufacturers might have additional requirements detailed in non-disclosed documents.

All mentioned above documents use a variety of tests and inspection procedures that generally can be divided into three groups: (i) screening gr.A, (ii) screening gr.B and (iii) qualification. Screening gr.A inspections and testing is carried out for 100% of samples in each lot and have a purpose of removing parts with manufacturing defects from the population. Burning-in is considered a major element of the screening because it supposed to prevent early, defect related (infant mortality) failures.

Screening gr.B is carried out using samples from each lot (sometimes called lot acceptance testing, LAT), and its purpose is to ensure that the manufacturer continue production of parts that conform to the specification. Qualification testing is carried out periodically using samples from some lots to confirm the required quality level for a given type of production. Obviously, gr.A screening can reveal manufacturing defects only, and the robustness of the parts towards assembly, and post-assembly stresses should be addressed by gr.B screening and qualification tests.

Note that the notion of the lot of parts for commercial components is not defined as strictly as for military components. However, considering that MLCCs are produced by huge batches and the amount of a certain type of capacitors used in a space project is relatively small, the probability of having parts from different batches is low.

3.1. Comparative analysis of specifications

Tables 3.1 and 3.2 give a comparison of screening and qualification tests used in different specifications. In all documents, except for MIL-PRF-55681, there is a ban on use of pure tin for terminals' finishing. MIL-PRF-55681 has an option with pure tin, but warns against the possibility of whiskers growth. Some specifications limit the

thickness and dielectric constant of the ceramic layers and types of electrodes. For example, MIL-PRF-123 does not allow nickel electrodes and flexible terminations, limits dielectric thickness (*d*) to 0.8 mil, and the dielectric constant to 3000. In NASA/GSFC requirements, the values of *d* depend on the type of capacitors and can be as low as 0.28 mil (~7 μm), whereas JAXA specification QTS-2040 limits *d* to 3 μm. The latest military specification, MIL-PRF-32535, does not have limits for the dielectric thickness at all. Destructive physical analysis (DPA) is required by all specifications except for MIL-PRF-55681.

- Military specifications

Ultrasonic inspection when used for fully manufactured capacitors is limited to areas not covered by terminations, and likely for this reason, MIL-PRF-123 requires this inspection before the terminations are formed. However, formation of terminations might create a substantial stress to the capacitors and result in cracking, so the latest specification, MIL-PRF-32535, requires acoustic examinations before and after formation of terminations. Note that MIL-PRF-55681 (CDR-style capacitors) does not require ultrasonic inspection that might be the reason of several recent failures in space projects that were attributed to the presence of delaminations and cracks.

Every lot manufactured per MIL-PRF-123 and MIL-PRF-32535 specifications requires voltage conditioning or burning-in (BI) at two times rated voltage and 125 ºC for 168 hours minimum. BI requirements in MIL-PRF-55681 are somewhat relaxed: (i) the duration of testing is 100 hr, and (ii) the temperature might be less than 125 ºC and depends on the maximum operation temperature specified for the part. MIL-PRF-55681 also does not require DPA and thermal shock prior to BI. Considering high temperature processes during formation of terminations, the efficiency of temperature cycling before BI for unmounted capacitors is not clear.

Reliability of military grade capacitors is determined during accelerated life testing, typically at 2VR and 125 ºC. The failure rate (FR) for MLCCs is usually expressed as percent failures per thousand hours of test and indicates a maximum failure rate at operating conditions that is determined in the assumption of random failures (exponential distribution) [49]. To verify reliability level of 0.001%/1000hr with 60% confidence 91.6×10^6 unit-hours of testing at operating conditions (125 ºC and rated voltage) should be accumulated without failures (e.g. 91,600 samples during 1000 hours). The same FR level at 90% confidence would require testing of 230×10^6 unit-hours. To accelerate the testing, MIL-PRF-123 and MIL-PRF-55681 allow increasing test voltage two times that assumes 8X acceleration. However, even with this acceleration the testing might last more than half a year.

Capacitors manufactured to M32535 specification are not established reliability parts. Instead, two product quality levels are defined: standard reliability (M level) and high reliability (T level) that is intended for space applications. Both types are manufactured and tested similarly and the quality level is determined by (i) duration of life testing, and (ii) most importantly, by carrying out life testing on each lot of capacitors. Test duration for the T-level products is 4,000 hours for qualification and 1000 hours during gr. B screening testing, whereas qualification test for M-level capacitors requires 1,000 hours.

A sample size that is used for life testing varies from123 for MIL-PRF-123 and MIL-PRF-32535 to 25 for MIL-PRF-5681. Also, some lots might not be tested at all (e.g. CDR capacitors manufactured to MIL-PRF-55681 specification) and they are qualified by similarity with samples from other lots representing manufacturing process over a certain period. Considering that only a small proportion of capacitors might have defects that pose reliability risks, the efficiency of life testing to reveal lots with defects, and cracks in particular is limited. This efficiency is even lower when parts are tested in fixtures or soldered onto boards at conditions that are different compared to the actual assembly of flight cards.

Table 3.1. Requirements for screening of low-voltage MLCCs

Type of test	Test	MIL-PRF-123, T	MIL-PRF-55681	MIL-PRF-32535, T	S-311-P-829	S-311-P-838	ESA ESCC #3009	JAXA QTS-2040/M
Scope/limit		PME, d ≤ 0.8 mil, no pure tin, K_{max}= 3000		No pure tin	PME, no pure tin, d(PN), K_{max} =4000, X7R; 100 for NPO	BME, X7R, d ≥ 0.28 mil, N ≤ 300, Sn/Pb plated	Type I and II dielectrics	Sn/Pb by solder dip, d ≥ 3um $2000 < K < 4000$
Screening, gr.A	C, DF	100%	100%	100%	100%	100%	100%	100%
	IR @25C	100%	100%	100%	100%	100%	100%	100%
	IR@125C	100%	Sample	100%	100%	100%	sample	100%
	DWV/voltage proof	2.5 to 4×VR	2.5×VR	2.5 to 4×VR	2.5×VR	2.5×VR	2.5×VR	2.5×VR
	TS and Voltage conditioning	20c -55 to +125C, 168-264hr 2×VR, 125C	100hr 2×VR, at T_{max}	20c -55 to +125C, 168-264hr 2×VR, 125C	20c -55 to +125C, 168-264hr 2×VR, 125C	20c -55 to +125C, 168-264hr 2×VR, 125C	96hr at 2×VR, T_{max}	4hr/2VR/85 (in-process) 20c -55 to +125C, 21hr@ 3VR, 125C
	PDA*	3%	8%	5%	5%	5%	5%	-
	Ultrasonic inspection	100% before termination	-	Before and after termin. for size ≥0805	100% before or after termination	100% before or after termination	-	100%
	Visual exam.	100%	sample	100%	100%	100%	100%	20 pcs
Screening, gr.B	DPA	✓	-	✓	✓	✓	✓	✓
	TS and Life test	100c.,1000 hr, 2×VR, 125C	-	100c, 1000hr 2×VR, 125C	100c, 1000hr 2×VR, 125C	20c, 1000hr 2×VR, 125C	-	25(0) pcs, per JAXA-QTS-2040
	THB/moisture resistance	20c per M202 TM106, 10c at 50V	-	12(0) pcs., 85C, 85% RH, 96hr, VR	20c per M202 TM106	85C, 85% RH, 96hr, VR	-	12 pcs, 20c per M202 TM106
	Breakdown voltage	-	-	VBR ≥ 6×VR or 1200V	-	30(0) pcs, VBR ≥ 6×VR	-	As a part of evaluation
	Resistance to soldering heat	-	-	-	-	6(0) pcs, M202 TM210, J, Infared/convection but 1 cycle, within gr.B	-	4 pcs. Solder dip: +260°C, 10s. M202 TM210, B.
	HSSLV**	✓	-	-	✓	-	✓	✓
	PRVT***	-	-	-	-	✓	-	-

*PDA = percent defectives allowable

**HSSLV = humidity steady state low voltage test that is carried out at 1.3V for 240h at +85°C and 85%RH, typically using 12 samples.

***PRVT = Process Reliability Verification Test.

Table 3.2. Requirements for qualification testing

Test	MIL-PRF-123, T	MIL-PRF-55681	MIL-PRF-32535, T	ESA ESCC #3009	JAXA QTS-2040/M	AEC-Q200
TS	-55C to +125C, 100 c, 186 pcs	-55C to +125C, 5 c, 18 pcs	-55C to +125C mounted, 100 c (T) and 5c (M), 123 pcs	10 cycles T_{min} to T_{max}	18 pcs on alumina or FR4, -30 to +100°C x 1,000cy	77(0) 1000c -55 to +125C
Life testing	123(1) 1000hr 2×VR, 125C	25(1), 2000hr at T_{max}, 2×VR	123(1) 4000hr 2×VR, 125C	(20 or 40) 2000hr 2×VR, 125C	123pcs. 1.5VR, 4,000h@+125°C	77(0), 1000hr 125C, VR
HSSLV	✓	✓	-	Within gr.B (10 TS cucles before the testing)	Within gr.B	✓ (for PME only)
THB/moisture resistance	20c per M202 TM106	20c per M202 TM106	22(0), 85C, 85% RH, 1000hr, VR	-	-	77(0),), 85C, 85% RH, 1000hr, VR
Resistance to soldering heat	12(1) pcs, M202 TM210, B, solder dip, 230C, 10sec, gr.C	9(1) pcs, M202 TM210, J, Infared/convection reflow but 1 cycle, gr.C	22(0) pcs, M202 TM210, J, Infared/convection reflow but 1 cycle, gr.C	-	4(0), M202 TM210, cond.B Solder dip: +260°C, 10s.	30(0), M202, TM210, D. Wave solder, 260C, no preheat
Flex testing	-	12 pcs. 2mm deflection	12 pcs, 2mm deflection	-	1 mm deflection	2mm deflection

*The combination of the mounting process and 1 heat cycle is considered to be equivalent to 2 heat cycles.

Life testing of small size thin dielectric IDC style X7S BME capacitors manufactured to MIL-PRF-32535 showed that these parts couldn't pass testing and fail after 4000 hr at 125 ºC, 2VR. This was attributed to a higher acceleration factors compared to X7R capacitors with thicker dielectrics. For these parts, the exponent n in the Prokopowicz and Vaskas equation is in the range from 4.4 to 4.9 and E_a is between 1.2 and 1.6 eV, which is greater than what is usually assumed for PME capacitors (n ~ 3). For this reason, life testing for IDC capacitors is carried out at 1.5VR [37], which is consistent with conditions used for thin dielectric capacitors by JAXA [47].

Some X7S thin dielectric small size capacitors had failures when tested at 85 ºC 85% RH for 1000hr at rated voltages. This might be due to cracks formed during manufacturing or developed during assembly or testing. For these parts, requirements in MIL-PRF-32535 were also reduced, and instead of THB conditions (85 ºC and 85% RH), capacitors are tested at 40 ºC and 95% RH that are apparently less stressful. This relaxation of requirements would be reasonable if failures occur when test conditions exceed a certain threshold. In this case, no failures would be expected at normal operating conditions. Unfortunately, there is no proven predictive models for electrical failures of MLCCs with cracks in humid environments, and additional analysis is necessary to understand the reason of parts failures at 85 ºC and 85% RH.

- ### NASA/GSFC specifications

NASA/GSFC S-311-P-829 and -838 specifications (see Table 3.3.) describe requirements for extended range capacitors for space applications. Specification P-829 is related to precious metal and rigid terminal capacitors, whereas P-839 to the BME MLCCs manufactured with flex terminations only.

For some reasons, in both specifications DPA is required before terminations are formed. Considering that most cracks are associated with terminations, this excludes an important, reliability related area of MLCCs and allows inspections to be carried out by manufacturers only.

In spite of different materials and technologies used for PME and BME capacitors and differences in their performance, both specifications have the same requirements for AC and DC characteristics. Requirements for gr.A are also similar, but requirements for gr.B screening differ substantially. In particular, HSSLV testing in P-829 is

replaced by TBH as in MIL-PRF-32535. In addition, similar to MIL-PRF-32535, P-838 has requirements for flex testing and resistance to soldering heat that are absent in P-829.

Table 3.3. NASA/GSFC specification

Requirement	S-311-P-829 rev.J (2017)	S-311-P-838 rev A (2017)
Electrode	PME only	BME only
Voltage range	5V to 100V	16 to 100
Dielectric type	NPO and X7R	X7R
Ultrasonic examination	100% prior to termination (as in M123) or after, at the Mfr. option	Same as P-829
Termination	a) Ag/Pd alloy (type M in M123) b) Ni barrier with Sn/Pb plating (type Z) c) Ni barrier with Au plating (type G)	Flexible, Ni barrier and Sn/Pb plating
Size	0402 to 2225	0402 to 1812
Dielectric thickness	1 mil for 100V, 0.8 mil for 50V, down to 0.25 mil at lower voltages	0.28 mil minimum for VR<50V
Max. dielectric constant	4000 for X7R and 100 for NPO	-
Process Reliability Verification Test (PRVT)	Not required	A special procedure that evaluates acceptance (reliability) of the parts based on the number of grains in a dielectric layer
Dielectric microstructure	Not required	SEM examinations and average grain size measurements (as a part of PRVT)
Insulation resistance	10^{10} ohm or 100 ohm_F at 125C 10^{11} ohm or 1000 ohm_F at 25C	Same as P-829
Dielectric Withstanding Voltage (DWV).	2.5xVR per MIL-STD-202, TM 301	Same as P-829
Dissipation factor	X7R: ≤7.5% for VR ≤ 10V; ≤ 5% at VR=16V, ≤ 4% at 25V, ≤ 3.5% at 50V, and ≤ 2.5% at 100V NPO: ≤ 0.15% for all VR	≤ 5% at VR=16V and 25V, ≤ 2.5% at 50V and 100V
Percent Defective Allowable (PDA).	< 5% after voltage conditioning	< 5% after voltage conditioning and IR measurements at 125C
In-process inspection	DPA (pre-termination) Gr.A inspection includes: -Thermal shock (20 c -55C to +125C) -Voltage conditioning (≥ 168hr at 125C, 2VR; the number of failures detected during the last 48 hours of test < 0.1%, or one piece.) Gr.B inspection includes: B1: TS (100c -55C to +125C) and Life test B2: HSSLV per M123 B3: Voltage Temperature Limits and Moisture resistance test per M123 (for parts larger 0805) No resistance to soldering heat!	DPA (pre-termination) Gr. A is similar to P-829 Gr.B. 45 pcs for d ≥ 0.8 mil and 125 pcs for d < 0.8 mil. B1: – same as P-829 B2: HSSLV testing is replaced with TBH (96hr at VR, 85C, 85% RH) B4: Resistance to soldering heat B5: Shear stress B6: Breakdown voltage test B7: Board flex test

A major element of gr.B inspection in P-838 that makes it different from all other military and space specifications is the Process Reliability Verification Test (PRVT). A theory behind this test is that the ratio of dielectric thickness to the grain size is the most important parameter of BME capacitors that defines their reliability [50]. High reliability capacitors are recommended to be selected based on an empirical criterion:

$$F_t = 1 - \left[1 - \left(\frac{\bar{r}}{d}\right)^{\alpha}\right]^N < 0.00001$$

where F_t is the probability of failure, $\bar{r}$ is the measured average grain size, d is the average dielectric thickness, N is the total number of dielectric layers, α is a constant that is assumed to be 5 for capacitors with rated voltage exceeding 100 V and 6 for capacitors with rated voltage below or equal 100 V.

Multiple studies have shown that the grain size of ceramic materials affects characteristics and reliability of MLCCs. However, other factors, e.g. type and level of doping, the thickness of the shell, homogeneity of grain distribution, and built-in mechanical stresses are a few other factors that have a strong effect on quality and performance of

capacitors. For this reason, selecting MLCCs, and especially calculating their reliability based on the grain size might be misleading. In any case, this criterion is not relevant to the cracking related failures in MLCCs that constitute the majority of the observed failures.

- ## ESA and JAXA specifications

ESA Generic Specification ESCC-3009 (2017) [45] defines general requirements for qualification, procurement, and delivery of types I and II MLCCs for space applications. Specific requirements for the parts are in the detailed specifications available at the ESC web site: https://escies.org/specfamily/view. In general, these requirements are close to those used by NASA, but a substantial deviation exists in the use of ultrasonic inspection and burn-in conditions. ESCC-3009 does not require ultrasonic inspection and requirements for burning-in are limited to 96 hours at 2VR and maximum operation temperature (similar to MIL-PRF-55681) that is determined in the detailed specifications. Somewhat more flexibility compared to the military specifications exists for the operating life test temperature and the range of temperatures during thermal shock testing. Both tests are carried out at temperatures defined in detailed specifications instead of the standard conditions per military specifications: 125 ºC for life testing and from-55 ºC to +125 ºC for thermal shock.

ESA employs different quality assurance systems for ESCC qualified and non-qualified parts. Periodic testing (every 2 years, that is similar to gr.C or qualification testing) is required for qualified components only. The lot validation testing (corresponds to screening gr.B) for these components is not required, but can be requested in the purchase order.

The Japanese system for selection and QA of MLCCs for space applications benefits substantially from the extensive market for automotive components. Giants of MLCC manufacturing (Murata, TDK, et al.) have produced billions of capacitors for automotive industry for more than two decades and have great reputation for high quality and reliability of their products. Automotive grade BME capacitors are used as the base for MLCCs selected for space systems [51]. The selected capacitors are processed by solder dipping to replace pure tin finishing with Sn/Pb solder, ultrasonic inspection, and are up-screened by burn-in within gr.A inspections [52]. Periodically, the parts are verified by the quality conformance inspection (QCI) that in some aspects is more stringent than NASA requirements. Considering that capacitors per QTS-2040 can have dielectric thickness down to 3 µm, life testing is carried out at 1.5VR instead of 2VR that is typical for military standards.

Additional information necessary for better understanding of the test requirements, parts selection, equipment design, assembly and handling is detailed in JAXA-ADS-2040/M105 [47]. Life testing of 123 samples at 125 ºC and 1.5VR for 4000 hours can assure S-level FR (0.001%/1000HR) at room temperature. Voltage acceleration of this testing is assumed to follow 4.5 power law ($n = 4.5$), and temperature accelerates testing by the 10°C rule. To further reduce the risk of degradation and failures during applications, the parts are deratad to 50% of the rated voltage specified by manufacturers, and maximum operation temperature for some part types is limited to the range from -55 °C to +75 °C.

Additional testing to assure reliability of capacitors includes a combination of the thermal shock with the Pressure Cooker Bias Testing (PCBT) [47]. The parts (23 pcs) are mounted onto an FR-4 printed wiring board (PWB) with the thickness of 1.6 mm and subjected to 2000 TS cycles from -55 °C to +125 °C (temperature transition time is less than 5 min.). Following TS, the parts are tested by PCBT at +125 °C, 95%RH, 2 atm pressure, and rated voltage for 144 hours. This test is sensitive to the presence of cracks, but in the presented example, small cracks that were found during visual inspection in one capacitor after TS did not reach internal electrodes and the insulation resistance during PCBT stabilized at more than 1MΩ. This confirms that the reliability of the capacitor was not affected by small cracks.

In addition to a regular TS and humidity testing, an immersion cycling is carried out for special cases. During this testing 18 pcs are subjected to a combination of TS and immersion cycling. Capacitors soldered onto an alumina substrate are stressed by 250 cycles between -55 °C and +125 °C, and then tested per MIL-STD-202 TM104, cond. B: two immersion cycles between a hot (65 °C) and cold (25 °C) baths with salty water (saturated with NaCl). Passing this test gives assurance that the parts soldered onto ceramic substrates will not form cracks and can operated reliably even under severe environmental stresses.

- Automotive industry specifications

Automotive Industry Council, AEC-Q200, specification defines qualification requirements for passive components including MLCCs. It does not call for ultrasonic inspection and HSSLV testing and does not require burning-in and life testing for each lot of capacitors. AEC-Q200 does not describe screening procedures at all, but does not relieve the supplier of any additional requirements needed by the customers. In many cases, parts used in cars are built and tested to SCDs that have detailed specifications for S&Q. For some applications, IR measurements are required at 180 ºC and life testing for the under the hood parts is carried out at 2VR and 150 °C for 2000 hours.

AEC-Q200 describes only the minimum required stress tests and additional testing and analysis working in cooperation with capacitors manufacturers is often used to assure adequate quality parts for cars by using an appropriate mixture of qualification methodologies including step-stress testing, application-specific tests, physics-of-failure approaches, sequential stress tests, etc.

An example showing the difference of Murata requirements for auto (GCM series) and standard (GRM series) MLCCs is shown in Table 3.4 (https://www.murata.com/en-us/support/faqs/products/capacitor/mlcc/char/0004). Note, that MLCCs manufacturers are often trying to demonstrate that their product can exceed the AEC-Q200 requirements (e.g. thermal shock is not required per AEC-Q200), and different manufacturers might demonstrate their compliance to AEC-Q200 in different ways. In addition, AEC-Q200 does not specify acceptable variations of characteristics of the parts after environmental stresses and these requirements are presented in the SCDs.

Table 3.4. Quality requirements for automotive industry and general purpose Murata MLCCs

Test	GCM (AEC-Q200)	GRM (standard)
Temperature cycle	1000 cycles	5 cycles
Thermal shock cycle	300 cycles	-
THB	85 C, 85% RH, VR, 1000hr	40 C, 90% RH, VR, 500 hr
HSSLV	1000 hr	-
High temperature load (life)	1000 hr	1000 hr
Retention at high temperature (storage)	1000 hr	-

Automotive parts are built using more aggressive design rules compared to military MLCCs. Also, automotive industry requirements are more flexible in selecting test conditions compared to the military specifications and allow for some process and materials' changes. For example, IR can be measured at voltages much greater than VR, and the test voltage during the dielectric withstanding voltage (DWV) test can be increased to (6-10)×VR compared to 2.5×VR in military specifications. In some cases, humidity testing is carried out on mounted onto PCBs parts at 85 °C and 85% RH and voltages greater than VR (up to 2 times).

3.2. Qualification procedures and cracking problems in MLCCs

Soldering and post-soldering stresses might generate cracks in MLCCs, and for this reason, reliability of capacitors soldered onto PWBs and loose parts might differ substantially. Majority of MLCCs are used after soldering, so simulation of the assembly conditions should precede any environmental tests, and it is imperative that the QA system for MLCCs would address properly issues related to soldering.

The probability of cracking after soldering depends on the substrate material. For example, due to the differences in CTEs between the ceramic material and substrate, tensile stresses develop in MLCCs (CTE ~ 10 ppm/ºC) after soldering onto alumina boards (CTE ~ 7 ppm/ºC). These stresses were responsible for many observed failures in ceramic chip capacitors mounted on alumina substrates back in 80th [9]. Temperature cycling testing between -55 ºC and +125 ºC showed that proportion of failures is substantially greater for capacitors mounted onto alumina compared to FR4 boards [25]. Contrary to alumina substrates, FR4 or polyimide PWBs have a greater CTE (~17 ppm/ ºC) that should result in increasing compressive stresses in the parts. Considering that the compressive strength of ceramics is more than ten times greater than the tensile strength, the probability of cracking after soldering onto polymer boards should be substantially less compared to ceramic boards.

Although soldering related stresses cannot be ignored in the quality assurance of MLCCs, most military specifications do not address mounting conditions properly. For example, MIL-PRF-123 does not specify mounting before qualification testing and MIL-PRF-55681 allows mounting the parts on a suitable substrate (e.g., 96 percent alumina or FR4 glass epoxy) when specified in the test procedures, but does not have mounting requirements for life or HSSLV testing. MIL-PRF-32535 requires mounting onto an FR4 board before TS and life testing, whereas mounting for humidity testing is optional. GSFC specifications S-311-P-829 and P-838 do not have mounting requirements at all.

Even when mounting conditions are specified, there is typically a warning that "the substrate and mounting process shall be such that it will not be the cause of, nor contribute to, failure of any test for which it may be used." The interpretation of this warning might be that only tests that did not result in failures are valid. Otherwise, the parts might have been abused during soldering. However, it is reasonable to assume that high quality MLCCs should sustain possible deviations from an ideal soldering process and some variations in materials and design of PWBs from those used by MLCCs' manufacturers should not pose reliability risks.

- ### Thermal shock

Most specifications require TS cycling between -55 ºC and +125 ºC, and some between max and min temperatures specified for the part. However, the number of cycles and sample size varies substantially, from 1000 cycles and 77 samples in AEC-Q200 to 5 cycles and 18 pcs in MIL-PRF-55681. This variation might be partially due to the uncertainty in the efficiency of TS testing to reveal lots with excessive proportion of defects.

Although maximum temperature for MLCCs is typically limited to 125 ºC (apparently, to the Curie point), some applications involve higher temperatures. For example, qualification of military hybrid microcircuits require temperature cycling (100 cycles) between -65 ºC and +150 ºC. This means that military grade MLCCs cannot be used in military grade hybrid microcircuits without additional testing.

Changes in environmental temperature cause thermo-mechanical stresses in MLCCs for two reasons. The first is related to the presence of materials with different CTE within the capacitor and between the capacitor and PWB in case of mounted parts. In this case, the effect of temperature cycling depends mostly on the difference between minimal and maximal temperatures (temperature swing). The second reason comes to play when the temperature of the part changes drastically, so there is a substantial temperature gradient across the body of a capacitor. These conditions are defined as thermal shock that per ASTM C-1525 [53] is "a large and rapid temperature change, resulting in large temperature differences within or across a body". If temperature on the surface is greater than in the bulk, expansion of the surface areas of the part will be contained by the colder bulk areas thus resulting in compressive stresses at the surface and tensile stresses in the bulk. These stresses can develop even in homogeneous materials and depend strongly on both, the temperature swing and the rate of temperature variations.

Comparison of three different test conditions that create thermal shock in MLCCs: (i) terminal solder dip test, (ii) ice water test, and (iii) liquid nitrogen drop test showed that the heat conduction and direction of temperature changes (heating or cooling) are critical factors of thermal shock testing of MLCCs [8]. The probability of fracturing depends also on the level of residual mechanical stresses, mostly in terminal areas of ceramic capacitors.

The ice water test (IWT) when preheated to a certain temperature MLCCs are immersed into icy water is a reproducible and effective technique for evaluation of the susceptibility of MLCCs to fracturing during cold thermal shock conditions. Majority of the parts can withstand IWT at 150 °C and the average critical temperature varied from 170 °C to 222°C. In spite of a significant temperature difference that capacitors experienced during the liquid nitrogen drop test (capacitors at room temperature are dropped into liquid nitrogen that has temperature -196 °C), this testing resulted in much less severe cracking compared to the ice-water testing performed at conditions with similar temperature difference. The result is due to a rapid formation of a gaseous N2 film that shields the surface of the capacitors and significantly reduces the heat transfer from the part. This confirms that the heat transfer conditions are of critical importance for TS testing and for the assessment of the thermo-mechanical reliability of ceramic capacitors. Due to compressive stresses developed by the hot thermal shock conditions during manual soldering or terminal solder dip testing, the probability of cracking is much less compared to cold TS. For this reason, normal quality lots of large-size MLCCs (2220) can sustain terminal solder-dip testing at 350 ºC (see section 8.2).

Thermal shock testing that is required per military and space specifications for MLCCs is carried out according to MIL-STD-202, TM107. During this testing the parts are transferred between cold and hot air chambers during up to 5 minutes. Apparently this testing cannot create thermal shock conditions, and a better name for the test would be temperature cycling.

Built-in or residual stresses in MLCCs might affect their reliability [54, 55]. However, these stresses are mostly developed during cooling from high-temperature processes such as sintering (>1000 ºC) or termination firing (~400 ºC), and the range of temperatures during temperature cycling of unmounted parts has a relatively minor effect on the level of these stresses. However, temperature cycling might cause fractures and failures in MLCCs if they are mounted on the board. The probability of these failures depends on the size of capacitors. For example, some types of large size capacitors (size 2220) can pass up to 1000 cycles, but fail after 3000 cycles, whereas smaller size parts have a better stability under this testing. To assure adequate reliability of MLCCs, temperature cycling during qualification tests should be carried out after soldering, the number of cycles should be increased substantially (at least to 300 cycles), and electrical characteristics (at least DWV and IR) should be verified after the testing.

- Life testing

No electrical measurements are currently required after TS testing, and the effect of TS is assumed to be revealed by the life testing that follows TS and is carried out on the same parts. However, the sequential testing does not allow for revealing the origin of defects because they might have been preexisted even before TS. A similar sequence of test is required during screening when TS precedes voltage conditioning. The difference in the screening and qualification procedures is in the number of cycles, duration of biased testing, and most importantly, in the conditions of mounting. Obviously, testing during screening cannot reveal cracks that could have been caused by soldering and temperature cycling of the parts in the mounted conditions.

Requirements to combine TS and life test or voltage conditioning exists in most specifications except MIL-PRF-55681 and ESCC-3009 (however, ESA specification requires also mounting of the parts and 10 TS cycles before HSSLV testing). This, as well as neglecting mounting before qualification testing might be one of the drawbacks in manufacturing of the popular CDR- style capacitors.

As will be discussed in section 5.2, life testing of PME capacitors might reveal capacitors with cracks. However, because only short circuit failures are determined during life testing and BME capacitors with cracks can increase leakage currents but not fail short circuit, the effectiveness of this test to reveal BME MLCCs with cracks is relatively low. In the latter case, variations of leakage currents or IR after life testing might be better indicators of quality of the parts.

- Humidity testing

Moisture sorption in the cracks that cross opposite electrodes in ceramic capacitors reduces insulation resistance and facilitates dendrite growth that might cause short circuit failures. For this reason, humidity testing might be more sensitive to the presence of cracks compared to life test that occurs in dry conditions. Humidity testing in combination with soldering and TS stresses would be more efficient compared to life test. However, not all specifications require mounting, and none, except for ESCC-3009 requires temperature cycling.

Three types of humidity testing are used in different specifications:

- Moisture resistance test per MIL-STD-202, TM106 with exceptions described in MIL-PRF-123. The purpose of this test is evaluation of the resistance of components to the deteriorative effects of high humidity and heat conditions typical of tropical environments. During this test, mounted parts are subjected to 20 cycles between 25 ºC and 65 ºC at 80% to 100% RH (120 hr total at 65 ºC and 100% RH). A 50 V bias is applied during the first 10 cycles only.
- Temperature humidity bias (THB) testing per MIL-PRF-32535 (or AEC-Q200). The parts are tested for 1000 hours at rated voltages, 85 ºC and 85% RH.
- Humidity steady state low voltage (HSSLV) testing. Per MIL-PRF-123 this test is carried out using 12 samples at 85 ºC, 85% RH for 240 hours at a voltage 1.3 ±0.25 V applied through 100 kohm resistors. The post stress measurements of IR should be carried out also at 1.3 ±0.25 V.

Studies of moisture-related failures of first MLCCs (back in late 70th) have shown that the conductive paths that are formed in cracks can be destroyed by application of rated voltages, and for this reason, HSSLV testing had been

developed and even now is often considered as the most effective testing to reveal cracks in capacitors. However, NASA Engineering and Safety Center (NESC) studies in 2009 [56] have demonstrated that this test is not effective for the contemporary MLCCs for the following reasons:

- Historically, low voltage failures (LVF) were attributed to lots with a large proportion of manufacturing defects; however, currently, these failures are more likely to be caused by cracking caused by soldering, handling, and post-soldering environmental stresses. Technological advances in manufacturing processes and controls have produced much more uniform dielectric structure, thickness, and low porosity MLCCs that reduced substantially the probability of cracking during manufacturing.
- No LVFs were identified using HSSLV testing in NASA flight systems for at least the past 15 years and per manufacturers' information the HSSLV testing on military grade MLCCs has generated zero failures during last eight years. The hybrid manufacturers were unaware of any MLCC LVF problems in their products.
- Statistical analysis shows that at the confidence level of 60%, zero failures out of 12 samples that are currently required for testing can assure that the proportion of defective parts in the lot is less than ~ 10% only.

Comparative analysis of cracking related failures in PME and BME capacitors has shown that HSSLV testing can reveal PME capacitors with introduced cracks, but is not effective for BME technology [34]. For this reason, HSSLV testing has been replaced in MIL-PRF-32535 with THB that had been shown to be more effective for BME capacitors.

It is important to note, that reduced IR or short circuit failures during humidity testing of mounted capacitors might be caused by external conductive paths (e.g., metal dendrite formation) resulting from surface contaminations and formed either on the surface of capacitors [57] or on the surface of PWB as shown in Fig.3.1. A thorough failure analysis is required to confirm that the observed failures are actually caused by cracking in capacitors.

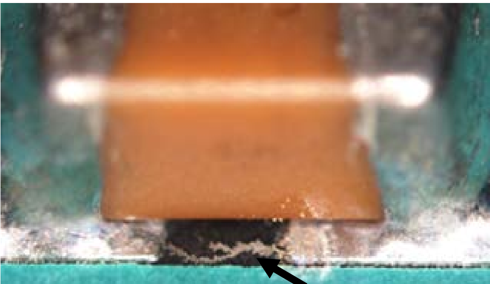

Figure 3.1. External Metal Dendrite on PWB beneath the MLCC that resulted in false short circuit failure.

- ### Resistance to soldering heat

A qualification test that supposed to verify the robustness of MLCCs against soldering stresses and simulate the worst case soldering thermal shock conditions is the Resistance to Soldering Heat (RSH) testing that in all specifications is carried out per MIL-STD-202, TM210. Recommended test conditions per this method are displayed in Table 3.4 and show that for most conditions the test temperatures are relatively benign and close to soldering temperatures that are described in manufacturers' and users' guidelines for soldering of MLCCs. Note also that extensive experience of using lead-free solder by commercial industry showed that chip ceramic capacitors are capable to withstand high-temperature solder reflow processes up to 260 ºC, that exceeds test conditions that are currently used in military specifications.

It is generally acknowledged [58, 59] that wave soldering causes the most severe thermal shock stress for ceramic capacitors. The effect is due to a high heat transfer rate when liquid metal comes into contact with MLCCs. These stresses might create visible cracks on the surface and sides of capacitors that start at or near the termination. Vapor phase reflow soldering uses the latent heat of vaporization of the condensing vapor as the heat transfer method and have a lesser effect compare to wave soldering. Infrared reflow soldering is also less stressful because of a low heat transfer by air convection and radiation, and normally does not result in thermal shock failures.

Manufacturers are often using wave soldering test without preheating to assess quality of their production. The maximum temperature during this test is 280° C for automotive industry capacitors and 235° C for military capacitors. However, the wave soldering test is not required in military specifications for MLCCs.

Table 3.4. Test conditions for the “Resistance to soldering heat” test per MIL-STD-202, TM210.

Solder technique simulation	Test cond.	T (°C)	Time (s)	Temp. ramp	Heat cycles	Typical soldering conditions	Comments
Solder iron	A	350 ±10	4 - 5	-	1	270C - 300C/ 5s	Not used for MLCCs
Solder Dip	B	260 ±5	10 ±1	25 ±6 mm/s	1	Resoldering or finishing replacement at T = 260C	Used for leaded parts and for caps per M123 (at T=230C) and JAXA
Wave: Topside	C	260 ±5	20 ±1		1	260C	Not used in the specifications
Wave: Bottomside	D	260 ±5	10 ±1	Preheat 1-4°C/s to within 100°C of solder temp. 25 mm/s ± 6 mm/s	1	260C	Used by AEC-Q200 w/o preheating.
Vapor phase reflow	H	215 ±5 (vapor temp)	60 ±5		1	215C	Not used in the specifications.
IR/convection reflow	I	215 ±5 (component temp)	30 ±5	1-4°C/s; 90-120s above 183°C	3	220-230C/10s for Sn/Pb solder. 250-260C/10s for Pb-free.	Not used in the specifications
	J	235 ±5 (component temp)	30 ±5	1-4°C/s; 90-120s above 183°C	3		Relaxed cond. J is used for chip cap per M55681
	K	250 ±5 (component temp)	30 ±5	1-4°C/s; 90-120s above 183°C	3		Not used in the specifications

Solder dip test for the same reason as soldering wave test creates severe TS conditions for chip capacitors and is the test that simulates manual soldering conditions more closely. According to Rawal and co-authors [60] different lots of MLCCs manufactured in 1980th had different resistance to this type of thermal shock testing (solder dip at 260 ºC) resulting in up to 74% of failures in some lots and no failures in others. However, the test temperature is reduced substantially in MIL-PRF-123 (to 230 ºC). Also, the test have a risk of damaging parts by tweezers that create unknown pressure and additional temperature gradients across the capacitor.

During solder dip, a ceramic capacitor experiences a hot thermal shock with an instant temperature increase that results in large transient compressive stresses at the surface and relatively small tensile stresses in the bulk of the specimen. Although this test provides good heat transfer conditions and results in formation of significant thermo-mechanical stresses, the probability of fracture and crack formation is relatively low. This is mostly due to a high compressive strength of ceramic materials that is typically in the range from 1 GPa to 4 GPa and is approximately an order of magnitude greater than the tensile strength [19]. This explains a substantial increase of the critical temperature during TSD testing over the data reported in literature [61, 62]. In the referred studies the critical temperatures were measured during cold thermal shock testing that creates tensile stresses at the surface, and hence requires much smaller temperature gradients to cause fracture. The critical temperature for the hot TS (ΔT ~350 $^{\circ}$C) is approximately two times greater than for the cold TS (~150 $^{\circ}$C) and is not proportional to the difference in compressive and tensile strength of ceramics. This can be explained considering that the probability of fracturing depends not only on the level of the temperature gradient and TS stresses, but also on the level of the built-in mechanical stresses that can vary from lot to lot due to variations in manufacturing processes.

Resistance to soldering heat test using soldering iron is described in MIL-STD-202 TM 210, condition A. The testing should be performed at a temperature of the soldering iron of 350 °C ±10 °C by contacting a solder pad with installed component for 4 to 5 seconds. Although this test simulated rather closely actual manual soldering conditions, for some reasons it is not used in specifications for space level MLCCs or by manufacturers of the parts.

Analysis of requirements to RSH testing described in military and space specifications allows for the following conclusions.

- In all specifications except AEC-Q200 the requirements for RSH testing are relaxed even compared to the conditions described in MIL-STD-202 TM210. For example, MIL-PRF-55681 and 32535 require only one reflow simulation cycle instead of 3 cycles per MIL-STD-202; solder temperature for dip testing in MIL-PRF-123 is reduced from 260 ˚C to 230 ˚C, whereas majority of commercial components are reflow soldered at temperatures exceeding 245 ºC. Considering that the requirements of MIL-STD-202 are close to the conditions recommended for soldering, the level of stress provided by RSH testing is not sufficient to reveal potentially weak lots.
- NASA/GSFC specification P-829 does not require RSH, but P-838 calls for 6(0) samples to be tested using solder dip testing (similar to MIL-PRF-32535) as a part of gr.B screening. Considering that PME capacitors might be more susceptible to cracking failures compared to BME parts, RSH testing should be included in the S-311-P-829 specification.
- From 9 to 22 samples are used for RSH testing (AEC-Q200 requires 30 samples). In some cases, one sample can fail and the lot will be still considered acceptable for high-reliability applications. Considering that the parts are tested at typical soldering conditions, the reason for allowing from 5% to 15% of capacitors fail the test is difficult to comprehend.
- None of the specifications requires the soldering iron test (cond. A per MIL-STD-202, TM210). Taking into account a wide use of manual soldering during assembly of space units and boards, this is a substantial drawback of the existing qualification system. Large size chip capacitors that are to be manually soldered should be first tested for the robustness against soldering stress conditions. A modified solder dip test that can be used for this purpose is described in section 8.2.

Flex testing

One of the major causes of MLCCs' cracking is deformations of the board that transmits stress to the chip through soldered terminals. This deformation can be caused by variety of reasons including:

- Thermo-mechanical stresses in the populated board during post-soldering cooling.
- Depenalization of the individual cards from the master panel.
- Attachment of components (e.g. insertion or removal of connectors, outlets, pins, etc.)
- Attachment of the board to the case.
- Vibration or mechanical shock. Note that vibration induced deformations and the risk of cracking increase substantially at the resonance frequencies.
- CTE mismatch between board material and soldered components during temperature cycling.

KEMET studies [63] have shown that increasing deflection of the board almost exponentially increases the probability of cracking. For example, bending of 1206 size capacitors on an FR4 board with 1.6 mm thickness at a span of 90 mm to 1.84 mm deflection has generated ~ 0.01% of failures, but increasing deflection raised the probability of failures to 0.1%, 1%, and 10% respectively at 2.2 mm, 2.25 mm and 2.56 mm of deflection.

Typically, flex cracks originate from the terminal ends at the bottom of the capacitor and have a diagonal direction inside the part usually at an angle of approximately 45º (see Fig. 2.8.b). In case of excessive amount of solder, the K-shaped cracks can also develop due to formation of tensile stresses at the top of capacitors [64].

The flex testing first had been developed to reduce cracking during de-panelization in commercial applications. Currently, this test is required for MLCCs by military and space specifications except for MIL-PRF-123, ESCC-3009, and S-311-P-829. Note, that NASA/GSFC P-838 specification requires flex testing within gr.B of the screening tests.

According to AEC-Q200-005 and MIL-PRF-32535, this test is carried out using a specified size FR4 board with a capacitor soldered in the middle of the board. The board is bent as shown in Fig. 3.2a to a certain deflection (typically 2 mm). AEC-Q200-005 defines failure as a condition when a part cracks that can be determined, for example, by acoustic emission, or by changes in the parameters being monitored. The MIL-PRF-32535 requirement is more specific and determines failure as capacitance change by more than 10% at a deflection ≥ 2 mm. However, KEMET studies have shown that 2% of capacitance variations might provide a better resolution for revealing the initiation of the cracks [10].

Figures 3.2.c, d show capacitance variations during flex testing of small size (0603) PME and BME MLCCs. Note, that variations of capacitance developing cracks during loading are reversible and electrodes separated during the bending rejoin when the strain is removed. This means that capacitance in parts with cracks can remain within the specified limits, and in general, capacitance measurements are not effective for revealing cracks. Degradation of capacitance by steps (Fig. 3.2c and d) indicates partial separation of electrodes during bending that is consistent with the results of cross-sectioning (Fig.3.2b).

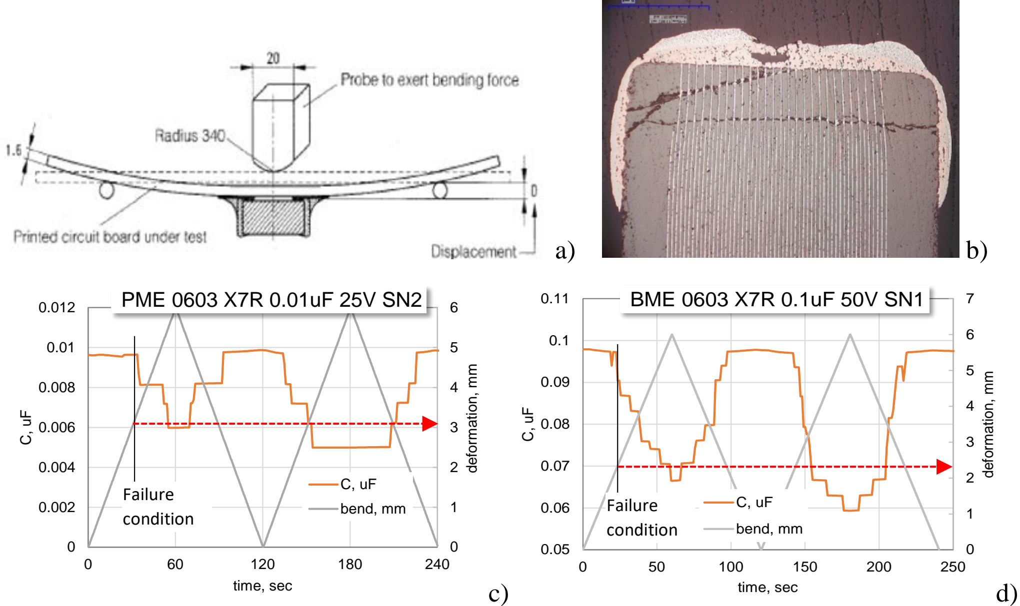

Figure 3.2. Schematic of the flex testing (a), cross-sectioning of a capacitor failed flex testing (b), and variations of capacitance and deflection with time for a PME (c) and BME (d) capacitors.

Multiple studies of the flex cracking showed that in addition to the quality of MLCC itself, variety of other factors might affect test results [32, 63, 65-68]. These factors include:

- Orientation of the component on the board.
- Type of attachment, e.g. mounting with Ag-epoxy or soft terminations in the parts absorbs stress and reduces cracking.
- The height and thickness of the solder fillet, and presence of solder under the chip.
- The type of solder. According to some research [66] less cracking was observed when Pb-free alloys are used because high-temperature soldering process creates a higher compressive stresses in MLCCs after cooling. However, Adam [69] reported that because Pb-free solders are quite rigid, cracks are generally more likely during bending of the boards when Pb-free solders are used.
- Ceramic material (X7R capacitors are weaker compared to COG capacitors).
- The size of the chip (larger chips experience greater stress and have greater susceptibility to cracking).

All researches indicate the effect of the chip size on results of flex cracking, so some application engineers utilize a rule of thumb that prohibits using MLCCs with a size of 1210 or larger. A strong size dependence of the probability of cracking failures means that commercial BME capacitors that have a smaller size compared to similar value military grade PME parts are less vulnerable to flex cracking. Application of parts with flex terminations manufactured by BME technology might reduce failures related to flex cracking substantially.

- ### Sample size

Qualification tests in military and space specifications are carried out using a relatively small sample size, typically from 6 to 22 pcs, and often require zero failures for the test to pass. However, statistical analysis (e.g. using a Fisher exact test) shows that when such a small number of samples is used, there is no significant difference between groups with zero and a few failed samples.

If we want to assure that the proportion of defective samples in a lot (e.g. samples with cracks that can be revealed by humidity testing) is below a certain value, P_f, the number of samples that has to be tested with a zero failure result (N) can be calculated as:

$$N(P_f) = \frac{\ln(1-c.l.)}{\ln(1-P_f)} \approx -\frac{\ln(1-c.l.)}{P_f} \quad ,$$

where *c.l.* is the confidence level.

At P_f = 0.1% and *c.l.* = 60% calculations yield $N \approx 1000$, which exceeds substantially a typical sample size for qualification testing. However, when multiple lots of components manufactured to military specifications passed the testing, then, considering consistency in manufacturing conditions and materials used, the significance of the testing is different. For example, if a dozen of lots passed HSSLV testing with 12(0) results, but one lot had one failure, 12(1), the latter can be considered as different at the confidence level of 90%.

This means that using a relatively small sample size for qualification testing might be sufficient for mature technologies with known consistent and successful results of testing. However, positive results of qualification testing per military specifications for a new technology or a commercial device does not give the required confidence and might be misleading.

4. Characteristics of MLCCs

Specifications for low-voltage MLCCs have only three electrical characteristics: capacitance (C), dissipation factor (DF) and insulation resistance (IR). Measurements of breakdown voltages (VBR) and mechanical characteristics are not required. However, VBR might be sensitive to the presence of cracks and mechanical characteristics might be used to assess the robustness of the parts to cracking. For these reasons, these tests are also described below.

- Rated voltage

The rated voltage (VR) is an important parameter of MLCCs that determines conditions of measurements and affects AC and DC characteristics of the parts and their reliability. It is often assumed that VR is limited by breakdown voltages in capacitors. However, it is not true for low-voltage ceramic capacitors because VBR exceeds rated voltages by dozens and hundreds times. Contrary to tantalum capacitors, this allows for highly accelerated testing of MLCCs at voltages exceeding VR many times and allowing for a substantial reduction of times to failure (orders of magnitude) compared to application conditions. However, high acceleration might increase risks of introducing new failure mechanisms and cause errors in the reliability prediction.

The rated voltage is selected from a set of standardized values that are changing with increasing increments. This is one of the reasons why VR is not directly related to physical properties of low-voltage MLCCs, cannot be measured, and might be skewed by the marketing trends.

Class II dielectrics have a strong dependence of the dielectric constant on the electric field that results in substantial variations of capacitance with applied voltage. This dependence, rather than VBR, is one of the most important factors limiting VR. Another important factor is that the probability of failures in MLCCs increases sharply with operating voltage. This factor is more important for military or space grade parts that should withstand life testing at 2VR and 125 ºC for 4,000 and even 10,000 hours, whereas commercial parts are typically life tested for not more than 1000 hours.

The rated voltage is a technical parameter chosen by manufacturers based on their experience and internal rules so that voltage dependent characteristics and reliability of the part remained within the specified limits.

4.1. Capacitance and dissipation factor

According to specifications, measurements of dissipation factors and capacitance for majority of MLCCs (capacitors in the range from 100 pF to 10 µF) should be made at room temperature, 1 kHz and 1Vrms of the AC signal. However, the values of C and DF for class II dielectrics are changing substantially with temperature, DC voltage, frequency and the amplitude of the AC signal. Note, that voltage and temperature stability of capacitance is required only for military BR or BX type capacitors, whereas military X7R and X7S capacitors are tested to temperature stability only.

The limit for DF might be several times greater than the actual values, whereas capacitance should remain within the specified tolerance. Considering that application conditions might vary substantially from conditions used for AC measurements, the specified parameters for MLCCs are rarely sufficient for electronic designers to make an informed choice.

Typical variations of DF for 10 μF 10 V capacitors manufactured by Murata with the level of stress during measurements are shown in Fig.4.1 [70]. Note that DF decreases with bias and temperature, but increases with frequency and AC signal. Values of DF are also increasing for thin dielectric capacitors, for example, capacitors with *d* ~ 2 to 4 μm typically have DF ~ 4%, whereas for *d* ~ 15 to 25 μm DF is in the range from 1 to 2%. AC characteristics of class II dielectric MLCCs might be affected by the prehistory of the parts, e.g. duration of the shelf life or exposure to high voltages (e.g., DWV testing). For this reason, deaging (e.g. 2 to 5 hours at 150 ºC) is recommended before measurements.

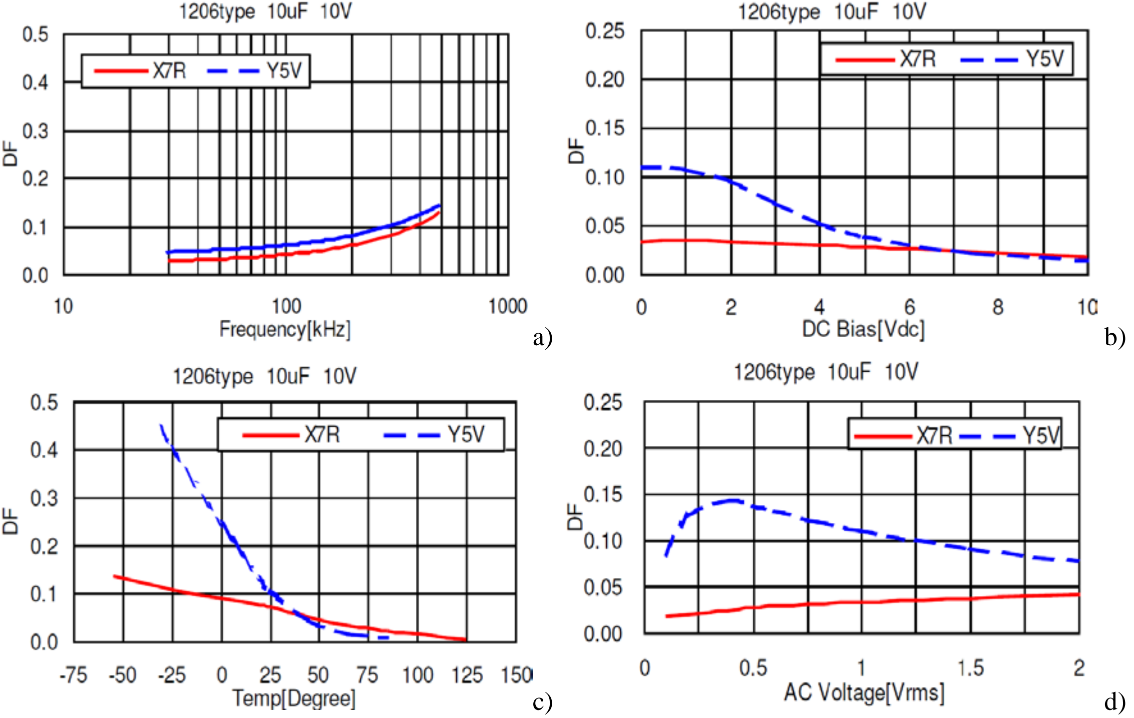

Figure 4.1. Variations of dissipation factor in 10 μF 10 V X7R and Y5V MLCCs with frequency (a), DC bias (b), temperature (c), and AC voltage (d) [70].

Dissipation factor determines the level of power dissipated in the part, $P = 2\pi fCV_{rms}^2DF$, that results in self-heating. In pulse application the self-heating can cause temperature cycling that might eventually result in cracking and failures. For example, a 1 μF 0402 size capacitor operating at 1 MHz at DF ~ 5% and V_{rms} =0.1 V would dissipate ~0.0031 W that might cause overheating by approximately 20 ºC.

Although military and space documents do not require limiting the maximum dissipated power, this factor might be critical for signal filtering applications in contemporary low voltage microcircuits operating at high frequencies. Typical values of the power rating determined by Johansen Dielectrics, JDI, [71] for various size commercial MLCCs are shown in Table 4.1. The rating is based on 25 ºC temperature rise for standard mounting conditions. For military and space specifications, it would be reasonable to set the maximum dissipated power and describe procedure for its measurements. During applications, the power should be derated to 75% of the maximum specified value.

Table 4.1 Typical power ratings for MLCCs

JDI Size	EIA Size	Rated Power, Watts
R07	0402	.005 W
R14	0603	.02 W
R15	0805	.04 W
R18	1206	.08 W
S41	1210	0.2 W
S43	1812	0.4 W
H42	1515	0.4 W
H47	2520	0.9 W
H51	3530	1.5 W
H62	4540	2.1 W
H66	5550	2.8 W
H70	6560	3.8 W

To assess the effect of cracking on AC characteristics, several types of PME and BME capacitors have been damaged either by cutting off corners of the parts (fractured capacitors) or by pressing the surface with a Vickers indenter (damaged capacitors). Figure 4.2 displays correlation of characteristics measured before and after the cracking.

Results show that cracking does not affect capacitance, which is consistent with the results of flex testing when in many cases capacitance recovers when the stress is removed. Dissipation factor shows some sensitivity and increases after cracking by 10 to 50%, but remains within the specified limits. Apparently, capacitance is not a useful characteristic to reveal the presence of cracks, and in some cases, increasing DF might be related to cracking. However, DF variations might be not related to the crack formation, but rather to mechanical stresses or acoustic waves associated with the cracking process [72]. Hitting the capacitors without introducing cracks increased DF by 20% to 30% initially, but DF gradually decreased with time and stabilized at the initial level after dozens and hundreds hours of storage.

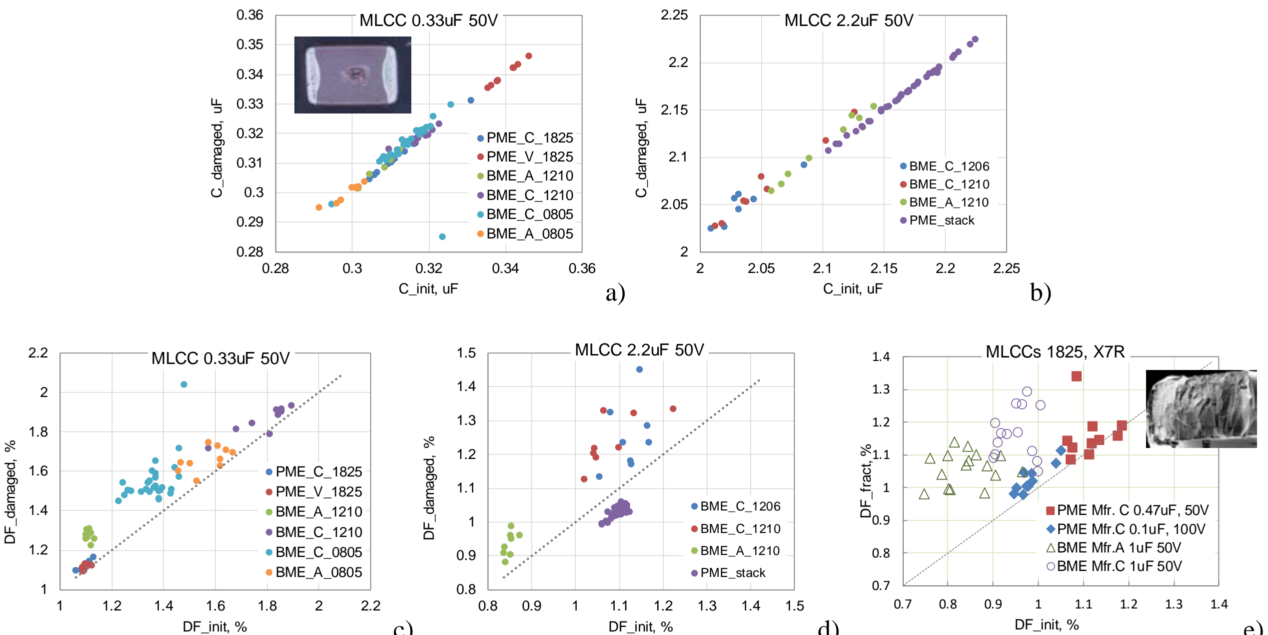

Figure 4.2. Effect of cracking on capacitance (a, b) and dissipation factors (c-e) of different types of MLCCs.

4.2. Insulation resistance and leakage currents

Leakage currents in MLCCs similar to other types of capacitors depend on the applied voltage and are decreasing with time under bias. For this reason, IR measurements are specified after 2 min of electrification at the rated voltage. However, if IR meets the specified limit, and is steady or increasing with time, the test may be terminated before the end of the specified period. Typically, manufacturers are testing IR within a few seconds using a go/no go test, so actual values of IR are rarely measured.

Manufacturers of commercial MLCCs or capacitors for automotive industry often use so-called flash IR measurements instead of regular measurements that require testing at VR. Voltage during flash testing might be up to 10 times greater than the rated voltage. Although these measurements formally deviate from the military specifications, it might be an effective means for quality assurance because IR at high voltages should be less than at VR, and passing the limit at higher voltages gives more confidence in quality of the parts.

Cracks in MLCCs increase leakage currents and might reduce IR, which makes it a characteristic potentially sensitive to the presence of cracks. To understand factors that affect the sensitivity of IR measurements to cracking, we need to understand the nature of leakage currents in MLCCs and their relation to the existing requirements for IR.

- Specified IR values

Although in many cases, and in particular when capacitors are used for filtering or decoupling in high frequency applications, circuit designers would be satisfied with IR values in the megohm range, the specifications typically require gigaohm values of IR (see Table 4.2). This means that the existing requirements for IR are driven by the quality assurance reasons, rather than by the needs of applications, so the requirements for high IR during screening are likely used to confirm that capacitors are defect-free.

IR requirements in all specifications except for JAXA QTS-2040M are similar to MIL-PRF-123: 100,000 megohms or 1,000 megohm-microfarads, whichever is less at 25 ºC. In most applications, the same IR requirements are applied to PME and BME capacitors. However, JAXA specifications for the thin dielectric BME MLCCs allows for 10 times lesser IR values.

Experience shows that high volumetric efficiency BME capacitors might have relatively low IR at high temperatures but excellent long-term reliability. Relatively high leakage currents in BME compared to PME capacitors reflect a different nature of materials used and are not directly related to the quality and reliability of the parts. Due to a higher intrinsic conductivity of BME compared to PME capacitors, IR requirements for commercial BME parts are typically ten times less stringent than for PME capacitors. Requirements of MIL-PRF-55325 to have the same IR values for BME and PME MLCCs, forces manufacturers of BME capacitors to have increased thickness of the dielectric and produce capacitors of a larger size that are more vulnerable to cracking.

Table 4.2. Requirements for IR in different specifications

<table>
<tr><th>Temp</th><th>VR</th><th>MIL-PRF-123, T</th><th>MIL-PRF-55681</th><th>MIL-PRF-32535</th><th>S-311-P-829</th><th>S-311-P-838</th><th>ESA ESCC #3009</th><th>JAXA QTS-2040/M</th></tr>
<tr><td>25C</td><td>≥25V</td><td>100 GΩ or 1000 Ω×F</td><td>100 GΩ or 1000 Ω×F</td><td>100 GΩ or 1000 Ω×F</td><td rowspan="2">100 GΩ or 1000 Ω×F</td><td rowspan="2">100 GΩ or 1000 Ω×F</td><td rowspan="2">Typical 1000 Ω×F</td><td>NA</td></tr>
<tr><td>25C</td><td><25V</td><td>NA</td><td>100 GΩ or 500 Ω×F</td><td>100 GΩ or 500 Ω×F</td><td>100 Ω×F</td></tr>
<tr><td>125C</td><td>≥25V</td><td>10 GΩ or 100 Ω×F</td><td>10 GΩ or 100 Ω×F</td><td>10 GΩ or 100 Ω×F</td><td rowspan="2">10 GΩ or 100 Ω×F</td><td rowspan="2">10 GΩ or 100 Ω×F</td><td rowspan="2">Typical 100 Ω×F</td><td>NA</td></tr>
<tr><td>125C</td><td><25V</td><td>NA</td><td>10 GΩ or 50 Ω×F</td><td>10 GΩ or 50 Ω×F</td><td>10 Ω×F</td></tr>
</table>

Increasing temperatures to 125 ºC reduces the specified IR values by 10 times, which corresponds to an effective activation energy of 0.23 eV. This value is substantially less that the activation energy for intrinsic leakage currents in MLCCs. The discrepancy is due to absorption currents that are typically prevailing in capacitors within minutes after voltage application.

Unfortunately, users have a limited information about actual IR values and their distributions, so the margin between the real values and the limit are rarely known. Without this information, it is difficult to assess the effectiveness of IR limits for quality assurance, and selection of the criteria in military and space specifications are often based on the "engineering practice", "historic data", and similar specifications rather than on statistical analysis of the test results. For the same reason, the necessity of two times relaxation of IR requirements for capacitors with VR < 25 V in MIL-PRF-55681 and MIL-PRF-32535 that might or might not have thinner dielectrics compared to 50 V capacitors is difficult to assess.

Experiments show that military requirements for IR at 125 ºC provide sufficient margin between actual values and the limit for PME (1 to 2 orders of magnitude) but might be not adequate for BME capacitors. To meet IR requirements, manufacturers have to increase the thickness of the dielectric for BME capacitors thus increasing the size of the parts and increasing risks of cracking.

- Absorption and intrinsic leakage currents

Dielectric absorption processes that result in transient leakage currents include dipole orientation, redistribution of ionic charges, or charge injection from electrodes into the traps in the dielectric. Currents caused by absorption, I_{abs}, decrease with time after a step voltage application and follow the empirical Curie - von Schweidler law, according to which the currents decrease with time as a power function, $I_{abs}(t) = I_0 \times t^{-n}$, where I_0 and n are constants, and n is close to 1. Similar absolute values, but different polarity transient currents flow through capacitors under applied voltage (polarization process) and under short circuit conditions (depolarization process). Intrinsic leakage currents, I_{il}, in MLCCs are attributed to electron injection from metal electrodes ito conduction band of the dielectric and can be described by the modified Schottky model [73].

In a general case, leakage currents in a capacitor can be presented as a sum of charging, absorption, intrinsic, and defect-related leakage currents:

$$I(t,T,V) = I_{ch}(t,V) + I_{abs}(t,T,V) + I_{il}(T,V) + I_{dl}(T,V,RH)$$

Charging currents, I_{ch}, correspond to currents in an ideal capacitor without losses, depend on the applied voltage, are limited mostly by the external circuit (power supply or limiting resistance), and might prevail at times below ~ 1 sec (see Fig. 4.3). Absorption currents depend strongly on time under bias and applied voltage. Intrinsic currents, $I_{il}(T,V)$, do not vary with time, increase exponentially with temperature and super-linearly with voltage. Defect- or crack-related leakage currents, $I_{dl}(T, V, RH)$, depend also on the relative humidity of the environment.

Figure 4.3 illustrates typical time variations of leakage currents in MLCCs at different voltages and temperatures. Absorption currents prevail at room temperatures, have a poor temperature dependence, and vary mostly with the value of capacitance. In high-capacitance MLCCs I_{abs} are large, and can mask the presence of cracks. Intrinsic leakage currents prevail at high temperatures and/or high voltages that are typically exceed VR.

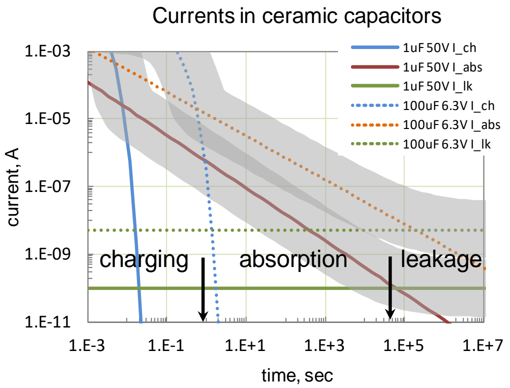

a) Currents in high-value MLCCs after voltage application. Gray area shows a typical range of current variations.

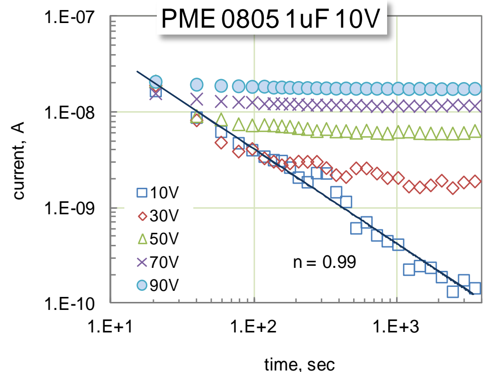

b) Absorption currents at RT and VR prevail during 1 hour of electrification, and increasing voltages increase currents exponentially.

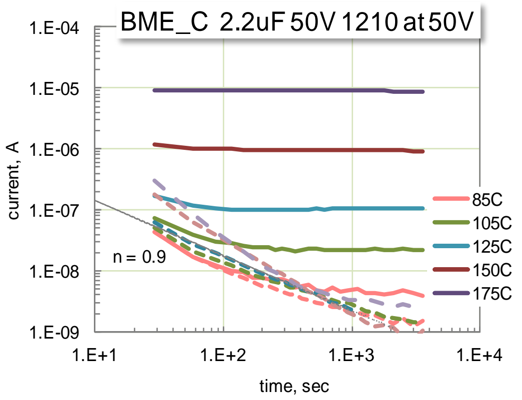

c) Dashed lines indicate depolarization, solid lines - polarization currents. Increasing T rises intrinsic currents exponentially and does not affect depolarization currents.

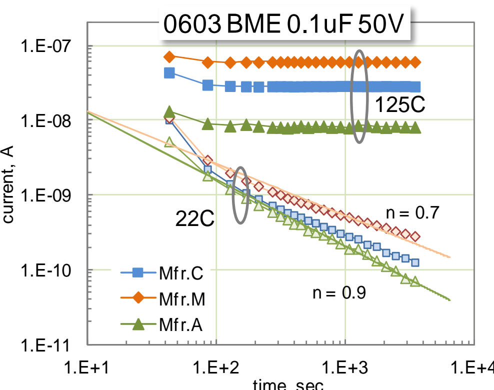

d) Same value capacitors from different vendors have similar absorption currents (at 22 ºC), but different intrinsic leakage currents (at 125 ºC)

Figure 4.3. Relaxation of leakage currents in MLCCs.

A linear increase of absorption currents with voltage at voltages close or below VR, allows for characterization of capacitors by a resistance that does not change substantially with voltage. However, at increasing voltages, above 2 to 3 times VR, absorption currents are saturating but intrinsic currents are rising exponentially thus resulting in a substantial decreasing of IR. Voltage dependence of leakage currents associated with cracks is likely less significant compared to the intrinsic leakage currents, so increasing voltages might not increase the sensitivity of IR measurements to the presence of cracks. Fig. 4.4.a presents an example of the current relaxation in a normal and in a capacitor with cracks. The difference can be observed only after ~ 100 seconds of polarization. This makes the presence of the defect undetectable by regular IR measurements.

An equivalent circuit of a capacitor that accounts for dielectric absorption, intrinsic, and defect-related leakage currents is presented in Fig. 4.4.b. The capacitor has a nominal value, C_0. Resistor R_{il} represents intrinsic leakage currents, and R_d is related to cracking.

Dow [74] has proposed a model for absorption polarization processes that presents a capacitor by a circuit with five r-C_t relaxators connected in parallel to C_0. The relaxation process can be simulated by a proper selection of the relaxation times, $\tau_i = r_i \times C_{ti}$, and absorption capacitances, C_{ti}. In this model, variations of the absorption currents with time after application of a step voltage, V_0, can be described by a simple equation:

$$I(t,V)_{abs} = \sum_i \frac{V_0}{r_i} exp\left(-t/_{\tau_i}\right)$$

Calculations based on modeling of absorption processes show that the IR values measured after ~ 100 sec corresponds to an effective absorption resistance that can be estimated as [73]:

$$IR = r > \frac{100 \times 10^6}{0.25 \times C_0} = \frac{4 \times 10^8}{C_0},$$

where, C_0 is in µF and r is in Ω. This corresponds to the absorption resistance: $R_{abs} \times C_0 > 400$ Ω×F, which is 4 times greater than the typical requirements for IR (IR×$C_0 > 100$ Ω×F) and provide ~ 40 times margin to the actual IR values.

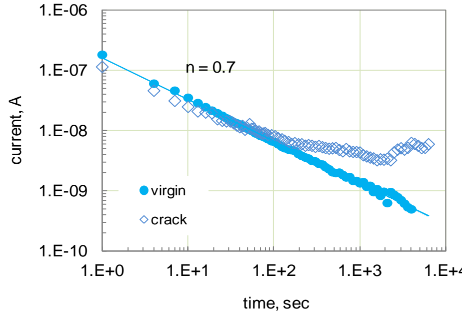

a) Relaxation of currents in a normal and fractured case size 0805, 3.3 μF, 6.3 V capacitors at RT and VR.

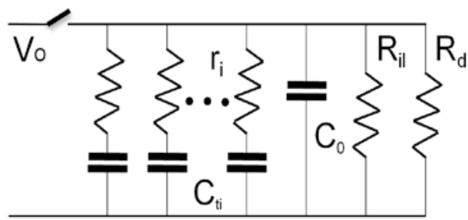

b) Equivalent circuit of a capacitor C_0 having intrinsic leakage current (represented by R_{il}) with absorption (elements r_i, C_{ti}) and defect (R_d).

Figure 4.4. Effect of cracking on relaxation of leakage currents (a), and an equivalent circuit of a capacitor with cracks (b).

The intrinsic current density through a dielectric layer is controlled by electron injection over a metal/dielectric barrier and can be described using the Schottky/Simmons model:

$$I(T,V)_{il} = AT^{1.5}\mu\, E\, exp\left(\frac{-\Phi_B}{\mathrm{kT}}\right)\, exp\left(\frac{\beta_s E^{0.5}}{kT}\right)$$

where A is a constant, μ is the mobility of electrons in the dielectric, E is the electric field in the dielectric, Φ_B is the barrier height at the metal/ceramic interface, $\beta_s = 2.7\times10^{-24}$ C× (m×V)$^{0.5}$ is the Schottky constant, k is the Boltzmann constant, T is the absolute temperature.

Experiments show that activation energy of the intrinsic leakage currents, $E_a = \Phi_B - b_s E^{0.5}$, at rated voltages is 1.19 ±0.14 eV for PME and somewhat less, 0.83 ±0.13 eV, for BME capacitors, which explains a higher leakage currents in BME parts [75].

Manufacturers' data on temperature dependence of IR, in the range from room temperature to 125°C and the requirements in military specifications, indicate much lower values of the activation energies, from 0.23 eV to 0.32 eV. This is due to the different nature of currents measured at room temperature and 125 °C. Absorption currents that have weak temperature dependence prevail at relatively low temperatures close to room temperature, whereas intrinsic leakage currents that have high activation energy prevail in the high temperature range.

- ## Effect of cracking on IR

Close correlation between IR values in 15 different types of virgin and fractured capacitors at room temperature (Fig. 4.5a) shows that that IR measurements during screening at room temperature might not detect fractured capacitors. Apparently, absorption currents that control IR are much greater than currents associated with tiny cracks. It is often assumed that IR measurements at high temperatures (125 °C) are more sensitive to the presence of defects, and thus are more effective in evaluating quality of capacitors. However, results of high-temperature measurements for 9 types of fractured and virgin MLCCs (Fig. 4.5b) also failed in revealing cracks. Obviously, this is due to a high level of intrinsic leakage currents that apparently exceeds the currents associated with the presence of cracks.

Considering a relatively large margin between the specified and actual IR values, the sensitivity of IR testing for revealing cracks is further reduced when actual IR values are not recorded and instead the compliance with the specifications is verified by the go-no go method.

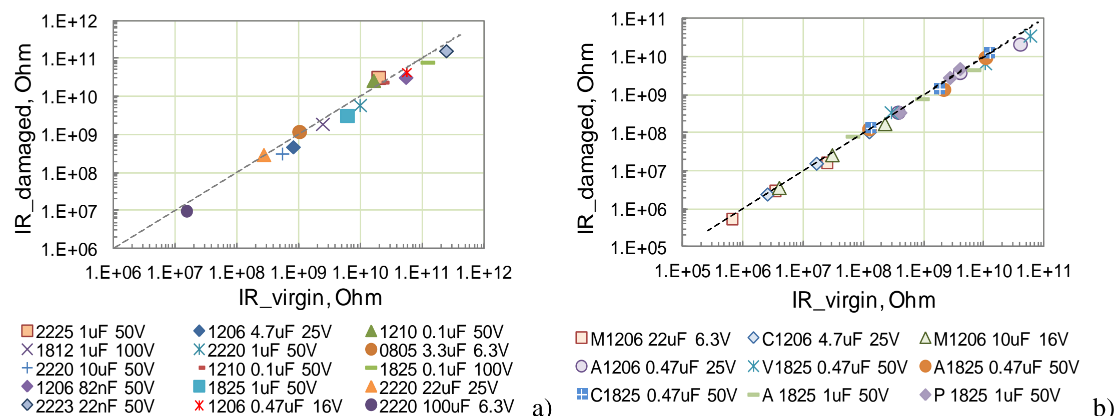

Fig. 4.5. Effect of cracking on insulation resistance in different types of ceramic capacitors. The IR measurements were carried out using a standard technique: 120 seconds of electrification at rated voltages. The dashed line corresponds to no-change values. (a) Room temperature measurements. (b) Measurements at 85 °C, 125 °C, and 165 °C.

4.3. Breakdown voltage

Breakdown voltage (VBR) is an important characteristic of ceramic capacitors that is sensitive to the presence of structural defects. Distributions of VBR can be used to assess the proportion of defective parts in a lot and evaluate quality of the product [76]. In many cases, distributions of VBR values for BME capacitors are bimodal (see Fig.4.6). For such distributions the intercept point indicates the proportion of parts with defects, and the spread of VBR towards low voltages indicates the significance of defects (more significant defects result in a more substantial reduction of VBR).

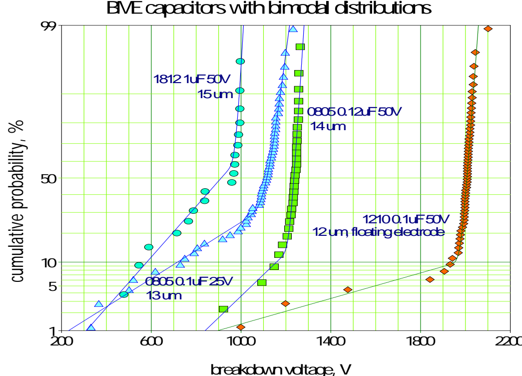

Figure 4.6. Examples of distributions of VBR for different types of BME MLCCs rated to 25 and 50 V.

Breakdown fields (E_{BR}) in ceramic capacitors increase substantially with decreasing of the thickness of the dielectric (Fig. 4.7a). Considering that the breakdown has a thermal nature, decreasing E_{BR} with increasing d is likely related to better thermal conditions for thinner dielectric layers. It is also possible that thin dielectrics have a reduced number of flaws that are responsible for breakdown.

Breakdown voltages in low-voltage MLCCs are several to more than a hundred times greater than the rated voltage, and there is a trend of decreasing the safety margin (defined as a ratio of V_{BR} to VR) with the rated voltage (Fig.4.7b). However, safety margins for capacitors with the same VR can vary up to two orders of magnitude, which is mostly due to a wide spread of the dielectric thicknesses for capacitors rated to the same voltage (see Fig. 4.7c).

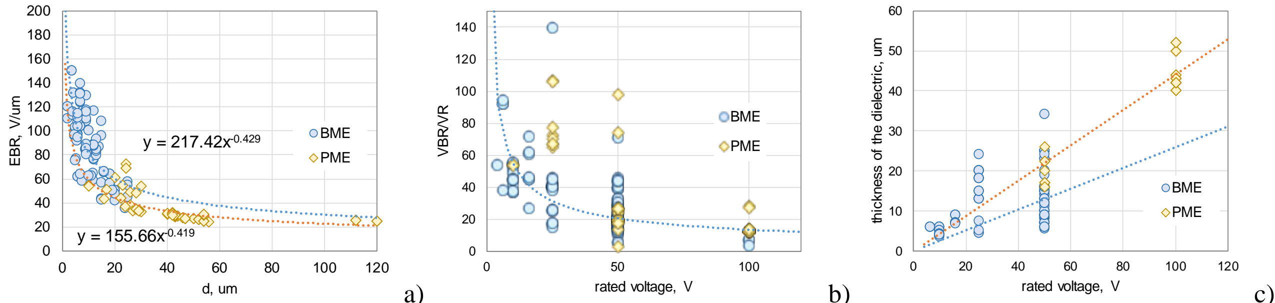

Figure 4.7. Relationship between breakdown field and thickness of the dielectric (a), normalized breakdown voltage vs. rated voltage (b), and variations of the thickness of the dielectric with VR (c) in different types of MLCCs.

Measurements and analysis of VBR distributions are not required by the military and space specifications. However, per MIL-PRF-32535 capacitors during qualification testing should demonstrate VBR exceeding VR by 30 times. Selection of this criterion for all types of capacitors is not justified, and based on results shown in Fig. 4.7b, a substantial proportion of parts, including military PME capacitors, would fail this criterion. JAXA employs measurements of VBR to demonstrate the level of the safety margin in MLCCs for space applications [47].

Most specifications require screening of the parts by the dielectric withstanding voltage (DWV) test that is typically carried out by exposure of the parts to 2.5VR. However, experiments show that low-voltage capacitors with cracks can pass this testing but cause failures during long-term operations at lower voltages. Note, that high-quality commercial MLCCs are often screened by DWV at voltages up to 10 times greater than VR [77].

Figure 4.8 shows an example of VBR distributions for virgin capacitors and capacitors with cracks. The cracks were introduced by mechanical fracture (MF) at the corner of the part, by cross-sectioning (X-sect), and by a thermal shock (TS). Similar testing with different types of capacitors showed that on average only ~ 20% of the mechanically fractured parts have VBR below 2.5VR. Cross-sectioned capacitors and capacitors with TS-introduced cracks had VBR exceeding DWV by several times. A large percentage of capacitors with tiny cracks created by thermal shock testing did not decrease substantially VBR compared to virgin parts.

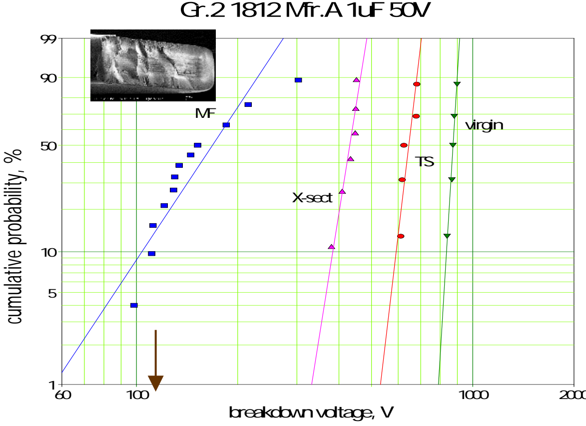

Figure 4.8. Distributions of VBR for case size 1812 1 uF 50V capacitors in a virgin condition (virg), and with cracks introduced by mechanical fracture (MF), cross-sectioning (X-sect), and thermal shock (TS). The insert shows fractured capacitor, and the error indicates voltage during DWV testing.

Results show that the probability of failure during DWV testing per the existing requirements is low even for capacitors with rough mechanical fractures. Increasing voltage during DWV test up to 50% VBR as suggested in [78] would increase the efficiency of the testing substantially.

4.4. Mechanical characteristics

Cracking of MLCCs occurs when the sum of external and internal mechanical stresses exceeds the strength of the part. It is reasonable to assume that selection of the most mechanically robust capacitors can reduce the risk of

cracking related failures. Mechanical characteristics that can be measured in-situ on MLCCs include flexural strength, Vickers hardness, and indentation fracture toughness. Below is the summary of mechanical tests that have been reviewed and detailed in the previous NEPP reports [79, 80].

- ### Flexural strength

Ceramic is a brittle material and its mechanical strength is typically measured using the three point or four point bending tests. AEC-Q200-003 describes a version of the test for the in-situ measurements of the break strength for MLCCs. Figure 4.9 gives a schematic and an example of the test set-up. A sample in a special holder is pressed with a metal rod in the middle until it breaks, thus indicating the fracture load. The specification requires that the minimum acceptable force to be set by the detailed specifications for the part. However, no methodology for selecting the minimal force is suggested, and no data for the acceptable limits were found in literature or in the manufacturers' specifications for automotive industry MLCCs. One of the drawback of the test is that it is limited to relatively large size (≥ 0805) capacitors. However, using a special fixture or parts soldered onto PWB, the tensile strength can be measured even for case size 0402 capacitors [81].

Assuming that the test conditions correspond to a three-point bending of a rectangular sample with the thickness *d* and width *b*, the flexural strength, or modulus of rupture, *MOR*, can be calculated as:

$$MOR = \frac{3FL}{2bd^2}$$

where *F* is the load during fracture, and *L* is the span of the fixture.

Distributions of MOR values, rather than the fracture loads *F* are used in technical literature to normalize the strength and compare results for different part types. Due to small sizes of MLCCs, the stress distribution in a capacitor under stress deviates from pure bending conditions, and strictly speaking, the above equation is not applicable. However, the purpose of the testing is mechanical characterization of capacitors rather than ceramic materials and the calculated MOR values should be considered as an effective flexure strength that characterizes a specific size of capacitors. In this case, the effective MOR values might allow for comparison of the mechanical robustness of different types of MLCCs.

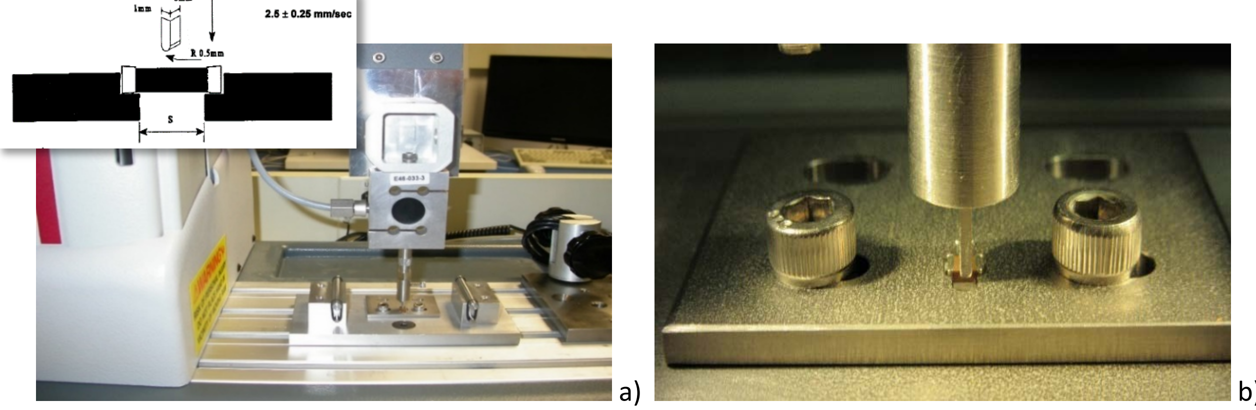

Figure 4.9. An overall view of the set-up for the flexural strength testing (a) and a close -up view of the fixture (b). Insert shows a schematic of the test per AEC-Q200-003

Samples of MLCCs made of the same materials but having different sizes might have a substantially different flexural strength. For this reason, this technique does not allow an accurate comparison of MOR values for different EIA size capacitors. However, for the same size capacitors, but with different thickness, normalization allows for a more accurate comparative analysis. Still, two times difference in the thickness can cause ~ 12% MOR variations, and thicker samples tend to have smaller strength.

Figure 4.10 shows the effect of surface treatment and the presence of cracks on distributions of MOR in CDR35 style capacitors. Polishing, immersion into solder flux (Kester 1544 Rosin) and exposure to humid conditions did not affect the distributions. The latter is somewhat surprising because it is known that cracks can propagate with time of moisture

exposure. A thermal shock caused by a solder dip testing at 350 ºC (TSD350) also did not reduce mechanical strength of the capacitors. No cracking was detected on the parts after TSD350, which is consistent with the measurements of the flexural strength.

Results indicate that microcracks with a size of a few micrometers or less as well as the presence of water molecules or contaminations on the surface do not affect significantly the strength of MLCCs. However, cracking caused by a Vickers indenter applied in the center of the part at forces 2.5 N, 5 N, and 10 N reduced the strength substantially, from 2 to 5 times. Considering that the size of the cracks increases with the applied force from ~20 µm to ~ 100 µm, this means that only relatively large cracks, above a few micrometers, reduce the strength of MLCCs.

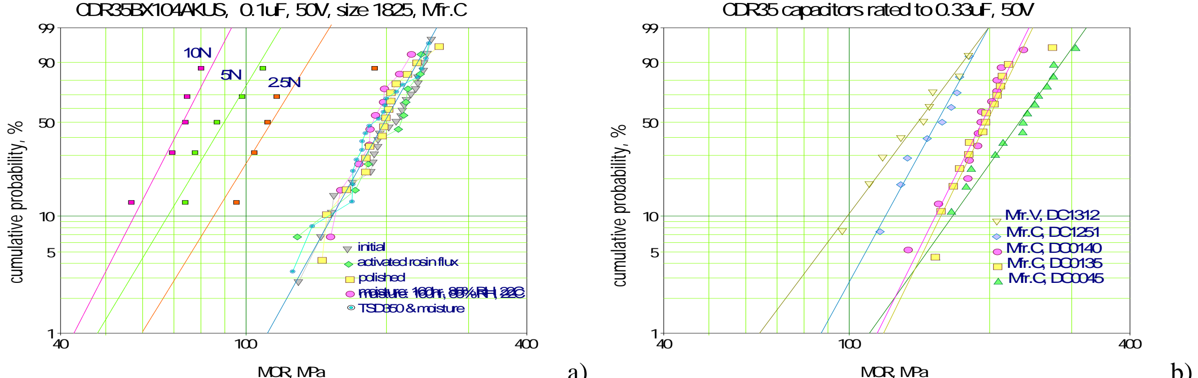

Figure 4.10. Weibull distributions of MOR for CDR35 capacitors after different treatment before testing (a) and different lot date codes and vendors (b).

MOR distributions for five different lots of CDR35 capacitors (see Fig.4.10b) indicate that both factors, lot date code and vendor are significant and the flexural strength technique is capable of revealing lots with reduced strength. The results show that the mechanical strength is a lot-related characteristic of MLCCs and variations of MOR values from lot to lot might exceed 50%. However, a substantial amount of statistical data should be obtained to develop acceptance criteria and use the flexural strength testing for quality assurance.

Measurements of mechanical characteristics of MLCCs from a lot of CDR35 capacitors that had flight failures in comparison with a reference lot of similar parts that did not have failures (see Fig. 4.11a) showed a statistically significant difference in the MOR values [28]. Similar results indicating that that 1825 CDR-05 capacitors that were susceptible to cracking and also caused flight failures had substantially lower MOR values compared to the reference capacitors have been reported by the Indian Space Research Organization, ISRO, [82]. This confirms the effectiveness of MOR testing for selecting capacitors resilient to soldering stresses.

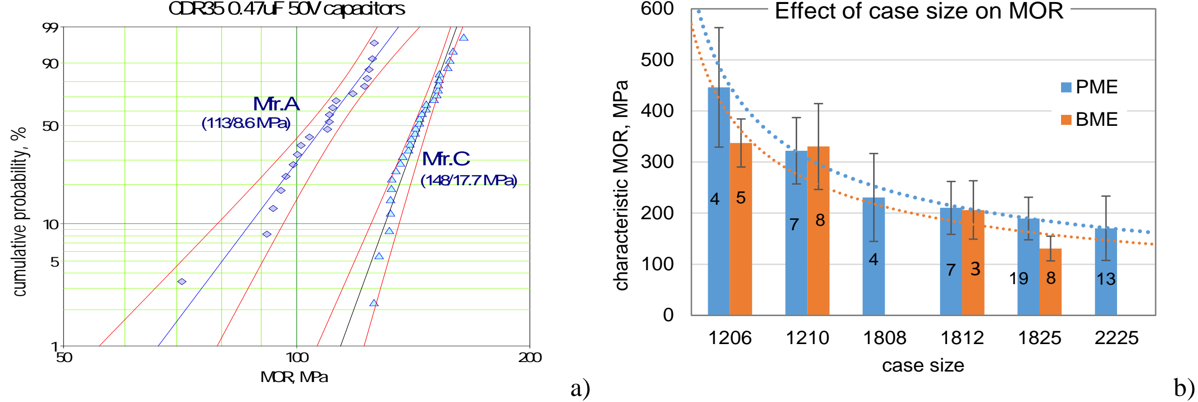

Figure 4.11. Distributions of the flexural strength (MOR) for Mfr.A capacitors that caused flight failures and reference, Mfr.C, capacitors (a) and characteristic MOR values of the relevant Weibull distributions for different lots of MLCCs (b). Red lines in (a) indicate 90% confidence bounds; error bars in (b) correspond to the standard deviations and numbers indicate quantity of the tested lots.

Results of MOR measurements for different size capacitors are shown in Fig. 4.11.b and indicate a trend of increasing the strength for the smaller size parts. Case size 1206 MLCCs have MOR values approximately twice the value for 2225 capacitors. This trend is similar to what is observed during the board flex testing and indicates that smaller size MLCCs are more resilient to bending stresses. Considering that there is no substantial difference in the strength between BME and PME capacitors, and the first have typically smaller size for the same CV values compared to PME capacitors, a wider use of BME capacitors in space applications would likely reduce the probability of cracking related failures.

- Vickers hardness

Hardness of materials can be defined as a resistance to indentation. A square-based diamond pyramid indenter is used during the Vickers hardness testing that is specified in ASTM C1327-15 (2015). Vickers hardness is calculated as a ratio of the applied force *P* to the surface area of the footprint:

$$VH = \frac{1.854 \times P}{D^2},$$

where *D* is the diagonal of the footprint, see Fig. 4.12.

If *P* is measured in kgf and *D* in mm, *VH* number is in kgf/mm2. If *P* is in newtons and *D* is in meters, then VH is measured in GPa.

Analysis shows that in-situ measurements of Vickers hardness are possible for capacitors with relatively thick cover plates. The effect of metal electrodes can be neglected if *P* is low enough so the depth of the indentation is more than ~2 times less that the thickness of the cover plate.

Vickers hardness testing of 30 lots of PME and 8 lots BME X7R capacitors (see Fig 4.12b) did not reveal any substantial difference between PME and BME MLCCs. The observed average VH values varied from 8.5 GPa to 10.2 GPa at a typical standard deviations in the range from 0.5 to 0.6 GPa.

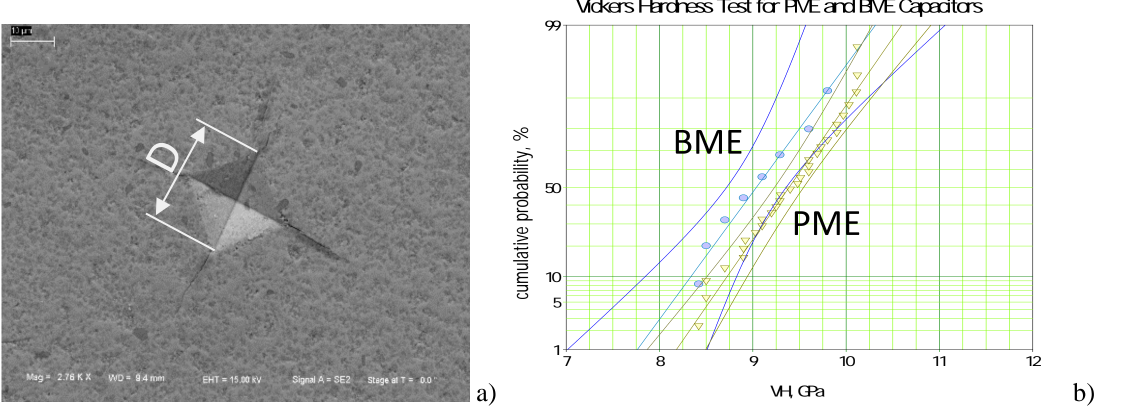

Figure 4.12. An example of the footprint during Vickers hardness testing (a) and distributions of average VH values for different lots of PME and BME capacitors. Dashed lines in (b) indicate 90% confidence range.

Contrary to plastic materials, where the hardness is approximately three times greater than the strength, there is no correlation between the hardness and strength for brittle ceramics. Although this testing is used sometimes to characterize ceramic in MLCCs and during failure investigations, it is most likely not effective for prediction of the susceptibility of capacitors to cracking.

- Indentation fracture toughness

Microcracks existing at the surface of a capacitor might not affect its performance if they do not cross opposite electrodes. However, stresses created during or after soldering might result in enlargement and propagation of small preexisting cracks resulting in electrical failures with time of operation. Obviously, capacitors using materials with higher fracture toughness can better resist cracks' extension and would be more reliable. The ability of a material to resist fracture and withstand stresses in the presence of cracks is determined by its fracture toughness, *Kc*.

Fracture toughness for ceramics in general is one of the controversial issues in materials testing, with more than 30 different tests and many variations for each test available [83]. In-situ measurements of *Kc* using indentation fracture technique (IFT) is the most controversial, and has not been standardized so far. Nevertheless, this method has been used by many researchers because of its simplicity and the applicability to small size samples. This technique is considered an unrivalled quick, convenient and economical means for comparative, site-specific evaluations of the toughness of ceramics [84].

This method consists of using a Vickers indenter in order to generate cracks at the corners of the indent (see Fig. 4.12a) and calculating K_c based on the length of cracks, c. A commonly used equation for the radial-median cracks relates K_c with the load P, Vickers hardness H, and Young's modulus E:

$$K_{c(R_M)} = \xi_{R_M}\left(\frac{E}{H}\right)^{0.5}\left(\frac{P}{c^{1.5}}\right),$$

where $\xi_{R_M} = 0.015$ is constant.

Results of IFT measurements on samples from different lots of PME capacitors having the same part number are shown in Fig. 4.13b. No significant difference between lots with different date codes was observed. However, it appears that the fracture toughness for M123BX474 capacitors is ~ 30% less than for CDR35BX334 capacitors. It is possible that in spite of the controversy, IFT in-situ measurements of the fracture toughness can provide useful information regarding robustness of capacitors to the cracking failures. However, improvements in the accuracy of measurement to better than ±20% are required.

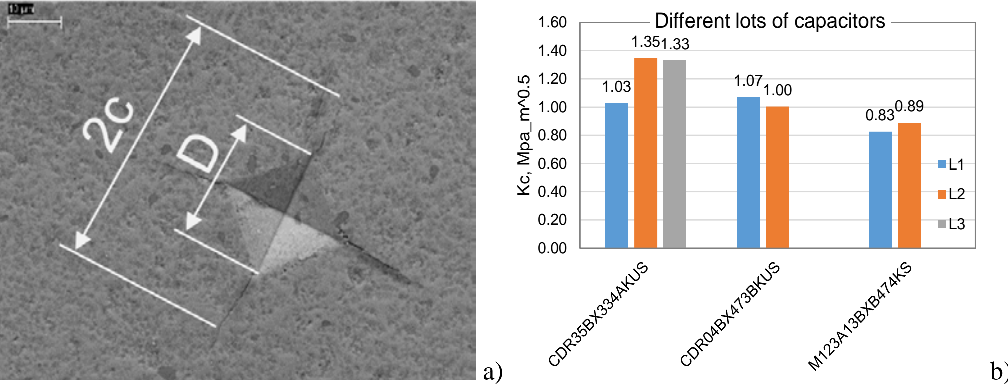

Figure 4.13. An example of the footprint during indentation fracture toughness testing (a) and Fracture toughness for different lots (L1, l2, and L3) for three types of military grade capacitors.

Experiments show that K_c values for MLCCs are in the range from 0.8 to 1.4 MPa×m$^{0.5}$ for PME BX, from 1.3 to 1.6 MPa×m$^{0.5}$ for PME BP, and from 0.7 to 1.3 MPa×m$^{0.5}$ for BME class II dielectric capacitors. Considering the accuracy of measurements, there is no statistical difference between fracture toughness of PME and BME capacitors.

5. Failure mechanisms in MLCCs with cracks

Failures of MLCCs with cracks are commonly explained by moisture sorption that increases conductivity along the surface of the crack or causes electrochemical migration (ECM) of electrode materials and formation of shorting metal dendrites. Silver that is used in PME capacitors is a metal most susceptible to ECM. Migration of silver can be observed at voltages as low as 0.4 V [85] and relative humidity down to ~ 40% RH [86], which is the reason of so-called low-voltage failure phenomena in capacitors. Fig.5 shows an example of a capacitor failed due to silver electromigration along an internal crack shorting opposite electrodes. Note, that this part passed screening testing per MIL-PRF-55681.

Much less is known about ECM in BME capacitors with internal electrodes made of nickel, which is often considered as a non-migrating metal. In the absence of moisture in environments, e.g. during life testing at 125 ºC or at low temperatures in vacuum, degradation and failures in capacitors with cracks might also happen, but the mechanism of the process is less obvious compared to humid environments.

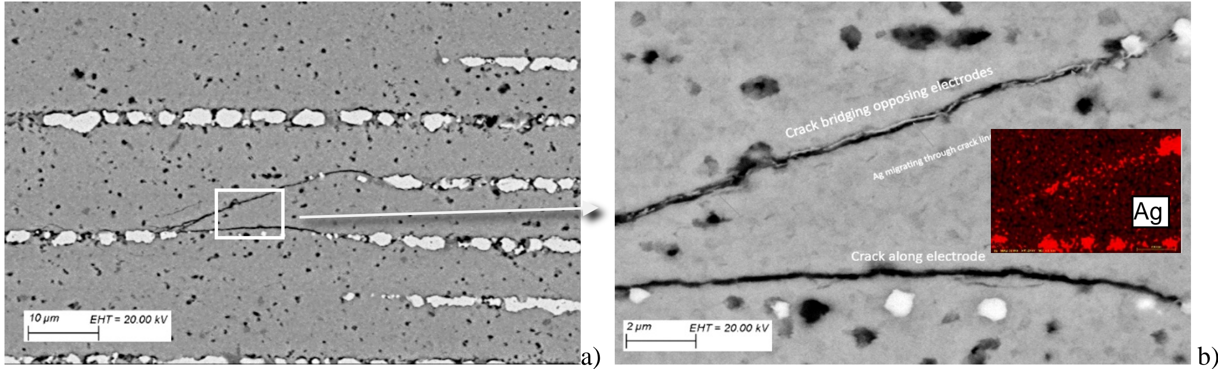

Figure 5. An overall (a) and close-up (b) views of a shorting crack in 0.1 µF 16 V PME capacitor. The part was tested at 6 V and started showing increased and unstable leakage currents after 110 hr at room temperature and then failed eventually short circuit due to silver electromigration after 50 hr at 60 °C. (Pictures courtesy of Ron Weachok, Jacobs Technology Inc.)

5.1. Degradation of PME and BME capacitors in the presence of moisture

Capillary condensation can fill tiny cracks with water even at relatively low level of humidity in environments and remain trapped in the crack even after several days in dry conditions [87]. To simulate electrochemical processes in capacitors with cracks filled with condensed water, a water layer testing (WLT) at low voltages, from 0.5 V to 1.5 V, was used in [88]. The parts were cross-sectioned perpendicular to the internal electrodes and a quarts slide pressed against the surface with exposed electrodes formed a few micrometers' gap filled with deionized water. Formation of dendrites was observed using an inverted metallurgical microscope (Fig.5.1).

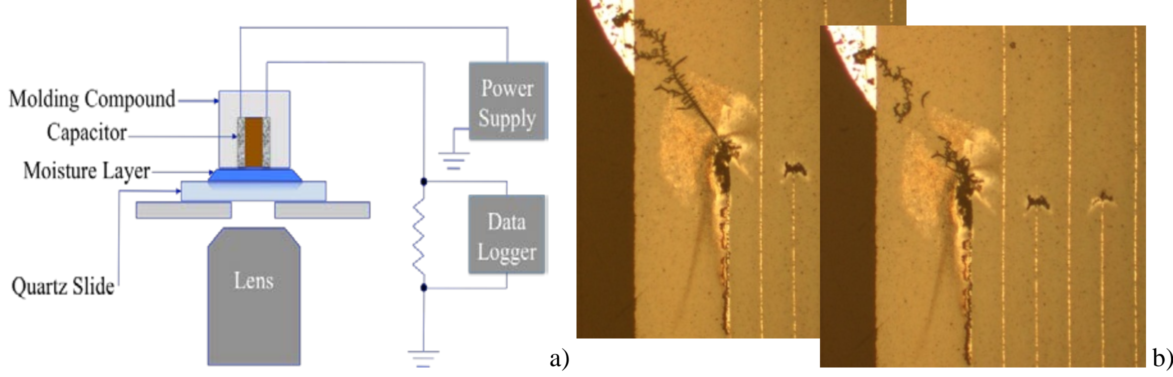

Figure 5.1. Schematic of the water layer test set-up (a) and an example of dendrites formed between the termination and the tip of the negatively biased electrode on the surface of 1825 0.1 µF 100 V PME capacitor that was shorted after 3.6 min at 1.3 V and blown after shorting (b).

Results show that the presence of condensed water in relatively wide cracks can result in formation of shorting dendrites within a few minutes even at voltages below 1.5 V. Formation of dendrites bridging electrodes and their blowing after short circuit (Fig. 5.1b) might explain intermittent behavior of failures in MLCCs in humid environments. When electrodes are bridged by a tiny dendrite, this blowing might clear the short, after which the process repeats. However, when a relatively large dendrite is formed, the resistance of the short is less and the dissipated power is larger. This might result in a micro explosion creating a more severe damage to the structure of capacitors and cause melting of ceramic and catastrophic failures (see an example in Figure 5.2.). It is also possible that during such an event the melted metal will be forced to fill out other areas of the crack that during cross-sectioning might be misjudged as metal migration.

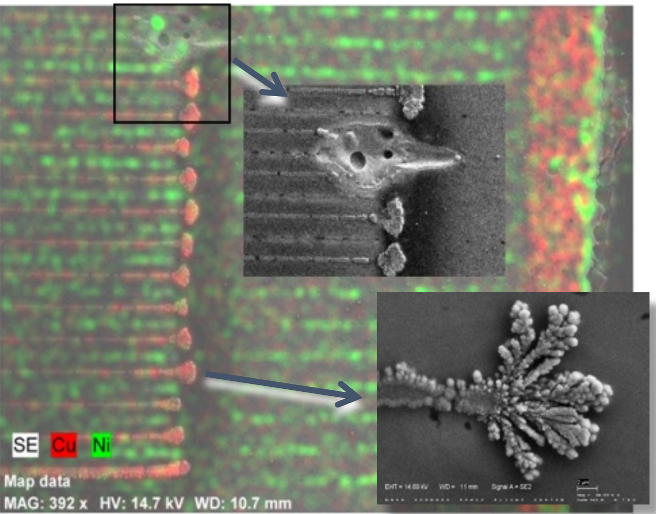

Figure 5.2. An example of a catastrophic failure caused by copper dendrites growth on a surface of a BME, 1 μF 50 V, case size 1812, capacitor. These dendrites grew for 5 min at 3 V, 95% RH, but the short circuit failure occurred when a rated voltage was applied after the testing. An overall SEM image is overlapped with EDS mapping and the top insert shows the area of a blown dendrite resulted in damage of ceramic, and the bottom shows a clos-up of a copper dendrite.

Surprisingly, dendrites in PME capacitors in many cases were formed not by silver, that was expected initially, but by lead (Fig. 5.1b) or tin (Fig. 5.3a). Similar tin dendrites were also observed on the surface of BME capacitors (Fig. 5.3b). Apparently, anodic dissolution, diffusion, and migration of Pb and Sn ions in water occurs faster than dissolution of silver in the Ag/Pd alloy used in internal electrodes. This is likely due to the impeding role of palladium oxide that is formed on the surface of electrodes in PME capacitors and is likely the major protection against development of Ag dendrites [89, 90]. Alloying of silver with palladium reduces the probability of dendrite growth, but it still might happen due to Ag diffusion along the grain boundaries of ceramics during sintering.

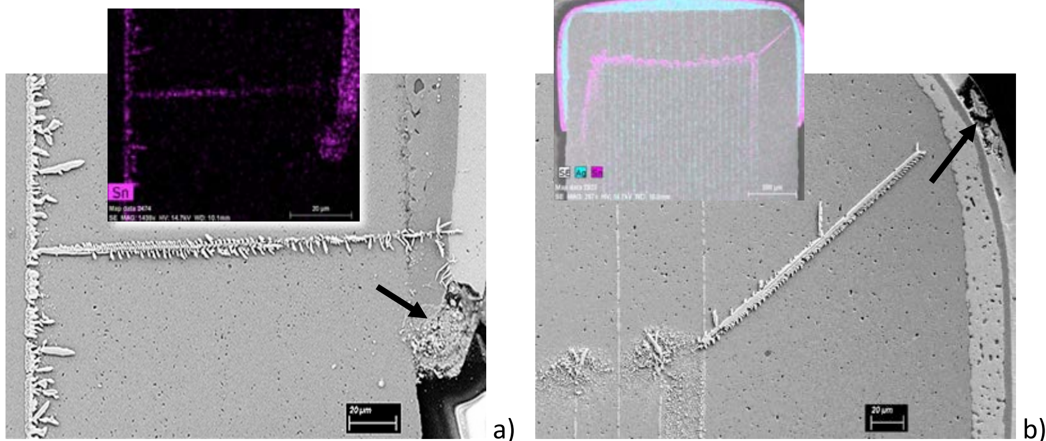

Figure 5.3. Growth of tin dendrites at the edge cathode electrodes in a BME 1825 0.47uF 50V capacitor that failed at 0.8 V after 23 minutes of testing (a) and in a PME capacitor that failed short circuit after 18 min at 0.8V (b). Errors indicate location of anodic dissolution of tin in the termination. Inserts show EDS mapping of the dendrites.

Figure 5.4.a shows silver dendrites formed on the surface of a PME capacitor at the tips of negatively biased electrodes and along the portion of the electrodes near terminations. Location of the dendrites indicates that the silver base frit, rather than the positively biased internal electrodes was the source of silver. Copper dendrites on the surface of BME capacitors (Fig. 5.4b) were also formed at the tips of electrodes and pitting corrosion of the copper frit termination indicates the source of the metal used to form dendrites. Results show that in both types of capacitors, BME and PME, shorting dendrites can be formed by materials used in terminations and/or solder used for attachment to the board.

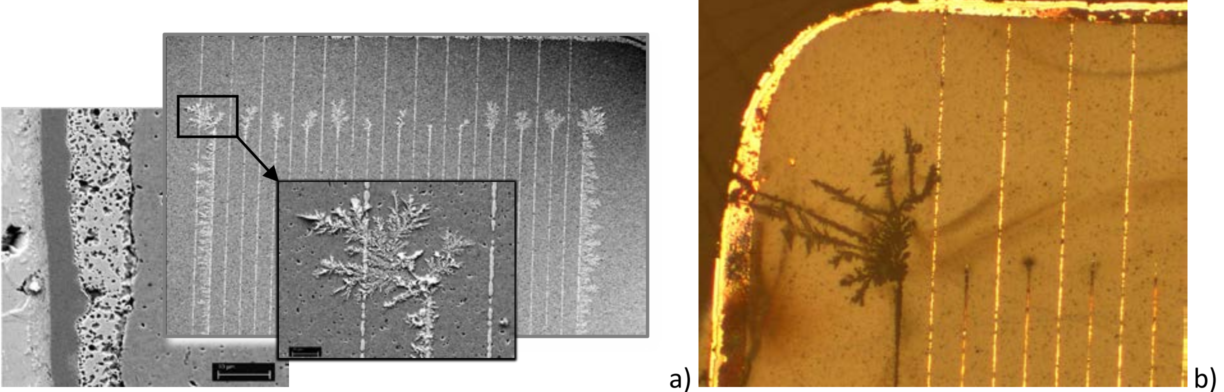

Figure 5.3. Dendrite growth during WLT at 1.3V in PME (a) and BME (b) 0.47 uF 50 V MLCCs. Silver dendrites were formed after 2.5 min in PME (a) and copper dendrites were formed after 8 min in the BME capacitor (b). Note pitting corrosion in the Ag (a) and Cu (b) base metal terminations for PME and BME capacitors respectively.

Contrary to WLT, only a few (from 2 to 4) monolayers of water are absorbed during humidity testing at 85% RH and 85 ºC. This retards significantly processes of the anodic dissolution and ion migration. At these conditions, formation of silver and/or Ag/Pd dendrites and failures due to short circuit or intermittent contacts in PME capacitors was detected after hours of testing (Fig. 5.4.a). Also, silver precipitates between the electrodes were formed by a colloidal silver oxide [85, 91]. Considering that silver oxides have relatively high conductivity [92], these deposits can cause increased leakage currents and parametric failures even without development of shorting dendrites.

Testing of the damaged by cross-sectioning BME and PME 0.47 μF 50 V capacitors having the same thickness of the dielectric (~1 mil) in humidity chamber at 1.3 V (HSSLV testing) showed that failures occurred in ~85% of PME capacitors, whereas BME capacitors had no failures. Typical variations of leakage currents in the parts are displayed in Fig. 5.4, and Fig.5.5 shows typical formations observed on the surface of the parts after the testing.

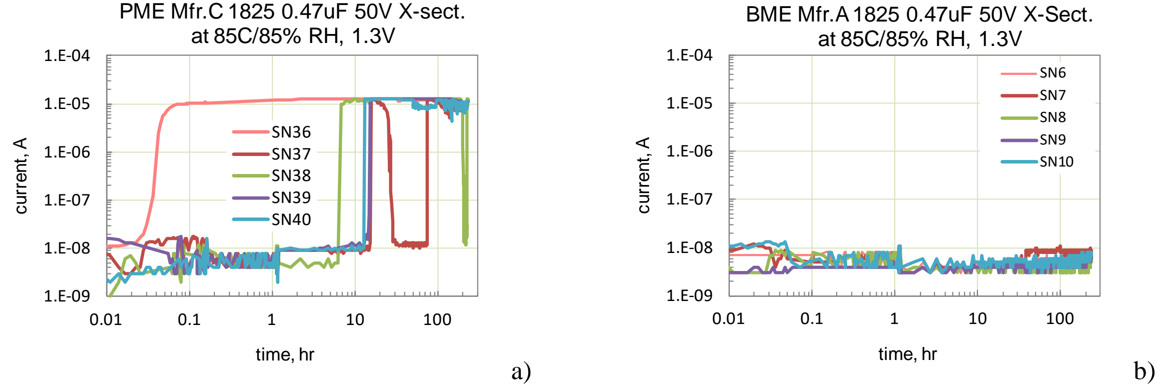

Figure 5.4. Variations of leakage currents with time during HSSLV testing of PME (a) and BME (b) 0.47uF 50V cross-sectioned MLCCs. Note that the currents were limited to ~ 10^{-5} A by external resistors.

BME capacitors after HSSLV had IR typically exceeding 10 MOhm, whereas PME capacitors had IR in the kilo-ohm range. Although BME capacitors did not fail electrically, SEM examinations revealed nickel carbonate compositions formed around anode electrodes. These compositions had high resistivity and did not short the capacitors. Note that similar formations were detected on the surface of fractured BME capacitors after humidity testing, whereas silver deposits were present on the surface of PME capacitors (Fig. 5.5 c, d).

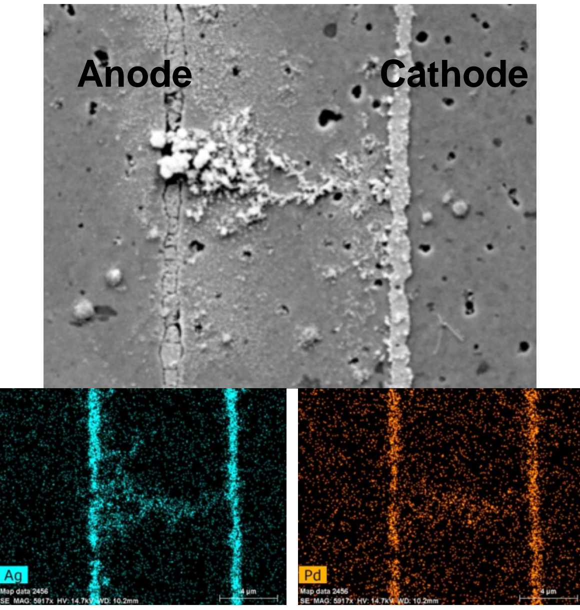

a) Ag/Pd dendrites on the surface of a PME capacitor failed after HSSLV testing. Note erosion of the anode electrode indicating the source of metal ions used to form dendrites.

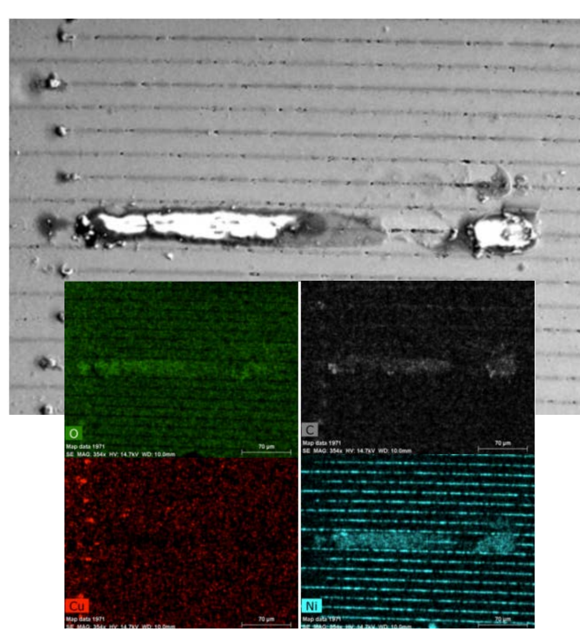

b) surface of a BME 1 μF 50 V capacitor after 44 hr of HSSLV testing. Note copper formations at the tips of anode electrodes.

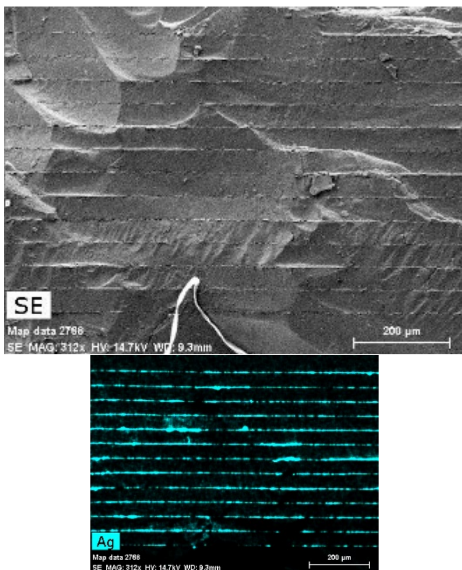

c) PME, case size 1825, 0.1 μF, 100 V capacitor, after testing at 22 °C, 85% RH, and 5 V. Although Ag dendrites were not found, EDS mapping indicates the presence of silver deposits between electrodes.

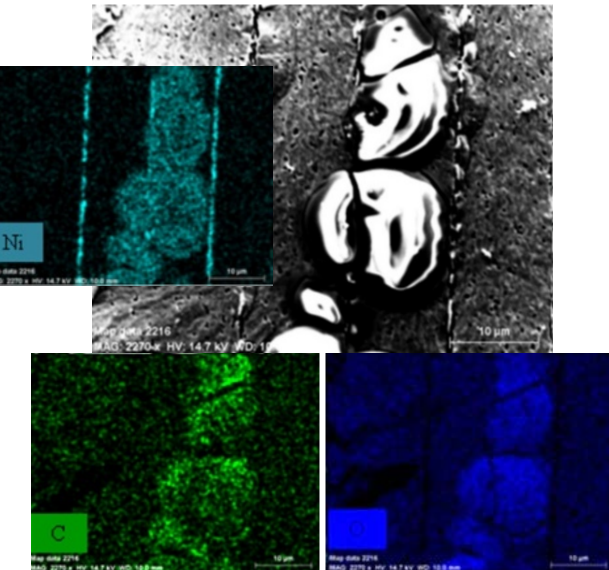

d) BME, case size 1825, 1 μF, 50 V, capacitor, after testing at 22 °C, 85% RH, and 15 V for 300 hours. High-resistivity Ni/C/O formations at anode electrodes are similar to Fig.b.

Figure 5.5. SEM and EDS images of formations on the surface of PME (a, c) and BME (b, d) cross-sectioned (a, b) and fractured (c, d) capacitors after humidity testing.

In a simplified form, processes of ECM on the surface of BME and PME capacitors that result in dendrite growth at cathode electrodes, formation of precipitations between the opposite electrodes, or formation of deposits at anode electrodes are shown in Fig. 5.6. The process of dendrite growth (Fig.5.6a) occurs in three-steps: (i) anodic dissolution

of metal ions, (ii) migration of ions along the surface, and (iii) deposition at the cathode. Anodic dissolution is an essential part of all ECM processes.

Depending on the type of materials and test conditions, the precipitates might be conductive (typical for PME capacitors) or isolative (typical for BME capacitors). Silver oxides are conductive and the resistivity of Ag2O/Ag2O3 varies from 10^{-5} to 10^{-3} Ω-cm. At this resistivity, even tiny areas of the crack can cause substantial IR degradation and failures. For example, in a 100 µm wide crack with a 10 µm spacing between electrodes, a thin, 10 nm thick crack filled with Ag-oxide would have resistance from 1 Ω to 100 Ω.

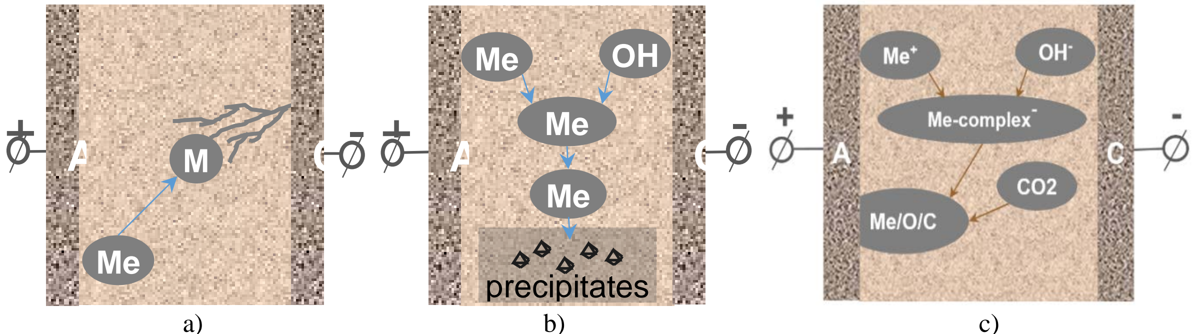

a) b) c)

Figure 5.6. Simplified schematic of electrochemical processes in MLCCs: cathode dendrites growth (a), formation of precipitations (b), formation of anode deposits (c).

ECM of silver in test structures consisting of conductive elastomer land grid array sockets did not result in formation of dendrites. Instead, leakage current degradation and failures occurred when surface insulation resistance dropped substantially due to silver ion accumulation prior to the dendritic formation [93]. In this case, the time necessary for the ion accumulation to reach a certain critical concentration determines the time-to-failure.

Analysis of the surface of fractured BME capacitors after humidity testing revealed evidence of the electrochemical migration of nickel at voltages as low as 1.3 V. However, similar to cross-sectioned samples, nickel formed amorphous, bulbous deposits on the anode electrodes (Fig.5.5 b, d). These deposits covered large areas of capacitors and were mostly comprised of nickel oxide, with the addition of carbon. Formation of these deposits can be explained by the anodic dissolution of Ni^+ ions from the internal electrodes that form complex cations through reactions with water and CO_2 in air. This subsequently leads to reduction of the complex cations at the anode (Fig.5.6c) and formation of agglomerates of nickel oxides (NiO) and nickel carbonates ($NiCO_3$) around anode electrodes of the capacitor.

The following reactions might explain ECM processes in BME capacitors:

$Ni^{2+} + 2H_2O \rightarrow HNiO_2^- + 3H^+$

or $Ni\text{-}OH + CO_2 \rightarrow NiOCO_2^- + H^+$.

At the anode nickel carbonates and oxides are formed:

$3HNiO_2^- + H^+ \rightarrow Ni_3O_4 + 2H_2O + 2e^-$

or $NiOCO_2^- + 4H_2O - e \rightarrow NiCO_3(H_2O)_4$

Pure stoichiometric NiO crystals are perfect insulators (~10^{13} Ω-cm) [94], but even doped, non-stoichiometric oxides still have high resistivity (10 to 10^6 Ω-cm). Formation of highly resistive composites does not degrade substantially IR and does not cause electrical failures in BME capacitors.

Due to a high susceptibility of metals used in terminations (Cu, Sn, Pb, Ag) to electromigration, generation of ions by the anodic dissolution and their diffusion from terminations along the moisture absorbed layer on the surface of MLCCs (see Fig. 5.7) can cause failures in both types, PME and BME capacitors. This mechanism might prevail over ECM of internal electrodes in BME capacitors, whereas silver migration originated either from terminations or internal electrodes and formation of conductive oxides deposits is prevailing in PME capacitors.

An example of behavior of leakage currents with time of operation in capacitors with cracks is shown in Fig. 5.8. Leakage currents at 22 ºC and 85% RH were monitored for 1000 hours in CDR35 capacitors after simulation of stresses associated with manual soldering by the terminal solder dip (TSD350) testing (see section 8.2). Seven out 20

samples after TSD350 failed the testing. In spite of the presence of cracks, electrical failures even at a relatively high humidity were observed only after long periods of testing ranging from 100 to 860 hours (Fig. 5.8b). The failures were intermittent and the parts exhibited unstable currents even before reaching the level of the formal failure.

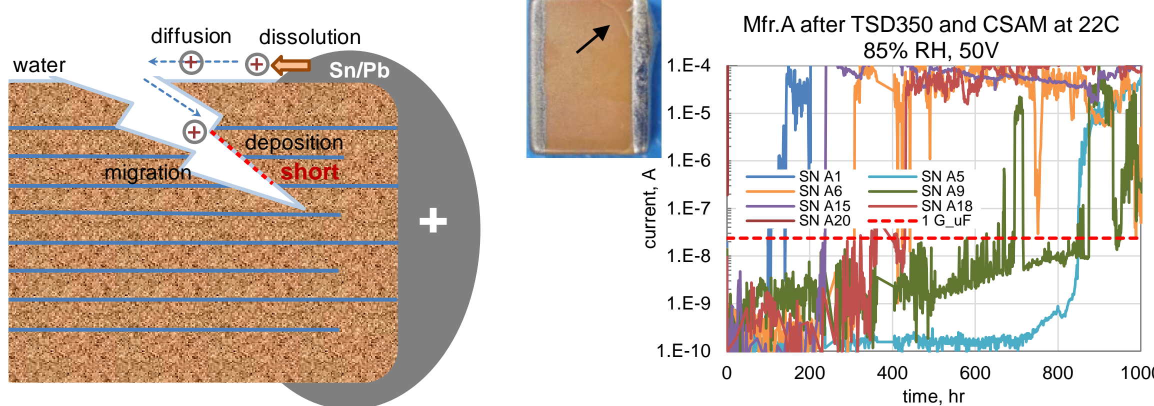

Figure 5.7. Schematic of failures in MLCCs with cracks caused by migration of ions that are anodically dissolved from terminations.

Figure 5.8. Leakage currents in CDR35 0.47 μF 50 V capacitors during 1000 hour testing at 22 °C, 85% RH, and 50 V. An insert shows example of cracks formed by TSD350.

Moisture adsorption on the surface of cracks reduces the surface energy of ceramics, thereby decreasing the critical stress needed for the crack growth [95]. Delayed cracking under operating electric fields is one of the major reliability issues for ferroelectric devices [96] and the effect has a strong dependence on humidity and voltage. Results for potassium sodium niobate ferroelectric ceramics show that crack growth occurs in humid air of 70% and 90% RH but was not observed at RH ≤ 30%. It is assumed that the critical humidity for crack growth without an electric field is ~50% RH. Crack growth can also occur in dry air when the electric field is larger than a certain threshold value, and the incubation time decreases for larger fields.

Considering that cracks might grow with time in the presence of moisture in environments, it might take months and even years of operation at normal conditions to form a short. Incresed humidity, temperature and voltage would accelerate the degradation process substantially. However, due to the difficulties in predicting behavior of cracks and complexity of the ECM processes involved, there is no reliable models to assess acceleration facors for cracking related failures.

Derating, that is one of the major means to increase reliability of components during operation, might be not effective to mitigate cracking related failures. For example, decreasing temperature of operation might have an adverse effect due to the associated increase of relative humidity. Because ECM can occur at very low voltages (below 1.5 V), reduction of voltage does not eliminates the risk of electrical failures.

Operation in dry environments after the parts with cracks have been exposed to humid conditions might not eliminate the risks of failures. For space electronic modules stored or operating at the ground, a gradual diffusion of water molecules inside a capacitor is possible, and the presence of moisture on the surface of cracks and associated degradation of *IR* can be observed with time of operation at normal conditions. It is also possible that a certain amount of moisture remains trapped in the cracks in flight modules operating in space. Water molecules in cracks are bonded to the surface by strong physical and chemical forces (in the form of –OH groups), which makes their removal without high-temperature baking extremely difficult even in vacuum. This allows for ECM processes in cracks to continue after launch, but it might take much more time for the failure to occur compared to the ground operations (unless the crack developed further, for example due to vibration during the launch).

A specific trait of silver is that it can migrate even in dry conditions through the ceramic grain boundaries and eventually cause shorts [97]. The activation energy of silver migration through the glass is relatively large, 1 to 1.3 eV [98], so the process at room temperatures might take thousands of hours. At a low rate of the ECM process, formation of dendrites is unlikely due to the effect of poisoning by contaminations, and the failures are most likely due to formation of silver oxide deposits.

Results of testing of BME and PME MLCCs with cracks in humid environments can be summarized as follows [34, 88]:

1. In the presence of condensed water, dendrite growth on the surface of cracks in PME and BME ceramic capacitors can occur at voltages in the range from 0.5 V to 1.3 V and metals the most susceptible to dendrite growth are Pb > Sn > Ag for PME capacitors and Pb > Sn ≥ Cu for BME capacitors.

2. The specific of ECM in fractured MLCCs is the presence of different metals forming galvanic cells in the termination that enhance substantially anodic elution of metal ions such as Pb, Sn, and Cu at low voltages. PME capacitors, due to the presence of Sn/Pb – Ag galvanic cells, are more susceptible to Pb and Sn dendrite growth compared to BME capacitors that have Sn/Pb – (Ni or Cu) cells with more compatible anodic indexes.

3. At a similar level of cracking, BME capacitors have lower probability of failures compared to PME capacitors. Leakage currents in BME capacitors typically degrade relatively slowly, and require higher voltages than in PME capacitors. This is due to different electro-chemical behavior of the nickel and silver/palladium electrodes. In PME capacitors, formation of conductive silver dendrites or silver oxide deposits results in short-circuits between the electrodes, whereas in BME capacitors, highly resistive nickel/carbon/oxygen compositions are formed.

4. In humid environments, the rate of degradation of leakage currents in BME capacitors with cracks increases with the applied voltage. For this reason, HSSLV testing that is used for PME capacitors, is not effective for BME capacitors, and instead, THB testing at 85 °C, 85% RH, and rated voltages for 240 hours is recommended.

5.2. Degradation in dry environments

Due to a reducing atmosphere during sintering of BME capacitors, the concentration of charged oxygen vacancies (V_O^{++}) in the ceramic is increased, and the mechanism of degradation during life testing is attributed to migration and accumulation of V_O^{++} at the grain boundaries and metal/ceramic interfaces. This causes decreasing of the energy barriers and increasing of leakage currents by enhanced electron injection according to the Schottky mechanism. For this reason, BME capacitors are much more susceptible to wear-out failures compared to PME capacitors.

Improvements in materials and process control reduced degradation in BME MLCCs substantially, and currently, the inception of the intrinsic wear-out failures became much greater than the mission duration in most high-reliability applications. However, in capacitors with defects degradation processes might accelerate substantially and cause infant mortality (IM) failures. Studies have shown that roughness and presence of voids in metal electrodes result in local field enhancement causing reduction of insulation resistance [52, 99, 100]. This might affect performance of capacitors with thin dielectrics.

A thermal runaway model that relates the presence of defects resulting in thinning of the dielectric to reduction of breakdown voltages and decreasing times to failure has been suggested in [101]. According to this model, the same degradation process that is responsible for the intrinsic wear-out failures might result in IM failures for capacitors having defects. In this case, voltage and temperature reliability acceleration factors that are determined for wear-out failures might be used to predict IM failures. The model can also explain degradation of leakage currents in BME capacitors with cracks during operation at high temperatures in dry conditions by enhanced migration of oxygen vacancies along the surface of cracks.

Compared to BME, PME capacitors have much lower leakage currents and lower probability of thermal breakdown. Failures in these parts are likely due to the time dependent dielectric breakdown (TDDB) caused by generation of traps in the dielectric. According to the percolation model, breakdown occurs when concentration of defects reaches the critical level [102]. During breakdown, the energy stored in the part is released instantaneously resulting in adiabatic overheating and melting of a local area of the dielectric and metal electrodes. Contrary to PME, degradation in BME capacitors occurs gradually and the energy generated at the defect can be balanced by heat dissipation. This explains why "leaky" BME capacitors often degrade, but do not fail catastrophically, whereas PME capacitors with prevailing avalanche-like breakdown [103] might not degrade, but fail short circuit instantly (see Fig. 5.9.d).

Variations of leakage currents in BME and PME capacitors with introduced cracks (Fig.5.9) show that cracking did not affect leakage currents in capacitors measured after a few minutes of testing. This confirms that IR measurements at 125 °C might be not sensitive to the presence of cracks. However, currents started increasing after ~ 1 hour and

raised more than two orders of magnitude after 10 to 100 hours (Fig. 5.9.a, b). After that, the currents stabilized or decreased with time, so no catastrophic failures happen.

Degradation of leakage currents in BME capacitors can be explained assuming that migration of V_O^{++} along the surface of cracks occurs faster than in the bulk of the dielectric. This facilitates accumulation of V_O^{++} at local areas of metal electrodes near the crack, and accelerates degradation of leakage currents. After reaching the ceramic/electrode interface, oxygen vacancies can diffuse along the interface thus charging areas close to the crack and reducing the barrier height at metal/ceramic interface (see Fig. 5.9.c). According to this mechanism, relatively minor cracks with a size of a few micrometers might increase leakage currents during HALT, but not cause catastrophic failures. However, a short circuit failure due to a thermal runaway might happen in a case of extensive cracking.

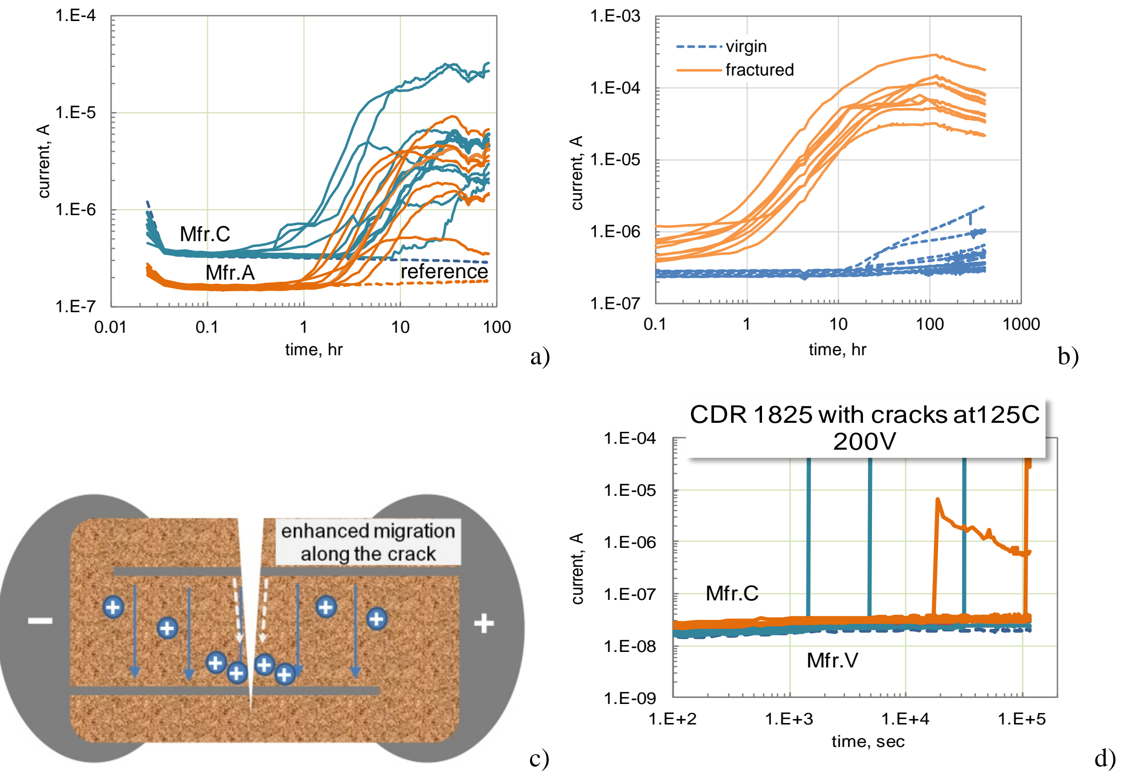

Figure 5.9. Variations of currents through HALT testing in BME (a, b) and PME (d) capacitors with cracks. BME capacitors, 0.33 µF 50 V (a) and 1 µF 50 V (b) were tested at 125 ºC, 100 V and PME capacitors, 0.47 µF 50V, at 125 ºC and 200 V. Dashed lines correspond to virgin and solid lines to capacitors with cracks introduced by Vickers indenter. Fig.c shows a schematic of degradation processes in BME capacitors with cracks.

Due to the thermal nature of breakdown in BME capacitors, degradation caused by migration of V_O^{++} after HALT not only increases leakage currents, but also reduces breakdown voltages. Capacitors with defects reduce VBR after HALT to a much greater degree compared to the defect-free capacitors. This makes high-voltage DWV testing after burning-in or life test a useful instrument to reveal capacitors with cracks.

Analysis shows that low-voltage BME capacitors with defects during life testing in dry conditions are more likely to fail parametrically, whereas catastrophic failures are more probable for PME capacitors, which is attributed to different mechanisms of breakdown for PME (electronic) and BME (thermal) capacitors. This situation is reversed compared to humid environments when PME capacitors with cracks are more likely to fail compared to BME capacitors.

6. Special cases of MLCC cracking during manufacturing, assembly, and testing

Common reasons for cracking are associated with:

- stresses during manual soldering, rework, or touch-up to improve appearance of the fillets;
- flex bending of the boards during depanelization, handling, mounting, or vibration testing;
- temperature cycling of MLCCs soldered onto PWBs;
- Excessive power during ultrasonic cleaning of the assembled boards.

To reduce the risk of failures during ultrasonic cleaning some manufacturers [104] and JAXA [47] recommend using cleaners with power not exceeding 20 Watts per liter at a frequency of 40 kHz for not more than 5 minutes. The cleaning process might cause substantial damage to MLCCs in case of resonance of PWB, so Murata recommends testing the cleaning equipment before starting the process to ensure it does not degrade capacitors [31].

Several less often discussed reasons of cracking are described below.

6.1. Hydrogen-related cracking

Anomalies in a module operating in space have been detected after months of work and were attributed to excessive leakage currents in CDR35 0.47 µF 50 V capacitors, These parts have been soldered manually and were suspected of having cracks [28]. Testing of a spare unit on the ground also showed increasing leakage currents after several weeks of operation. Failure analysis investigation confirmed that increased leakage currents were due to delaminations and cracking in the part. No external cracks on the failed lot were observed; however, acoustic microscopy showed that a substantial proportion of parts had delaminations at the termination areas.

Simulation of manual soldering stresses by TSD350 testing using virgin capacitors from the failed lot showed that cracks initiated at the surface continued as metal/ceramic delamination and facilitated formation of internal cracks crossing electrodes (see Fig. 6.1). Most likely, delaminations or weakening of the metal-ceramic adhesion occurred during manufacturing and grew further due to manual soldering stresses. Delaminations facilitated formation of crack crossing electrodes and resulted in electrical failures with time during biased testing. Corner location of delaminations indicates that they developed during formation of terminals.

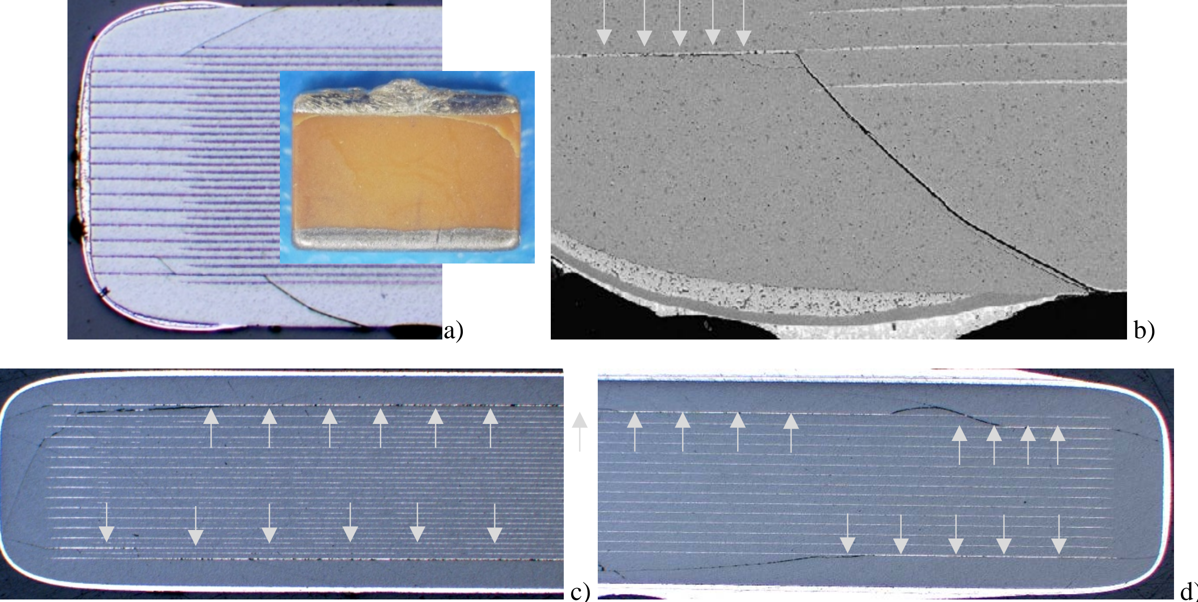

Figure 6.1. Crack reveled in MLCCs after TSD350 cross-sectioning across (a, b) and along (c, d) terminals.

One of the reasons for corner delaminations is evolution of hydrogen during electroplating of nickel and solder finishing. Several publications have discussed effect of hydrogen on ceramic materials and capacitors. Severe degradation of physical properties of ceramics has been reported by H.Zhang et.al. [96]. Hydrogen generation and its diffusion through ceramics during electroless nickel plating was attributed to failures of MLCCs by W. Chen and co-workers [105].

J. Piper [7] reported on failures of capacitors operating in the battery hydrogen atmosphere. The failures were attributed to the splitting of the side margins caused by hydrogen absorbed by the palladium electrodes. H.Zhang at.al. studied the effect of hydrogen on the fracture properties of the lead-free ferroelectric ceramics [96, 106]. Hydrogenation decreased the fracture toughness measured by IFT linearly with increasing concentration of hydrogen and delayed propagation of unloaded indentation cracks.

Y.Saito at al., studied degradation and failures of BME capacitors during biased testing at 120 ºC and 85% RH [107]. Leakage currents during the testing started increasing after dozens to hundreds of hours of testing and were unstable. Experiments with terminals having different thicknesses showed that moisture can penetrate to the active areas of MLCCs by permeation through relatively thin terminals and produce hydrogen by electrolysis of water molecules. The hydrogen reduced nickel oxide at the cathode electrodes and caused cracking due to release of internal stresses in the capacitors.

Using impedance spectroscopy and diffusion analysis Heidary and Randall [108] have demonstrated that increased leakage currents in MLCC after hydrogen diffusion are mostly due to decreasing Schottky barriers at the electrode/ceramic interface. It has been shown that the fastest path for diffusion in BME X7R capacitors is along the Ni/ceramic interface and somewhat slower along the grain boundaries. The pre-exponential factors D_0, and activation energies, E_a, for diffusion along electrodes, along the grain boundaries and through the grains respectively are 0.88, 0.28, and 0.002 cm^2/sec and E_a = 0.73, 0.76, and 0.52 eV. At these conditions, the effective diffusion coefficient of hydrogen is ~1.1×10^{-7} cm^2/sec at 250 ºC and the diffusion length is ~ 0.2 mm after 1 hour of exposure to the forming gas (5% H2 and 95% N2).

In PME capacitors, palladium in Ag/Pd electrodes forms a layer of PdO, which is considered the major protection against silver migration and development of silver dendrites [89, 90, 97]. Reduction of PdO in the presence of hydrogen removes the barrier and facilitates electrochemical migration of silver. This process occurs also with a substantial volumetric changes because palladium volume increases during oxidation by 68% [97]. According to R.Newnham [7], the lattice parameter of PdO decreases from 3.902 A to 3.891 Å during the reduction. Volume expansion due to the oxidation of Pd and contraction during reduction of PdO can have a detrimental impact on the microstructure of not only the metal, but also of surrounding ceramic [97].

Based on the effect of hydrogen, failures of MLCCs that have caused flight anomalies can be described as follows (see Fig. 6.2). Initially, due to some anomalies in the Ni plating process, a relatively thick Ni layer was formed and an excessive amount of hydrogen was generated at the terminals. The hydrogen diffused inside the ceramic and due to a high solubility of hydrogen in palladium (up to several percent [7]) accumulated mostly in the first electrode layers in areas close to terminals. Because the solubility of hydrogen in palladium decreases with temperature, heating of the parts during manufacturing, e.g. burning-in, can release some hydrogen that caused volumetric changes by oxide reduction, decreased adhesion and fracture toughness, and caused some relatively minor delaminations at the corner areas of the capacitors. A more severe heating during manual soldering or TSD350 simulation increased further delaminations by the same mechanism and also because of a relatively large tensile stresses created by expansion of thick Ni layers. Increased delaminations might facilitate formation of corner cracks caused by thermo-mechanical stresses during the soldering induced thermal shock. In the presence of moisture, electrochemical migration in cracks crossing opposite electrodes resulted in increased and unstable leakage currents. Reduction of PdO by hydrogen also facilitated electromigration of silver and electrical failures during biased testing.

Experience gained during MLCC manufacturing shows that cracking and delaminations caused by Ni plating occur more often with PME than with BME capacitors, which is due to a much higher level of hydrogen absorption in Ag/Pd electrodes compared to Ni electrodes. Absorbed hydrogen can also create a pop-corn-like effect during fast heating of capacitors that occurs during manual soldering of the parts.

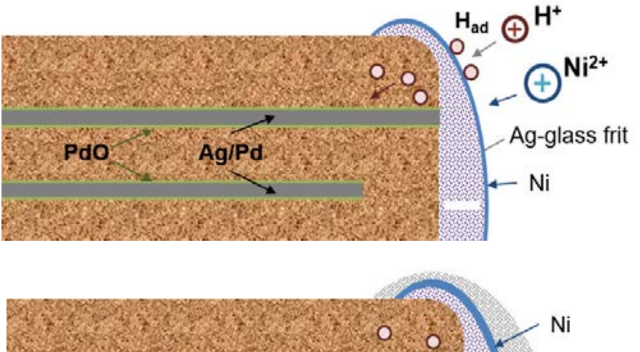

a) Electroplating of Nickel results in hydrogen generation at the surface and its diffusion inside the capacitor at the terminals.

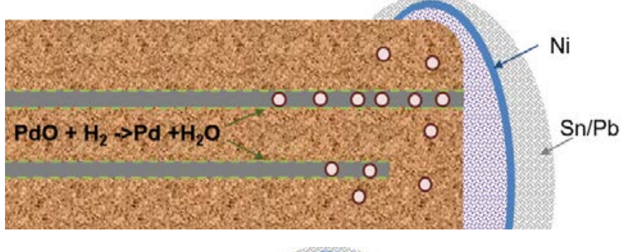

b) In the formed capacitors, hydrogen is mostly absorbed in electrodes close to the surface and terminations. Hydrogen absorption goes along with reduction of the protective PdO layer and decrease in metal-ceramic adhesion.

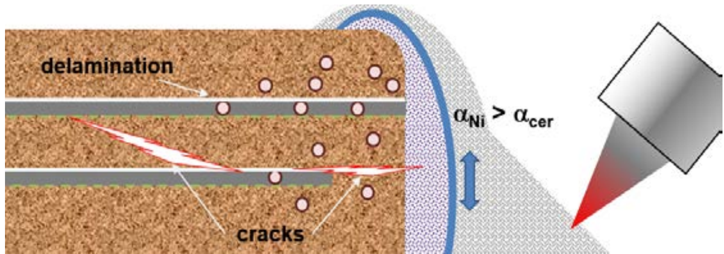

c) Manual soldering creates a thermal shock and together with mechanical stresses caused by the difference in CTE between Ni and ceramic, results in delaminations and cracking.

Figure 6.2. Schematic of the delaminations and cracking in MLCCs caused by hydrogen evolved during nickel electroplating.

6.2. Effect of pick and place machine

During automatic assembly processes, MLCCs are picked up by a vacuum tool or tweezers and either placed on bond pads with solder paste for reflow, or glued to the board in preparation for wave soldering. In either case, damage and crack formation in the parts are possible. A trend of rising the probability of damaging by the pick-and-place machine for small size (0402) ceramic components (capacitors and resistors) and possible techniques to assess the susceptibility to this kind of damage was discussed by S.Meyer at al. [81]. Stresses created by the pick-and-place machines might be not revealed by initial optical inspections and electrical testing, but cause failures during operations. In some cases, partially cracked components had electrical parameters within the specification, but their mechanical stability was compromised.

Testing techniques that can assess the tensile strength of SMD components have been suggested and used to differentiate damaged and faultless components. One of the techniques used was measurements of the impact strength to evaluate the critical energy of cracking for ceramic components. Another technique included measurements of the tensile strength that is similar to the flexural strength method (section 3.2), but uses a special fixture for small-size capacitors. A version of this test employs capacitors soldered onto PWB instead of loose parts in fixtures.

Results show that variations of the parameters of the pick-and-place tools (placement force and energy absorption in the spring systems) affected the tensile strength of 0402 SMD components. It was found that adjustments in the spring system of the pick-and-place equipment had the most significant effect on the probability of cracking and failures.

6.3. Electro-mechanical resonance

Class II and III dielectrics in MLCCs are ferroelectric materials that exhibit piezoelectric (generation of charges under stress) and reverse piezoelectric (formation of mechanical strain under applied electric field) effects. The reverse piezoelectric effect results in small, but measurable deformations in the capacitors. For example, ~ 0.75 μm displacement was detected in a 300 V, 9 μF capacitor at the rated voltage [109].

Rapid deformation under bias results in generation of acoustic waives when an AC signal is applied to polarized (biased) ceramic capacitors. At these conditions, a capacitor operates as a resonator and can be characterized by a series of resonance frequencies (see Fig. 6.3). The electro-mechanical resonance (EMR) effect is observed in all types of MLCC except for class I dielectrics and has a strong dependence on the DC bias.

The major resonance that corresponds to a maximum amplitude spike corresponds to the standing wave spread along the width of the capacitor. Independent on the part type and/or manufacturer, the major resonance frequency is determined by the width, W, of the capacitor and can be predicted using a simple relationship $f_{res} = v/(2W)$, where v is the sound velocity (longitudinal waves) in the ceramics. Experimental data illustrating the relationship between f_{res} and W are shown for X7R capacitors in Fig. 6.3. The results correspond to v ~4.1×10^3 m/sec, which is close to typical values for the sound velocity reported in literature [110].

Impedance spikes on the frequency dependence of biased MLCCs might not only result in excessive noise in the system, but cause a mechanical damage to the part and catastrophic failures. Such a failure has happened with stacked 9 μF 300 V capacitors used in a beam power supply system in the NEXT PPU project [109]. The part operated normally at ripple currents of 20 A p-p, frequency 200 kHz, and 80 to 160 V DC bias for many hours during multiple air and vacuum testing, but failed short circuit eventually after 345 hours of operation. Fig. 6.3.f shows the failed capacitor with a crack caused by the EMR effect in the part. Note, that the width of the capacitor corresponded to a resonance frequency of approximately 200 kHz that coincided with the operational frequency of the system.

Electro-mechanical resonances might be especially detrimental when capacitors are used in power applications and operate under large DC and ripple voltages. NASA/GSFC guidelines for selection of MLCCs [111] is warning about the EMR effect and suggests using impedance spectroscopy to make sure that the major resonance frequency is outside the range of operating conditions.

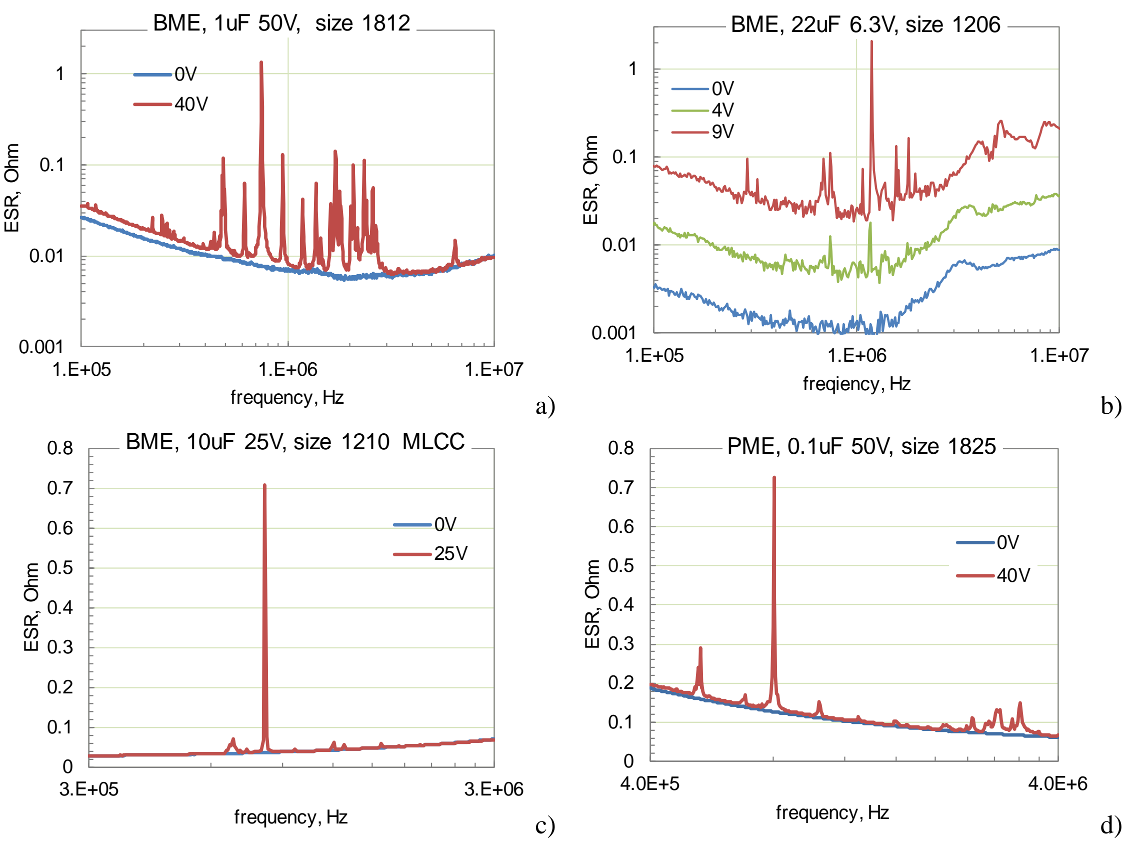

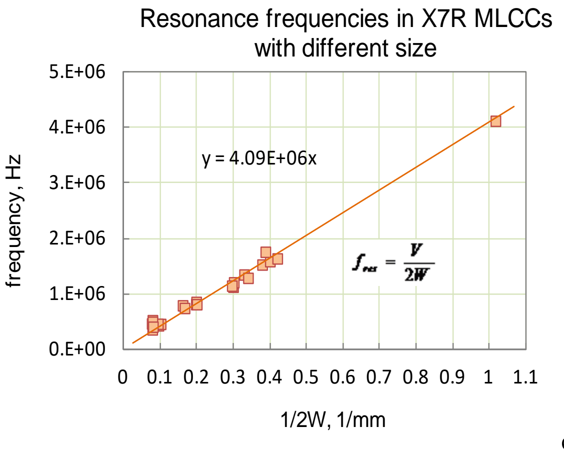

e)

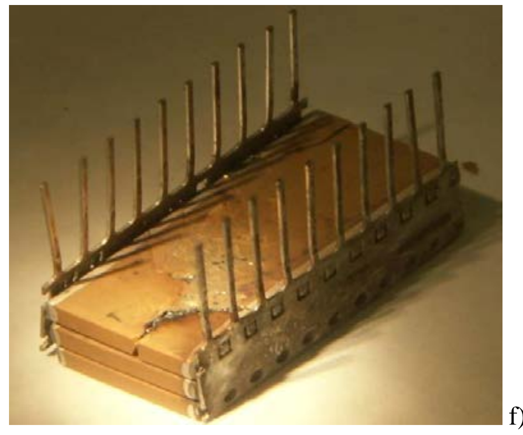
f)

Figure 6.3. ESR spectrums for different types of X7R capacitor with and without DC bias (a-d), variation of the major resonance frequency with the width of capacitors (e), and a 9 µF 300 V stacked ceramic capacitor that has been damaged when operating frequency was close to f_{res} (f).

7. Revealing cracks

Commonly used techniques to detect cracks include external visual examination, ultrasonic inspection, electrical measurements of capacitance, dissipation factors and IR. These techniques have been used for screening and qualification in military and space specifications and have been discussed in previous sections. It has been shown that they have a limited capability in detecting small cracks in MLCCs, are used mostly to reveal defects created during manufacturing and cannot be relied on to reliably detect damage caused by soldering and post-soldering stresses.

The most common technique to reveal cracks and delaminations is by ultrasonic microscopy that can reveal gaps even as small as ~ 0.1 µm. Until recently, this technique could be applied to horizontal cracks only, but Sonoscan has developed a method that images cracks and delaminations in unmounted MLCCs, regardless of their direction [69].

Although the latest development in X-ray imaging, especially using computer tomography 3D or CT-scan imaging system, have been used successfully in revealing flex cracking in assembled large size (1812) capacitors [112], more work has to be done to assess its sensitivity for smaller size capacitors with cracks caused by soldering.

A brief description of new or less frequently used methods that have been suggested for detecting cracks in MLCCs is given below. Although these methods have been successfully used in lab environments, none has been widely adopted for inspection by manufacturers and require further work and improvements. Nevertheless, they might be beneficial for end users during failure investigations or evaluation of new board designs, assembly processes or new technology components.

7.1. Optical examinations

• Vicinal illumination

Fine cracks are difficult or impossible to detect using standard visual inspection even using high-power microscopes due to the lack of contrast. Using dye penetrants and examinations under the black light illumination might be more effective, but contaminates the part. The effectiveness of optical inspection can be increased substantially by application of the vicinal illumination technique [113]. Examples of revealing cracks using vicinal illumination are shown in Fig. 7.1. This technique employs a high power bright field microscope with a small aperture. Light from a small bright spot on the ceramic is scattered by near-by cracks thus creating a sufficient contrast for easy detection. This technique is widely used for failure analysis of ceramic components, but it is time consuming because requires scanning of relatively large areas using small light spots (~200 µm) and high-power microscopes. For this reason, its application for screening purposes is limited. A restricted access to the parts soldered onto PWBs for the close proximity inspection using high-power microscopes limits application of this technique for soldered MLCCs.

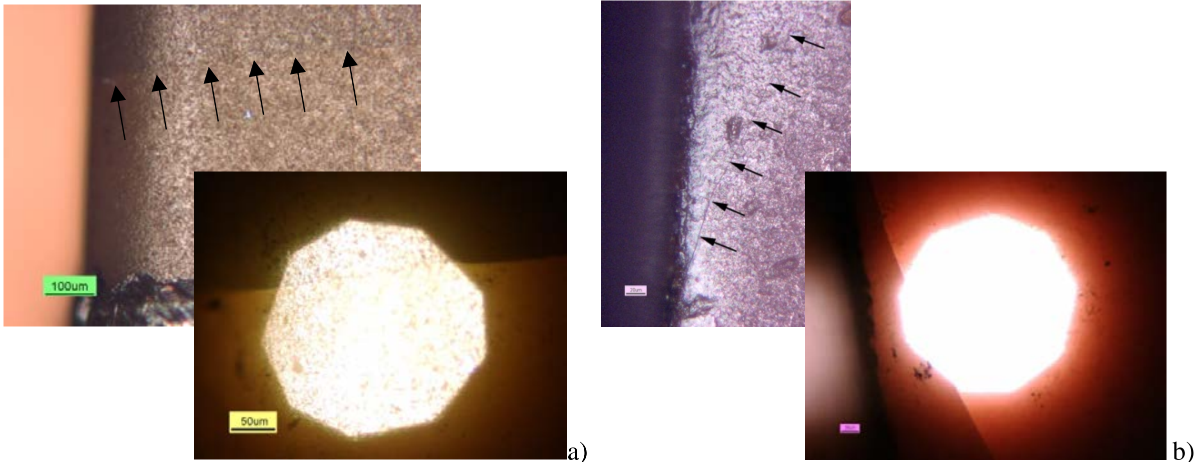

Figure 7.1. Examples of cracks exposed in MLCCs by the vicinal illumination technique. Top images show regular dark field high-power (X200 magnification) images of the cracks indicated by errors, and bottom images were obtained using vicinal illumination.

- Revealing delamination by discoloration of ceramic layers.

Optical examination of cross-sectioned samples during DPA might sometimes reveal discoloration of ceramic layers similar to those shown in Fig. 7.2. These discolorations were attributed to internal mechanical stresses formed during sintering and caused by the CTE mismatch between ceramic and metal electrodes. Cracks and delamination are formed with time when the stress is released. Formation of these defects might cause failures when terminal electrodes are not compact enough and do not block electroplating solutions from penetrating inside the capacitor. This phenomena affected mostly BME COG capacitors [26]. It was noted that the dielectric discoloration can be more easy found after terminal firing than after tumbling.

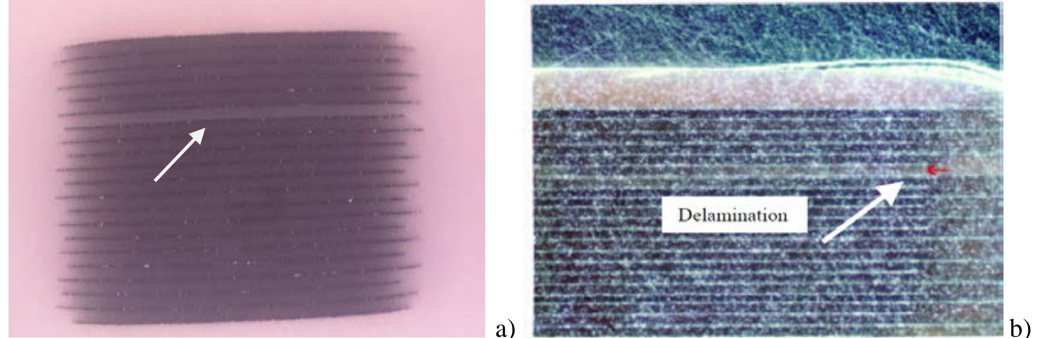

Figure 7.2. Discoloration in a dielectric layer of MLCCs revealed by a dark field inspection during DPA a) attributed to stresses [26], b) attributed to delamination [114].

7.2. Electrical measurements

Insulation resistance (IR) is a parameter sensitive to the presence of cracks, and in some cases up to 60% of damaged parts exhibit a detectable change in IR [115]. However, only a minority of MLCCs can be actually identified as potential failures before use. In addition, in-circuit tests can rarely apply sufficient voltage and/or time for realistic IR measurement. For capacitors soldered onto circuit cards, leakage through the circuit might be greater than through the capacitor, and the electrical problem may be intermittent [40]. Most functional tests of the assembled electronic cards are not sensitive to IR values, and many decoupling or EMC suppression capacitors may be damaged and defective without affecting circuit function in normal conditions initially.

The reason by which IR measurements might be not sensitive enough to the presence of fine cracks are discussed in section 4.2. A procedures that might improve the sensitivity of IR measurements for the cracks' detection and techniques that do not require measurements of leakage currents are described below.

- Methanol test

Methanol is a conductive, low-viscosity liquid with a perfect capillary action that allows penetration into tiny cracks in ceramics. A methanol test was used to further increase the sensitivity of leakage current (or IR) measurements to cracking [116]. During this test, the parts are preheated to 85 ˚C for 15 minutes and then immersed into methanol at room temperature for 3 minutes. DCL measurements were repeated after methanol removal and drying the part for ~1 minute. This test has been used successfully for revealing cracks in MLCCs; however, several factors may also lower the insulation resistance, thus obscuring the effect of cracks. These factors include contaminated cleaning solvents or large amounts of dissolved flux residue [115]. In several cases, application of methanol for parts with excessive DCL values decreased leakage currents, thus casting doubt on the effectiveness of this test [79]. It is possible that this was due to preheating at 85 ˚C that was used before immersing capacitors into methanol. Overall, the success of using methanol testing to reveal cracks was less than expected.

- Temperature dependence of capacitance

Exploiting thermal mismatch between the capacitor and the organic board to create tensile stresses and expand the crack in the part was used in [117] to reveal cracks by monitoring variations in capacitance with temperature. The idea of this technique is similar to flex testing, but instead of bending, the tensile force is created by the CTE mismatch between the capacitor and the board. However, class II and III dielectrics have a strong temperature dependence of capacitance that might obscure capacitance decay caused by damage.

- Time Domain Reflectometry (TDR)

Using TDR technique was suggested by M. Azarian to detect cracks in assembled MLCCs [118]. A short high-frequency pulse is applied by probes close to a capacitor, and a reflection of the signal that is detected at the input terminal can indicate the presence of cracks. A reliable detection of cracks was possible for large, case size 1812, capacitors with severe cracking. However, the testing was much less successful for smaller size capacitors (0805).

- Absorption voltage

A relatively poor sensitivity of traditional IR measurements to the presence of cracks is due to high level of absorption currents that prevail in MLCCs during first minutes after voltage application and mask currents related to cracks. However, time dependence of absorption voltages, V_{abs}, can be used to assess IR values related to the intrinsic currents in capacitors that are much lower than absorption currents.

The absorption voltage is due to releasing charges absorbed in the dielectric back to electrodes after a brief short circuit of a pre-polarized capacitor. When polarized at VR and then short-circuited for a few seconds, absorption voltages in X5R and X7R MLCCs typically increase within a few hours and can reach several volts. Subsequently, V_{abs} decreases slowly and can remain above one volt even after hundreds of hours (Fig. 7.3). The time to V_{abs} roll-off and the rate of voltage decrease are related to the leakage currents in the capacitor. A simple model that is based on the Dow equivalent circuit for capacitors with absorption allows for estimations of the insulation resistances in MLCCs that are not skewed by absorption currents [119]. The method is based on monitoring long-term variations of V_{abs} and allows for estimations of the insulation resistances up to 10^{14} Ω.

In the presence of cracks, the roll-off occurs earlier and maximum values of V_{abs} are substantially less than for virgin capacitors (see Fig.7.3a). Estimations of IR values for capacitors with cracks showed a substantial reduction compared to the values for virgin capacitors (see Fig 7.3.b). Note, that all damaged capacitors, except one, had IR exceeding 1 GΩ, which is acceptable per the existing requirements. Measurements of insulation resistance in MLCCs using a standard technique fail to reveal capacitors with cracks (see section 4.2), whereas the voltage absorption technique was effective in more than 70% of cases. However, the technique is time consuming and cannot be used for assembled capacitors.

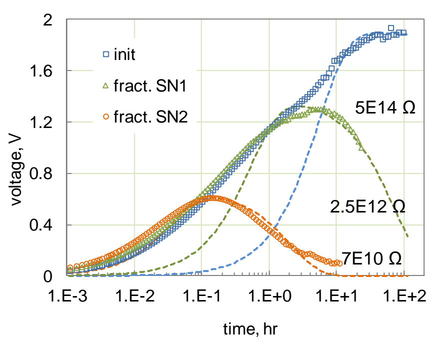

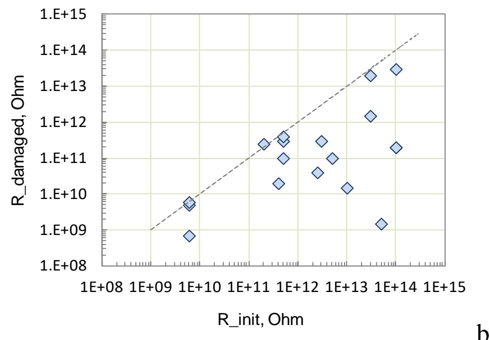

Figure 7.3. Absorption voltages in normal and damaged case size 1825, 0.1 μF 100 V capacitors (a) and effect of fracturing on IR, calculated based on absorption voltage model for 20 different types of capacitors (b). Dashed lines in (a) are calculations at the indicated values of IR and in (b) the dashed line corresponds to no-change values.

7.3. Electro-mechanical effects

Methods employing electro-mechanical effects are based on excitation and registration of mechanical waves in MLCCs by different techniques. Changes in the spectrum of the observed signals or in deformation of the part in the presence of cracks allow for revealing defective capacitors. These techniques include electromechanical resonance spectroscopy, resonance ultrasound spectroscopy, acoustic emission, and scanning laser interferometry.

- ### Variations of the electro-mechanical resonance spectrum

The spectrum of electro-mechanical resonances, similar to those shown in Fig. 6.3, is formed by the standing acoustic waves reflected from different interfaces. Cracks and delamination are additional sources for reflection and dissipation of acoustic energy and affect the spectrum. This effect was used by O. Boser at al. [110] to develop a non-destructive testing to reveal delaminations and cracks in capacitors. An automatic equipment for testing that can test a capacitor in 25 ms with 95% accept accuracy has been suggested.

Our experiments have confirmed that impedance spectroscopy might be sensitive to the presence of rough defects and cracks in capacitors. An example of variations in the spectrum shown in Fig. 7.4.a indicates that cracks introduced by the Vickers indenter on the surface of the part shift the resonance frequencies and substantially reduce the amplitudes of spikes. However, the changes in the amplitude and position of the spikes were much less noticeable for tiny cracks caused by thermal shock. Another problem with this method is that the spectrum depends on the prehistory of the part. In particular, long-term polarization can shift resonance frequencies with time even in defect-free capacitors (see Fig. 7.4.b).

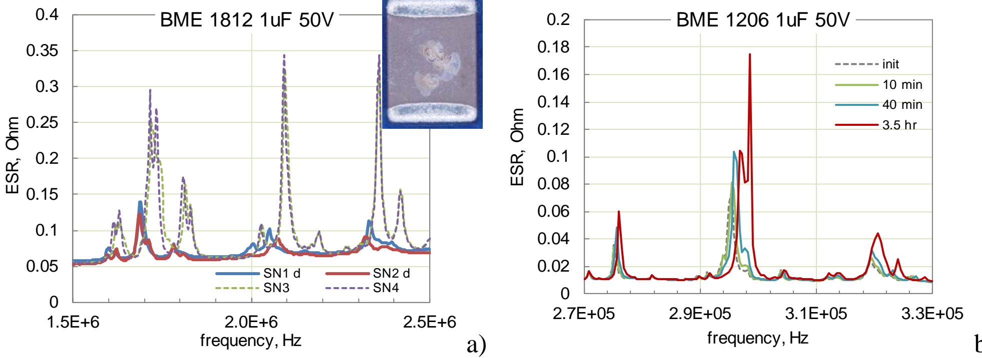

Figure 7.4. Electromechanical resonance spectrums. a) virgin (dashed lines) and capacitors with introduced cracks (solid lines). b) Spectrums in a virgin capacitor measured with time under 40 V bias.

- ### Resonant ultrasound spectroscopy (RUS)

Generation and detection of vibrational resonances in solids by resonant ultrasound spectroscopy (RUS) technique have been used to determine elastic properties of materials [120]. A version of the RUS method has been also

developped to detect cracks in MLCCs [121]. According to this technique, a driving transducer at a corner of a capacitor generates a range of vibrational frequencies that are detected by another piezoelectric transducer/receiver at the opposite corner of the part. To minimize damping effects due to transducer contacts, the two transducers hold the specimen with small contact areas at the diagonal opposing corners. The receiving spectrum is similar to those shown in Fig. 7.4 and indicate vibrational resonances in the capacitor that change their position and amplitude if cracks are present.

The benefit of this technique is that it does not require biasing of the capacitor and can be used for the parts soldered onto PWBs. RUS measurements made over the frequency range from 500 kHz to 3 MHz for virgin capacitors and capacitors subjected to thermal shock by the IWT (from 150 ºC to ice water) showed some changes in the spectrum. However, variations in the amplitude, contrary to the shift in frequency, might be also due to some changes in the position of the transducers. No significant changes in spectrums was detected after the flaws have been introduced by FIB milling and microindentation. It was assumed that the size of these flaws is too small to cause substantial changes in the resonant frequency. Apparently, more studies are necessary to increase the reproducibility of test results and sensitivity of this technique to tiny cracks.

- ### Tone-burst excitation

Phase analysis of electromechanical resonance with tone-burst excitation was used by Johnson at al. [122] to reveal cracks in X7R MLCCs. A ferroelectric transducer that generated radio-frequency tone bursts with durations of 0.2 ms in a 50 V capacitors biased at ~ 30 V formed mechanical waves in the part. The nonlinearity was quantified by shifts in resonant frequencies as a function of ferroelectric excitation level. Special algorithms of data analysis have been developed to characterize the non-linear effects in MLCCs. Acoustic non-linear measurements can provide data that are less sensitive to variations of frequencies but change significantly in the presence of defects. However, only 89 % of the MLCCs with visible cracks formed by the IWT (quenching preheated to189 ºC capacitors in ice water) have been detected. It is recognized that although the observed correlations indicate that nonlinear acoustic measurements offer a promising approach for nondestructive detection of cracks in MLCCs, further work to improve the level of detection should be pursued.

The technique was later upgraded by analysis of the dependence of phases and resonant frequencies on vibrational amplitude during ring down following the tone-burst excitation [123]. This improvement increased the proportion of detected MLCCs with visible cracks to 93%.

- ### Acoustic emission

Acoustic emission is a well known effect during breakdown events in capacitors. Measurements of acoustic signal caused by partial breakdown in capacitors with defects was used in [124] to screen out high voltage Z5U and X7R/BX capacitors with voids and delaminations. An AC-voltage-induced acoustic emission testing showed that the severity of delaminations correlates with the corresponding level of the acoustic signal.

Acoustic emission test for low-voltage MLCCs has been developed in [125]. Electrical pulses with amplitude of +-10V and duty cycle 80% applied to the parts soldered onto a PWB created vibration and resonances in capacitors. The pulses had frequency sweeps from 100 Hz to 2 MHz. The acoustic emission (in the megahertz range) induced by the electrical signal was measured directly from the component using a piezoelectric point contact sensor. Mechanical damage, such as flex cracks and delamination, changed acoustic behavior and was used to reveal MLCCs with defects. Acoustic signals were characterized with a numerical algorithm, and analysis has demonstrated that defects caused by the board bending affected the acoustic response. However, the precision and sensitivity of the acoustic measurements leave some room for improvement and more work is necessary to reduce errors and develop a technique that would detect capacitors with defects more reliably.

- ### Laser interferometry

A different technique to generate mechanical waives and detect the effect of cracks in MLCCs was suggested by Erdahl and Ume [126, 127]. A structural vibration was stimulated by a short, ~6 nsec, pulse of an infrared laser and the out-of-planer displacement of the surface was measured by a fiber-coupled laser interferometer (see Fig. 7.5a). Comparison of the waveforms between a reference, defect-free capacitor and device under test (see Fig. 7.5b) allows for revealing capacitors with defects. Because vibration of a capacitor depends on the attachment conditions, both,

the reference and the tested device should be attached to the same board in the same soldering process. A special signal processing technique improves the sensitivity of this method that had been successfully used for small size (0805 and 0603) capacitors.

The method can be automated and used for online quality assurance of MLCCs after soldering in mass production environments. The lack of reference capacitors on the board and insufficient statistics might limit application of this test for low-volume production of circuit assemblies. Although this method was able to detect flex cracks intentionally introduced in MLCCs, further testing and analysis are required to account for possible process-induced manufacturing variations.

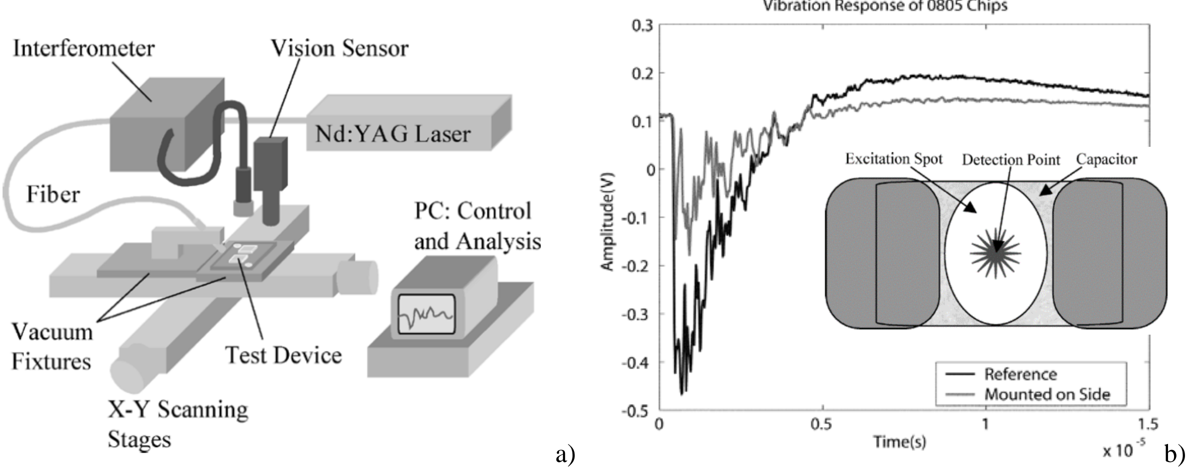

Figure 7.5. Set-up of the laser ultrasonic quality inspection system (a) and a time-domain vibration response (b). The insert shows a capacitor with laser excitation and measurement spots.

8. Cracking caused by manual soldering

Due to the process variations and dependence on operator skills, possible formation of significant temperature gradients, and deviations in the amount of solder, all manufacturers strongly discourage the use of hand soldering for MLCCs. However, due to the low volume production manual soldering is a common process for space electronic assemblies and hybrid microcircuits. In some cases, large size capacitors cannot be positioned using pick-and-place tools, and have to be soldered manually. In addition, high cost of the boards makes rework necessary in case of failures.

Experiments show that manual soldering have a detrimental effect on MLCCs with preexisting cracks [34]. A much greater proportion of case size 1825 capacitors failed environmental stress testing after manual soldering compared to the parts tested in fixtures. For different part types, the times to failure (TTF) during humidity testing of manually soldered capacitors decreased by one to three orders of magnitude in comparison with similar capacitors that have been tested in mechanical fixtures.

The risk of cracking during hand-soldering is increasing with the size of capacitors. J.Maxwell [11] suggested to "never use soldering irons" for parts with a case size of more than 1210. However, even small size capacitors (0603) might have a high probability of fracturing after hand soldering [128].

Volume of publications discuss the susceptibility of MLCCs to cracking caused by manual soldering. However, there is a lack of technical literature that analyses stresses during the attachment with soldering iron and describes physical mechanisms of cracking and failures.

In general terms, cracking in MLCCs occurs when the sum of internal stresses built during manufacturing and external stresses caused by soldering exceeds the strength of the part. Assuring that the level of soldering stresses is at the acceptable level is a workmanship issue and requires compliance with the existing guidelines. Assuring that MLCCs can withstand soldering stresses (have low built-in stresses and a high strength) is a part's issue and should be achieved by adequate selection and qualification tests. Commonly used workmanship requirements and suggestions for

qualification tests to assess the robustness of MLCCs are described below. The workmanship requirements are based on decades of industry practice and studies, are well-developed and documented. However, procedures that would allow selection of the most robust to manual soldering capacitors has not been sufficiently developed yet.

8.1. Workmanship recommendations for manual soldering

The international standards for rework, modification and repair of electronic assemblies, IPC-7711C/7721C and IPC J-STD-001G [129, 130] warn against touching components by the soldering iron and recommend preheating and limiting temperature heating rate to below 2 - 4 °C/sec to avoid thermal shock conditions. However, it does not provide any specifics related to the hand soldering procedures for MLCCs and refers to manufacturers' data sheets for additional information.

NASA and ESA guidelines for manual soldering [131-133] are mostly applicable to connectors and also lack information related to MLCCs. JAXA [47] has a more specific guidelines for manual soldering that mostly follow recommendations by Murata and TDK.

Most manufacturers of MLCCs (see for example, [5, 31, 134, 135]) have similar guidelines to reduce the risk of cracking in case of rework or hand-soldering. These recommendations can be summarized as follows:

1. Direct contact by a soldering iron tip often causes thermal cracks, so the tip should be applied to the contact pad only. Use a soldering tip no greater than 0.120" [3.0 mm] in diameter, and transmit the heat through the soldering material to prevent contact with MLCC. The power of the soldering iron should be limited to 30 W (some manufacturers allow up to 60 W), and the duration of the process should not exceed 5 sec (preferably, a few seconds).
2. If lands are different, solder the smaller land first, and remove the tip quickly when the fillet is formed. The fillet should have a concave profile and be at least 25% of the chip height. Excess solder might cause mechanical stresses on components, increase the probability of flex cracking and thereby diminishing reliability. All thermal shock studies supported a moderate amount of solder, with excessive solder leading to a greater susceptibility to fault.
3. Compared to local heating with a soldering iron, air heaters result in a more uniform temperature distribution and a lesser thermal shock, so the hot air approach provides a more benign hand solder technique compared to soldering iron. Murata suggests setting a hot air outlet at a temperature 400 °C, application of the tool at a distance more than 5 mm and at the angle of 45° for less than 10 sec. When removal of a chip capacitor is necessary, a hot air pencil is the preferred tool.
4. After soldering, allow the chip to cool at room ambient conditions. Using forced cool air or refrigerated air for expediting the cooling process is not recommended and can create thermal shock cracks.
5. Some manufacturers specify different tip temperatures for different size capacitors. For example, ESA limits the maximum tip temperature, T_{max}, to 340 °C [133], Murata allows T_{max} 350 °C for capacitors of size 1206 and less and 280 °C for larger parts, whereas ATC limits tip temperature to 285 °C for all parts. Panasonic requires 270 °C for size 0805 capacitors and smaller and below 250 °C for size 1206 to 1812. It is unlikely that this difference is due to different thermal resistance and quality of the product from different manufacturers. Most probable, it reflects different experience with field failures and possibly different techniques used for testing. In any case, it would be reasonable to use the lowest tip temperature setting possible.
6. Preheating of the board and capacitor is likely the most important condition for safe soldering. Most recommendations suggest preheating by a hot plate or hot air flow to 150 °C minimum. Some manufacturers call for different preheating temperatures for different size capacitors. Panasonic requires preheating to a temperature that is 150 °C below the soldering temperature (the delta temperature, ΔT = 150 °C) for case size 1206 and smaller and 130°C for 1210 to 1812. Novocap suggests ΔT = 100 °C for case size 1812 and smaller and 50 °C for larger than 1812. According to Johanson Dielectrics ΔT should be approximately 100 °C. Some internal OEM guidelines suggest ΔT as low as 40 °C. Apparently, low ΔT values would improve safety of the process but might be harmful to other components on the board. During rework, the populated and tested boards cannot be exposed to high temperatures, so in practice the preheating temperature and possible level of ΔT should be determined in each case separately.

To illustrate the effect of preheating, several groups of case size 0603 BME 0.01 µF, 25 V capacitors have been soldered onto similar FR4 boards using manual and reflow soldering. Manual soldering was carried out with different tip sizes (0.03” and 0.08”) and different preheating temperatures of the board: cold (22°C) and hot (150 °C). After soldering, the parts were inspected visually and tested for breakdown voltages. Results of the inspection and measurements are displayed on Fig. 8.1. Visual examinations and cross-sectioning confirmed formation of cracks in capacitors manually soldered onto a cold PWB, whereas no defects were observed in MLCCs after solder reflow and after manual soldering onto a board preheated to 150 °C. Soldering iron tips of larger size increased the probability of failures during manual soldering from ~20% for 0.03” to ~70% for 0.08”.

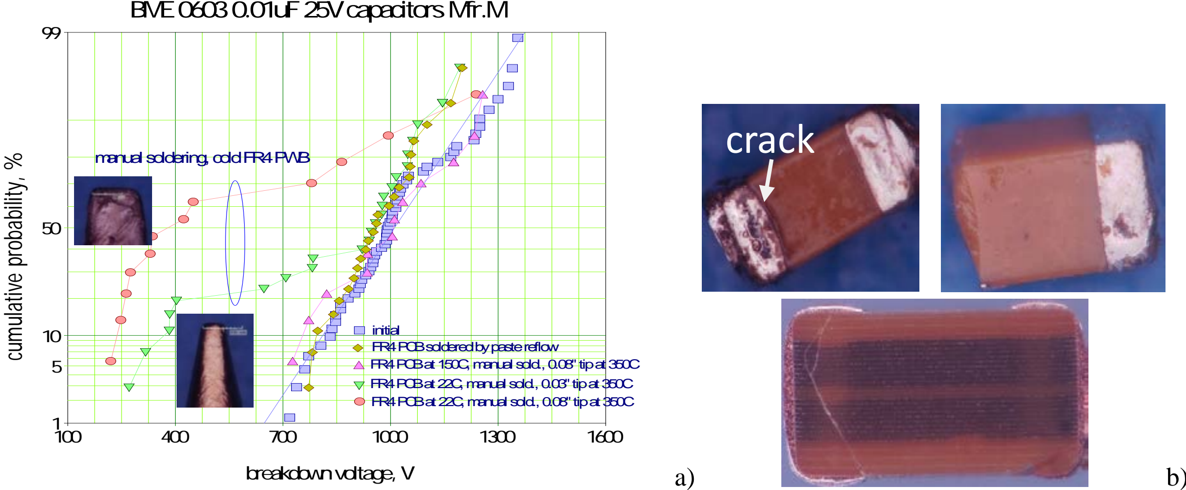

Figure 8.1. Distributions of breakdown voltages in 25 V, size 0603 capacitors (a) and examples of failed parts (b). MLCCs have been soldered onto FR4 boards using four methods: (i) standard reflow, (ii) assembly onto a PWB preheated to 150 °C using a soldering iron with 0.08” tip at 350 °C, (iii) manual soldering onto a cold PWB using a 0.08” tip at 350 °C, and (iiii) manual soldering onto a cold PWB using a 0.03” tip at 350 °C.

- Effect of touch-up

A touch-up with a soldering iron is often used after reflow soldering to improve appearance of the solder fillets and make them look nice and in compliance with the workmanship requirements. One of the reasons of cracking during the touch-up is thermal shock. Similar to manual soldering, hot air pencil creates lesser temperature gradients and is preferable for touch-up to soldering iron.

Another reason of cracking caused by the manual touch-up with a soldering iron is related to CTE mismatch between the board and ceramic capacitor. During the touch-up on a cold board, the capacitor heats up instantly and slightly expands (ΔL in Fig. 8.2a). After solidification of the solder, the capacitor tries to shrink back, but its deformation is limited by the board, so tensile stresses develop. An example of a touch-up induced cracking in a case size 0402 capacitor is shown in Fig. 8.2.b.

Because CTE of the board is greater than of a ceramic capacitor, compressive stresses in the part develop after reflow soldering. Ceramic materials can tolerate compressive stresses that are approximately an order of magnitude greater than tensile stresses and normally, no failures occurs after reflow soldering. However, formation of tensile stresses after touch-up might increase the probability of cracking substantially. If improvements in soldering and touch-up are necessary, preheating might be still useful because it expands the board and thus reduces the stress that can be relaxed during the following slow cooling because of creeping and stress relaxation in solder.

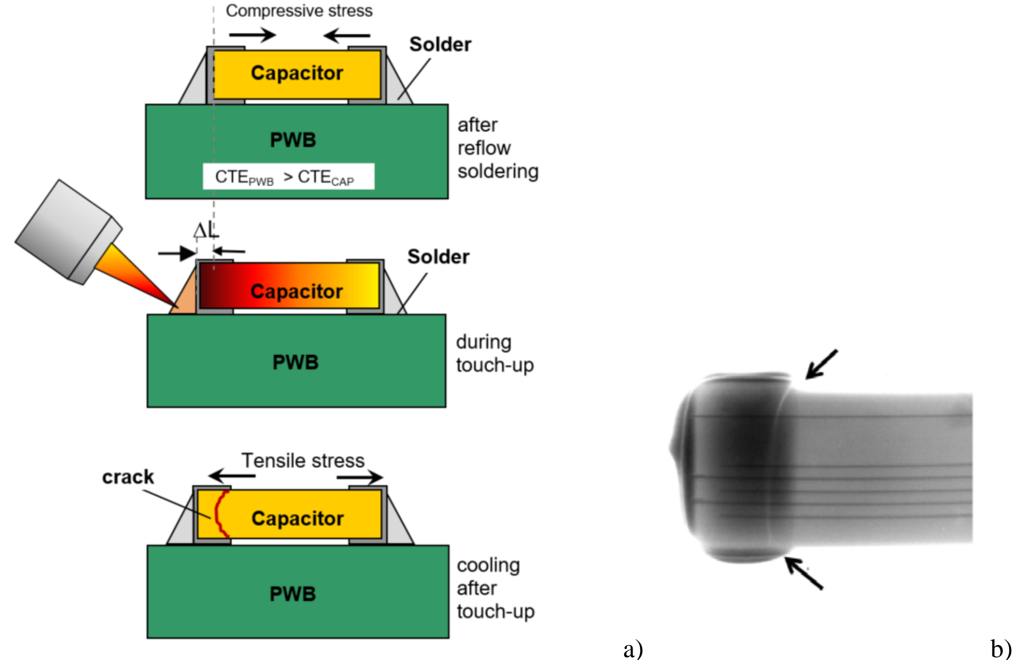

Figure 8.2. Formation of cracks caused by touch-up with a soldering iron (a) and an example of cracks formed by touch-up in X7R case size 0402 1000 pF 50 V capacitors (b).

8.2. Selecting capacitors robust to manual soldering

Data presented in this report show that no single inspection or testing provides reliable information regarding the susceptibility of a lot of capacitors to cracking. However, some tests have been shown to have a greater sensitivity than the others. These tests include monitoring of leakage currents during humidity testing after temperature cycling for capacitors soldered onto PWBs, acoustic microscopy, analysis of distributions of MOR, DF and IR. Another useful test that is described below is the terminal solder dip testing (TSD). A combination of these tests can be used to select the most robust to manual soldering capacitors and mitigate risks of failure.

- ### Terminal solder dip testing

Solder dip testing that is used in military and space applications requires immersing into molten solder at a relatively low temperature (230 °C) that is typically less than the temperature of the soldering iron and simulates wave soldering conditions rather than thermal stresses specific to manual soldering.

The terminal solder dip test is a modification of the standard solder dip testing that can be used to simulate conditions of manual soldering more adequately [136]. During this test, one terminal of a capacitor is clamped in a fixture while the other is touching molten solder (see Fig.8.3). This eliminates local pressure to ceramic and unpredictable changes in the temperature distribution caused by application of tweezers, stabilizes temperature at the clamped terminal, and creates a significant temperature gradient at another terminal. Experiments with the solder pot temperatures varying from 300 °C to 350 °C showed that practically no failures of large size capacitors occur at 300 °C, some cracks appear at 325 °C, and a much better discrimination of the lots regarding their robustness to soldering stresses can be achieved at 350 °C, TSD350 test. The latter condition also corresponds to the maximum soldering iron temperature recommended by manufacturers and is still less than the temperatures used sometimes during assembly of hybrid microcircuits (up to 400 °C).

During TSD350 testing, one terminal of each capacitor is dipped for 3-5 seconds into a pot of molten solder heated to 350 °C and then the parts are left to cool at room temperature for ~2-3 minutes. Typically, the dipping and cooling procedures are repeated three times for each part, after which all capacitors are examined visually and electrically.

Experiments using different lots of X7R MLCCs from five vendors using large size, (from 1210 to 2220) with 10 to 20 samples in a group showed that approximately half of the 26 tested lots can pass TSD350 without cracking (Fig

8.3.b). Approximately 60% of lots had less than 10% of cracks but ~ 20% had more than half of capacitors with cracks. Note that post TSD350 environmental tests in humidity chamber showed that not all capacitors with cracks have electrical failures. Obviously, shallow cracks that are not affecting active areas of capacitors do not cause failures.

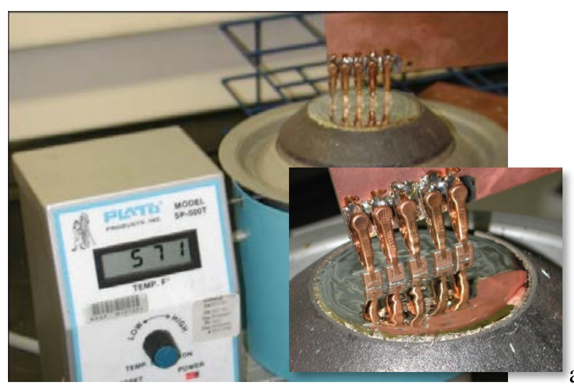

a)

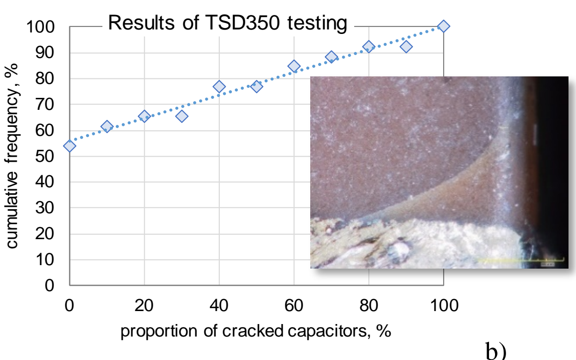

b)

Figure 8.3. A set-up for terminal solder dip testing with a simple fixture that can be used to test 5 samples at a time (a) and distribution of the percentage of lots of capacitors having a certain proportion of cracks after TSD350 based on testing of 26 lots (b). The insert in (b) shows a typical crack caused by TSD350 testing.

A relatively high robustness of MLCCs toward solder dip testing is mostly due to a high compressive strength of ceramic materials. Also, an increased thermal conductivity of capacitor along the metal plates mitigates the effect of high temperature gradients developed when the heat from molten solder is transferred to MLCC.

Two groups of tested capacitors were from two case studies when a large proportion of capacitors that have been soldered manually onto the flight cards had cracks. These cards had been reworked and MLCCs had been replaced with similar CDR-style capacitors from other batches. No cracking was observed on the cards after rework. Twenty virgin capacitors from the failed lots, as well as samples from the replacement lots have been tested by TSD350. In the first case, capacitors from the failed lot had 55% of failures whereas reference parts had zero failures. In the second case, all 20 samples from the failed lot had severe cracking, whereas only one shallow crack out of 20 samples had been detected in parts from the replacement lot.

Results show that different lots of military grade MLCCs might have different susceptibility to fracturing during manual soldering and TSD350 testing can reveal this difference.

- ## Assessment of the susceptibility to cracking

Tests and inspections that can be used for revealing MLCCs with cracks include temperature cycling after soldering onto test boards followed by monitored humidity testing, TSD350, and ultrasonic inspections (C-SAM). A combination of these tests is likely the most effective means to assess the robustness of MLCCs toward manual soldering stresses. Several types of tests that might be used for different level projects are presented in Fig. 8.4. Here, L1, L2, and L3 correspond to different levels of projects as they are defined in [137]. Note, that the criticality of MLCCs' applications should be also considered, and in cases when short circuit of a capacitor would result in a single point failure and/or significant loss of the system's functions, the level of scrupulosity during testing should be increased. Also, large size PME capacitors are especially sensitive to cracking under manual soldering and require extra precautions.

Groups of 20 samples minimum are suggested for test flows described below. For level 1 projects, a test flow in Fig. 8.4.a that includes manual soldering onto a test PWB that simulates actual soldering conditions is preferable. However, when details of soldering conditions are not known, the parts might be stressed by TSD350 as described in the flow in Fig. 8.4.b. One of the benefits of the second option is that it does not require soldering onto a board and thus eliminates problems with faulty leakage currents along the board during humidity testing.

For level 2 projects (Fig. 8.4.c), TSD350 can be also optional, and can be replaced by actual manual soldering onto a test board. A simple visual examination and electrical measurements after TSD350 are suggested to mitigate risks of failures for level 3 projects (Fig. 8.4.d).

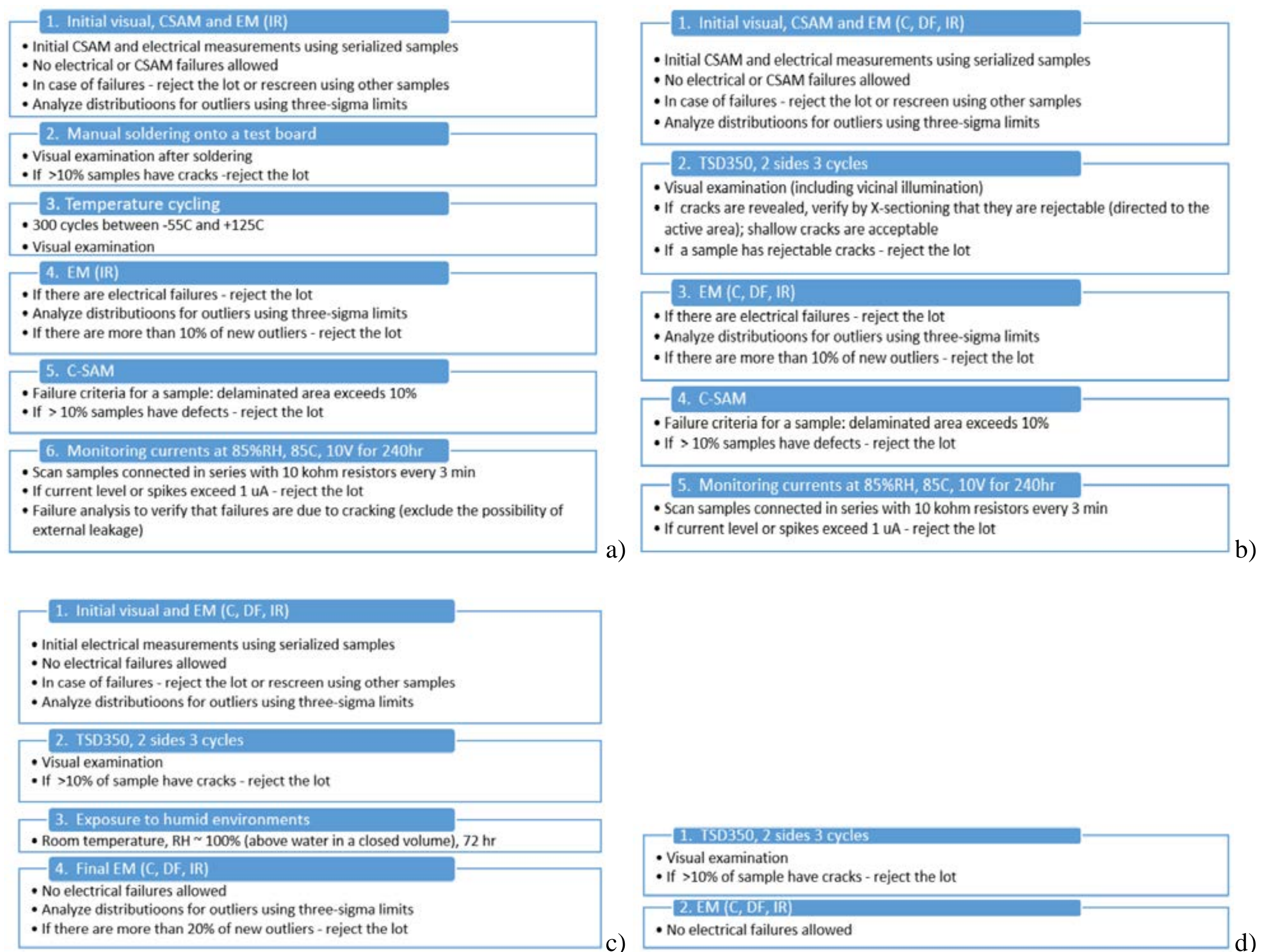

Figure 8.4. Test flows for the resistance to manual soldering testing for different level projects: L1 (a) –preferred, (b)-optional, L2 (c), and L3 (d) projects.

9. Conclusion

High-temperature manufacturing processes and materials with different CTEs that are used in MLCCs result in significant built-in mechanical stresses. Deviations from the optimal conditions and some anomalies in the manufacturing process might form hidden defects and reduce the strength of the parts. Additional thermo-mechanical stresses associated with soldering and post-soldering handling of the assemblies can increase stresses to the level sufficient for cracking. These cracks might not affect performance of the system initially, but result in failures with time of operation.

The existing military and space specifications are focused mostly on the quality of as build capacitors and do not address properly effects of soldering and post soldering stresses. Improvements in the existing qualification procedures and using tests that would reflect adequately environmental stresses experienced by capacitors after assembly is necessary to reduce risks of failures during applications.

In spite of substantial efforts that have been made to develop methods for revealing cracks in MLCCs after soldering, none is universal and can detect defective parts reliably.

Replacement of large size PME capacitors with a smaller size, thin dielectric BME capacitors with flexible terminations might reduce risks of cracking and failures in space systems.

The probability of cracking caused by manual soldering depends on the level of external stresses that is controlled by the workmanship and the robustness of MLCCs that depends on the level of built-in stresses, presence of defects and mechanical strength, and is lot-related. To mitigate risks of manual soldering and reduce the probability of cracking-related failures both, a tighter workmanship control and selection of parts robust against manual soldering stresses is necessary. Procedures to select MLCCs most resilient to manual soldering are suggested.

10. References

[1] A.Fletcher. (2018). *Restricted MLCC supply focuses on re-design activity*. Available: https://www.electronicspecifier.com/around-the-industry/restricted-mlcc-supply-focuses-on-re-design-activity[7/1/2018

[2] P. Ming-Jen and C. A. Randall, "A brief introduction to ceramic capacitors," *Electrical Insulation Magazine, IEEE,* vol. 26, pp. 44-50, 2010

[3] D. Brown, "Oxygen vacancy migration in MLCCS," in *2018 Pan Pacific Microelectronics Symposium (Pan Pacific)*, 2018, pp. 1-6.

[4] C.Hendricks, "Concerns with the long term reliability of MLCC for decoupling," presented at the Reliability and Energy Storage in Capacitors Workshop, Center for dielectric studies, PSU, 2011.

[5] L. Lambert. (2014). *Damage Prevention When Soldering Ceramic Chip Capacitors* Available: http://www.eptac.com/webinars/presentations/eptac_09_17_14.pdf

[6] D. M. Zogbi, "ELECTRONIC COMPONENTS FOR THE DEFENSE & AEROSPACE SECTOR: WORLD MARKETS, TECHNOLOGIES AND OPPORTUNITIES: 2017-2022," in *Paumanok Publications, Inc.*, 2018,

[7] "The Reliability of Multilayer Ceramic Capacitors, report NMAB-400," Washington DC 1983,

[8] A. Teverovsky, "Thermal Shock Testing and Fracturing of MLCCs under Manual Soldering Conditions," *IEEE Transactions on Device and Materials Reliability* vol. 12, pp. 413-419, 2012

[9] D. L. Kinser, S. M. Graff, and S. V. Caruso, "The relationship between reliability and bonding techniques in hybrid systems," *IEEE Transactions on parts, hybrids, and packaging,* vol. PHP-11, pp. 195-201, Sept. 1975 1975

[10] B. Sloka, D.Skamser, A. Hill, M. Laps, R. Grace, J. Prymak*, et al.*, "Flexure Robust Capacitors," in *The 27th symposium for passive components, CARTS'07*, Albuquerque, NM, 2007.

[11] J. Maxwell. (2006). *Capacitor Cracks: Still with Us after All These Years*. Available: http://www.johansondielectrics.com/technicalnotes/cra/

[12] S. Haishan and C. Shoutian, "Charge-discharge breakdown of dielectric ceramic," in *6th Intemational Conference on Properties and Applications of Dielectric Materials*, Xi'an, China, 2000, pp. 1029-1032.

[13] L. Bin, C. Wei, Z. Yajie, and C. Shoutian, "Distribution regularity of breakdown field strength of high voltage ceramic capacitor," in *Proceedings of the 6th International Conference on Properties and Applications of Dielectric Materials, 2000.*, 2000, pp. 1037 - 1040.

[14] J. Maxwell, "Cracks: the hidden defect," in *Proceedings of the 38th Electronics Components Conference*, 1988, pp. 376-384.

[15] T. Brennan, "Ceramic Capacitor Insulation Resistance Failures Accelerated by Low Voltage," *IEEE transactions on electron devices,* vol. ED-26, pp. 102-108, 1979

[16] B. V. Hiremath, "Evaluation of tumbling processes of multilayer ceramic capacitors for surface mount device applications," *IEEE Transactions on Components, Hybrids, and Manufacturing Technology,* vol. 16, pp. 822-827, 1993

[17] J. Maxwell. (2007). *Basics of Ceramic Chip Capacitors*. Available: https://www.johansondielectrics.com/downloads/jdi_mlcc-basics_2007-12.pdf

[18] EIA-198-1, 2002, Ceramic Dielectric Capacitors Classes I, II, III and IV – Part I: Characteristics and Requirements, https://ewb.ihs.com/#/document/VYVRABAAAAAAAAAA?qid=636682241794939520&sr=re-1-10&kbid=4%7C20027&docid=941257214#h961943d3

[19] R. C. Buchanan, *Ceramic materials for electronics*: Marcel Dekker, Inc, 2004.

[20] Tutorial, "Passive Electronic Component Reliability and Selection Criteria," in *CARTS*, Las Vegas, NV, 2012.

[21] H. Kishi, Y. Mizuno, and H. Chazono, "Base-metal electrode-multilayer ceramic capacitors: Past, present and future perspectives," *Japanese Journal of Applied Physics Part 1,* vol. 42, pp. 1-15, Jan 2003 <Go to ISI>://WOS:000181161300001

[22] "Recent Topics in the Field of Ferroelectric Materials for BME-MLCCs," in *Proceedings of the 12th Pacific Rim Conference on Ceramic and Glass Technology*, ed, 2018.

[23] M. R. Opitz, K. Albertsen, J. J. Beeson, D. F. Hennings, J. L. Routbort, and C. A. Randall, "Kinetic Process of Reoxidation of Base Metal Technology BaTiO3-Based Multilayer Capacitors," *Journal of the American Ceramic Society,* vol. 86, pp. 1879-1884, 2003 https://onlinelibrary.wiley.com/doi/abs/10.1111/j.1151-2916.2003.tb03576.x

[24] J. Maxwell, "Understanding Ceramic Capacitor Terminations," 2006, http://www.johansondielectrics.com/technical-notes/general/understanding-ceramic-capacitor-terminations.html.

[25] L. A. Mann, S. P. Gupta, and L. G. Jones, "The Influence of Termination Properties on the Thermal Shock and Thermal Cycle Performance of Surface Mount Multilayer Ceramic Capacitors," in *Electronic Components and Technology Conference*, 1991, pp. 437-441.

[26] P. Xiao, Z. Tan, and Y. Deng, "Analysis on Discoloration of MLCC Dielectric in DPA," in *CARTS USA*, Jacksonville, Florida, USA, 2009, pp. 289-297.

[27] J. W. Park, J. H. Chae, I. H. Park, H. J. Youn, and Y. H. Moon, "Thermo-mechanical stresses and mechanical reliability of multilayer ceramic capacitors (MLCC)," *Journal of the American Ceramic Society,* vol. 90, pp. 2151-2158, Jul 2007 <Go to ISI>://WOS:000247756500028

[28] A. Teverovsky, "Susceptibility to Cracking of Different Lots of CDR35 Capacitors," NASA/GSFC, Greenbelt, MD, NEPP report 2017, https://nepp.nasa.gov/files/29210/NEPP-TR-2018-Teverovsky-CDR35-Capacitors-TN52049.pdf

[29] B. S. Rawal, R. Ladew, and R. Garcia, "Factors responsible for thermal shock behavior of chip capacitors," *AVX technical information,* 1987 http://www.avx.com/docs/techinfo/factors.pdf

[30] D. K. Eli Bershadsky. (2016). *Vishay Vitramon MLCC End Termination*. Available: https://www.vishay.com/docs/45063/tn0029.pdf

[31] Murata, 2017, Chip Multilayer Ceramic Capacitors for Automotive, https://www.murata.com/~/media/webrenewal/support/library/catalog/products/capacitor/mlcc/c03e.ashx?la=en-us

[32] C. A. J.Prymak, P.Blais, "Flexible termination - reliability in stringeent environments," presented at the 29'th Passive Components Symposium, CARTS USA, Jacksonville, FL, 2009. https://www.mouser.com/pdfdocs/FlexibleTerminationAbstract.pdf

[33] TDK-Tech_Notes, Flex crack contermeasures in MLCCs, (https://product.tdk.com/info/en/products/capacitor/ceramic/mlcc/technote/solution/mlcc02/index.html

[34] A. Teverovsky and J. Herzberger, "Humidity Testing of PME and BME Ceramic Capacitors with Cracks," in *CARTS International*, Santa Clara, CA, 2014, pp. 15-29.

[35] EIA-469_D, 2006, STANDARD TEST METHOD FOR DESTRUCTIVE PHYSICAL ANALYSIS (DPA) OF CERAMIC MONOLITHIC CAPACITORS,

[36] R. Demco, "Ni Electrode for Auto Grade and High Reliability Applications," in *Components for Military and Space Electronics, CMSE'15*, Los Angeles, CA, 2015, p. 3.1.

[37] J. Marshall, "Ceramic Capacitor B.M.E. Technology and future developments for Space, Military Applications," in *21st Components for Military and Space Electronics, CMSE'17*, Los Angeles, CA, 2017, p. 2.6.

[38] KEMET, 2008, Flex Crack Mitigation, Tech Topic, https://www.mouser.com/pdfdocs/TechnicalOverviewofFlexMitigationSolutions.pdf

[39] TDK, 2013, High Reliability Automotive Use MLCCs, https://product.tdk.com/en/techlibrary/archives/vol06_mlcc/TDK_TJ_CAR_E_0711.pdf

[40] Tayloredge, Failure mechanisms in ceramic capacitors, https://www.tayloredge.com/reference/Electronics/Capacitors/MLC_FailureMechanisms.pdf

[41] D. Friedlander, "The use of COTS components in space: debunking 10 myths," *Intelligent aerospace,* July, 5 2017 https://www.intelligent-aerospace.com/articles/2017/10/electrical-electronic-and-electromechanical-cots-components-in-space-penalizing-policy.html

[42] D. Friedlander, "COTS in space: the 100 percent testing risk," *Intelligent aerospace,* November, 13 2017 https://www.intelligent-aerospace.com/articles/2017/10/electrical-electronic-and-electromechanical-cots-components-in-space-penalizing-policy.html

[43] NASA_GSFC, 2015, SPECIFICATION CONTROL DRAWING Capacitor, Ceramic, Multilayer Chip, Space Applications, S-311-P-829, http://www.presidiocomponents.com/products/S-311-P-829-Rev-J.pdf

[44] NASA_GSFC, 2016, SPECIFICATION CONTROL DRAWING Capacitor, Ceramic, Multilayer Chip, Space Applications, S-311-P-838, https://nepp.nasa.gov/files/27161/S-311-P-838A.pdf

[45] ESCC-3009, 2017, CAPACITORS, FIXED, CHIPS, CERAMIC DIELECTRIC, TYPES I AND II, ESCC Generic Specification No. 3009, https://escies.org/download/specdraftapppub?id=3232

[46] JAXA-QTS-2040/M, 2016, "CAPACITORS, MINIATURE, HIGH-CAPACITY, SURFACE MOUNT, FINE CERAMIC DIELECTRIC (J2040/M105), HIGH RELIABILITY, SPACE USE, DETAIL SPECIFICATION FOR", https://eeepitnl.tksc.jaxa.jp/en/qts/q_level_1/QAE2040_M105B.pdf

[47] JAXA-ADS-2040/M105, 2012, "APPLICATION DATA SHEET FOR COMMON PARTS/MATERIALS, SPACE USE", https://eeepitnl.tksc.jaxa.jp/en/ads/a_level_1/AAE2040_M105.pdf

[48] AEC-Q200, 2010, STRESS TEST QUALIFICATION FOR PASSIVE COMPONENTS, AEC-Q200 REV D, http://www.aecouncil.com/Documents/AEC_Q200_Rev_D_Base_Document.pdf

[49] MIL-STD-690, 2013, FAILURE RATE SAMPLING PLANS AND PROCEDURES, https://landandmaritimeapps.dla.mil/Downloads/MilSpec/Docs/MIL-STD-690/std690.pdf

[50] D. Liu, "How to Select/Screen/Quality Conformance Inspection (QCI) BME Capacitors for Space Applications," presented at the ETW, NASA/GSFC, 2013. https://nepp.nasa.gov/files/24681/Liu_2013_n217_NEPPETW_Pres_QCI.pdf

[51] "JAXA Report," in *G-12 Meeting*. San Antonio, TX, 2012,
[52] Y. Yamada, "Introduction of Small Size MLCC to Aero-Space Application and its technology, Murata," presented at the ESA 1st International Symposium 'Space Passive Component Days', Noordwijk, The Netherlands, 2013. https://escies.org/webdocument/showArticle?id=984&groupid=6
[53] ASTM, "C1525-04," in *Standard Test Method for Determination of Thermal Shock Resistance for Advanced Ceramics by Water Quenching*, 2009,
[54] J. d. Toonder, C. Rademaker, and C. Hu, "Residual stresses in multilayer ceramic capacitors: measurement and computation," *Journal of Electronic Packaging,* vol. 125, pp. 506-511, 2003
[55] G. Yang, Z. Yue, T. Sun, W. Jiang, X. Li, and L. Liz, "Evaluation of Residual Stress in a Multilayer Ceramic Capacitor and its Effect on Dielectric Behaviors Under Applied dc Bias Field," *Journal of American Ceramic Society,* vol. 91, pp. 887-892, 2008
[56] M. Sampson, J. Brusse, and A. Teverovsky, "Humidity Steady State Low Voltage Testing of MLCCs (Based on NESC Technical Assessment Report)," in *CARTS USA*, Jacksonville, Fl, 2011.
[57] A. Raman, S. Sahasrabudhe, L. Dietz, and M. Hossain, "Phenomenological understanding of Sn migration in ceramic-chip capacitors," in *Electronic Components and Technology Conference (ECTC), 2011 IEEE 61st*, 2011, pp. 541-546.
[58] J. Maxwell.) Surface mount soldering techniques and thermal shock in multilayer ceramic capacitors. *AVX Technical information* issue, pp., Available: http://www.avx.com/docs/techinfo/soldmlc.pdf
[59] G. De With, "Structural integrity of ceramic multilayer capacitor materials and ceramic multilayer capacitors," *Journal of the European Ceramic Society,* vol. 12, pp. 323-336, 1993 <Go to ISI>://A1993MK16700001
[60] B. Rawal, M. Childs, A. Cooper, and B. McLaughlin, "Reliability of multilayer ceramic capacitors after thermal shock," *Proceedings of the 38th Electronics Components Conference,* pp. 371 - 375, 9-11 May 1988 1988
[61] Y. C. Chan, Y. Wang, Z. Gui, and L. Li, "Thermal effects on the dielectric and electrical properties of relaxor ferroelectric ceramic-based MLCs," in *Proceedings of 1995 Japan International, 18th IEEE/CPMT Electronic Manufacturing Technology Symposium, International* Omiya, 1995, pp. 328-333.
[62] C. Koripella, "Mechanical behavior of ceramic capacitors," *IEEE Transactions on Components, Hybrids, and Manufacturing Technology,* vol. 14, pp. 718 - 724, 1991
[63] J. D. Prymak and J. Bergenthal, "Capacitance Monitoring while Flex Testing," *IEEE transactions on components, packaging, and manufacturing technology, part A,* vol. 18, pp. 180-186, 1995
[64] J. A. Ahmar, E. Wiss, and S. Wiese, "Four-point-bending experiments on multilayer ceramic capacitors: Microstructural details on crack initiation and propagation," in *2018 19th International Conference on Thermal, Mechanical and Multi-Physics Simulation and Experiments in Microelectronics and Microsystems (EuroSimE)*, 2018, pp. 1-6.
[65] K. Franken, H. R. Maier, K. Prume, and R. Waser, "Finite-Element Analysis of Ceramic Multilayer Capacitors: Failure Probability Caused by Wave Soldering and Bending Loads," *Journal of the American Ceramic Society,* vol. 83, pp. 1433-1440, 2000 http://dx.doi.org/10.1111/j.1151-2916.2000.tb01407.x
[66] M. Keimasi, M. H. Azarian, and M. G. Pecht, "Flex Cracking of Multilayer Ceramic Capacitors Assembled With Pb-Free and Tin–Lead Solders," *IEEE transactions on device and material reliability,* vol. 8, pp. 182-192, 2008
[67] J. Prymak, M. Prevallet, P. Blais, and B. Long, "New Improvements in Flex Capabilities for MLC Chip Capacitors," in *The 26th symposium for passive components, CARTS'06*, Orlando, FL, 2006, pp. 63-76.
[68] J. Al Ahmar, E. Wiss, S. Wiese, and Ieee, "Fracture Probability of MLCC in Dependence of Solder Fillet Height," *2017 18th International Conference on Thermal, Mechanical and Multi-Physics Simulation and Experiments in Microelectronics and Microsystems (Eurosime),* 2017 <Go to ISI>://WOS:000403217700045
[69] T. Adams, "Preventing MLCC Failures," *Circuits assembly,* August 2009 http://www.circuitsassembly.com/cms/sea-award/8686-preventing-mlcc-failures
[70] Murata. (2007, Capacitance and Dissipation Factor Measurement of Chip Multilayer Ceramic Capacitors. *(TD No.C10E)*. Available: https://www.murata.com/~/media/webrenewal/support/faqs/products/capacitor/mlcc/char/0007/07_capmeasureen.ashx?la=en
[71] JohansenDielectrics. (2005, AC power computation for DC rated capacitors. Available: https://www.johansondielectrics.com/downloads/jdi-ac-power-2005-05.pdf
[72] A. Teverovsky, "The Effectiveness of Screening Techniques for Revealing Cracks in High Volumetric Efficiency MLCCs," in *46th International Symposium on Microelectronics, IMAPS*, Orlando, FL, 2013. https://nepp.nasa.gov/files/24723/2013_n241_Teverovsky_IMAPS_Paper.pdf
[73] A. Teverovsky, "Insulation Resistance and Leakage Currents in Low-Voltage Ceramic Capacitors With Cracks," *Components, Packaging and Manufacturing Technology, IEEE Transactions on,* vol. 4, pp. 1169-1176, 2014
[74] P. C. Dow, "An Analysis of Certain Errors in Electronic Differential Analyzers II-Capacitor Dielectric Absorption," *Electronic Computers, IRE Transactions on,* vol. EC-7, pp. 17-22, 1958

[75] A. Teverovsky, "Leakage Currents in Low-Voltage PME and BME Ceramic Capacitors," presented at the 7th International Conference on Electroceramics (ICE2015), Penn State Conference Center, State College PA, USA, 2015. https://nepp.nasa.gov/
[76] A. Teverovsky, "Breakdown voltages in ceramic capacitors with cracks," *IEEE Transactions on Dielectrics and Electrical Insulation,* vol. 19, pp. 1448-1455, 2012
[77] EPCOS. *Multi Layer Serial Ceramic Capacitor, 2005*. Available: http://www.epcos.fr/Produits/pdf/Presentation_MLSC.pdf
[78] A. Teverovsky, "The Significance of Breakdown Voltages for Quality Assurance of Low-Voltage BME Ceramic Capacitors," in *CARTS International*, Santa Clara, CA, 2014, pp. 129-144.
[79] A. Teverovsky, "Effect of Manual-Soldering-Induced Stresses on Ceramic Capacitors," NASA Electronic Parts and Packaging (NEPP) Program, Part I 2008, https://nepp.nasa.gov/files/16346/08_002_01%20GSFC%20Teverovsky.pdf
[80] A. Teverovsky, "Mechanical Testing of MLCCs," NASA/GSFC, Greenbelt, MD, NEPP report 2016, https://nepp.nasa.gov/files/27587/NEPP-TR-2016-Teverovsky-TGR-Paper-MLCCs-TN39992.pdf
[81] S. Meyer, H. Wohlrabe, K. J. Wolter, H. Rcuter, and M. Keil, "Investigations on the mechanical stability and integrity of chip components after picking and placing in the surface mount technology process chain," in *Electronics Packaging Technology Conference (EPTC 2013), 2013 IEEE 15th*, 2013, pp. 873-877.
[82] S. K. Dash, P. Kumar, M. P. James, S. Kamat, K.Venkatesh, V.Venkatesh*, et al.*, "Study of Cracks in Ceramic Chip Capacitors (CDR-05) of Two Different Makes," *International Journal of Emerging Technology and Advanced Engineering,* vol. 3, pp. 85-90, 2013
[83] M. Szutkowska, "Fracture toughness of advanced alumina ceramics and alumina matrix composites used for cutting tool edges," *Journal of Acheivements in Materials and Manufacturing Engineering,* vol. 54, 2012
[84] D. B. Marshall, R. F. Cook, N. P. Padture, M. L. Oyen, A. Pajares, J. E. Bradby*, et al.*, "The Compelling Case for Indentation as a Functional Exploratory and Characterization Tool," *Journal of the American Ceramic Society,* vol. 98, pp. 2671-2680, Sep 2015 <Go to ISI>://WOS:000362229400001
[85] J. J. Steppan, J. A. Roth, L. C. Hall, D. A. Jeannotte, and S. P. Carbone, "A review of corrosion failure mechanisms during accelerated tests - electrolytic metal migration," *Journal of the Electrochemical Society,* vol. 134, pp. 175-190, Jan 1987 <Go to ISI>://WOS:A1987F664400035
[86] M. J. Ditz and I. N. T. Asm, *Determination of the moisture threshold for silver migration*, 1994.
[87] M. Ciccotti, M. George, V. Ranieri, L. Wondraczek, and C. Marlière, "Dynamic condensation of water at crack tips in fused silica glass," *Journal of Non-Crystalline Solids,* vol. 354, pp. 564-568, 2008/01/15/ 2008 http://www.sciencedirect.com/science/article/pii/S002230930701109X
[88] J. Herzberger and A. Teverovsky, "Dendrite growth in PME and BME ceramic capacitors," in *CARTS International*, Houston, TX, 2013, pp. 3.3 1-25. https://nepp.nasa.gov/
[89] J. C. Lin and J. Y. Chan, "On the resistance of silver migration in Ag-Pd conductive thick films under humid environment and applied d.c. field," *Materials Chemistry and Physics,* vol. 43, pp. 256-265, 1996 http://www.sciencedirect.com/science/article/pii/0254058495016428
[90] N. J. Donnelly and C. A. Randall, "Refined Model of Electromigration of Ag/Pd Electrodes in Multilayer PZT Ceramics Under Extreme Humidity," *Journal of the American Ceramic Society,* vol. 92, pp. 405-410, Feb 2009 <Go to ISI>://000263358000017
[91] S. J. Krumbein, "METALLIC ELECTROMIGRATION PHENOMENA," *Ieee Transactions on Components Hybrids and Manufacturing Technology,* vol. 11, pp. 5-15, Mar 1988 <Go to ISI>://WOS:A1988M705300002
[92] U. Kumar Barik, S. Srinivasan, C. L. Nagendra, and A. Subrahmanyam, "Electrical and optical properties of reactive DC magnetron sputtered silver oxide thin films: role of oxygen," *Thin Solid Films,* vol. 429, pp. 129-134, 2003 http://www.sciencedirect.com/science/article/pii/S0040609003000646
[93] S. A. Yang and A. Christou, "Failure model for silver electrochemical migration," *Ieee Transactions on Device and Materials Reliability,* vol. 7, pp. 188-196, Mar 2007 <Go to ISI>://WOS:000248067500023
[94] P. S. Patil and L. D. Kadam, "Preparation and characterization of spray pyrolyzed nickel oxide (NiO) thin films," *Applied Surface Science,* vol. 199, pp. 211-221, 2002 http://www.sciencedirect.com/science/article/pii/S0169433202008395
[95] B. Jiang, Y. Bai, J. L. Cao, Y. J. Su, S. Q. Shi, W. Y. Chu*, et al.*, "Delayed crack propagation in barium titanate single crystals in humid air," *Journal of Applied Physics,* vol. 103, Jun 2008 <Go to ISI>://WOS:000256706200131
[96] H. Zhang, J. X. Li, W. Y. Chu, Y. J. Su, and L. J. Qiao, "Effect of humidity and hydrogen on the promotion of indentation crack growth in lead-free ferroelectric ceramics," *Materials Science and Engineering B-Advanced Functional Solid-State Materials,* vol. 167, pp. 147-152, Mar 2010 <Go to ISI>://WOS:000277532400004
[97] S. F. Wang, J. P. Dougherty, W. Huebner, and J. G. Pepin, "Silver-Palladium Thick-Film Conductors," *Journal of the American Ceramic Society,* vol. 77, pp. 3051-3072, 1994 http://dx.doi.org/10.1111/j.1151-2916.1994.tb04549.x
[98] G. DiGiacomo, *Reliability of Electronic Packages and Semiconductor Devices* McGrow Hill, 1996.
[99] M. M. Samantaray, A. Gurav, E. C. Dickey, and C. A. Randall, "Electrode Defects in Multilayer Capacitors Part I: Modeling the Effect of Electrode Roughness and Porosity on Electric Field Enhancement and Leakage Current," *Journal of the American Ceramic Society,* vol. 95, pp. 257-263, 2012 http://dx.doi.org/10.1111/j.1551-2916.2011.04769.x

[100] M. Nakano, A. Saito, and N. Wada, "E–J Characteristics in Multilayer Ceramic Capacitors with the Thin Dielectric Layers," *Key Engineering Materials* vol. 421-422, pp. 277-280, 2009

[101] A. Teverovsky, "Failure models for low-voltage BME ceramic capacitors with defects," in *2017 IEEE International Reliability Physics Symposium (IRPS)*, 2017, pp. 6C-5.1-6C-5.8.

[102] I. Stolichnov, A. Tagantsev, N. Setter, S. Okhonin, P. Fazan, J. S. Cross*, et al.*, "Constant-current study of dielectric breakdown of Pb(Zr,Ti)O-3 ferroelectric film capacitors," *Integrated Ferroelectrics,* vol. 32, pp. 737-746, 2001 <Go to ISI>://000167524400006

[103] B. Rawal and H. Chan, "Conduction and failure mechanisms in barium titanate based ceramics under highly accelerated conditions"," AVX Technical information,

[104] PSA-Walsin-Tech, 2017, MLCC APPLICATION GUIDE, http://www.passivecomponent.com/document/MLCC/MLCC_application_guide.pdf

[105] W. P. Chen, L. T. Li, J. Q. Qi, Y. Wang, and Z. L. Gui, "Influence of electroless nickel plating on multilayer ceramic capacitors and the implications for reliability in multilayer ceramic capacitors," *Journal of the American Ceramic Society,* vol. 81, pp. 2751-2752, Oct 1998 <Go to ISI>://WOS:000076450800039

[106] H. Zhang, Y. J. Su, L. J. Qiao, W. Y. Chu, D. Wang, and Y. X. Li, "The effect of hydrogen on the fracture properties of 0.8(Na1/2Bi1/2)TiO3-0.2(K1/2Bi1/2)TiO3 ferroelectric ceramics," *Journal of Electronic Materials,* vol. 37, pp. 368-372, Mar 2008 <Go to ISI>://WOS:000252483100017

[107] Y. Saito, T. Oguni, K. Uchida, J. Ikeda, K. Kawasaki, T. Nakamura*, et al.*, "Mechanisms of MLCCs Insulation Resistance Degradation Under Highly Accelerated Temperature and Humidity Stress," in *CARTS*, Santa Clara, CA, 2014, p. 4.7.

[108] D. Sohrabi Baba Heidary and C. A. Randall, "Analysis of the degradation of BaTiO3 resistivity due to hydrogen ion incorporation: Impedance spectroscopy and diffusion analysis," *Acta Materialia,* vol. 96, pp. 344-351, 2015/09/01/ 2015 http://www.sciencedirect.com/science/article/pii/S135964541500347X

[109] L. P. James F. Soeder, Robert Scheidegger. (2012). *Capacitor Failure Investigation Results for the NEXT Ion Thruster Power Processing Unit (PPU)*. Available: https://ntrs.nasa.gov/archive/nasa/casi.ntrs.nasa.gov/20150010352.pdf

[110] O. Boser, P. Kellawon, and R. Geyer, "Electromechanical resonances in ceramic capacitors and their use for rapid nondestructive testing," *Journal of the American Ceramic Society,* vol. 72, pp. 2282-2286, Dec 1989 <Go to ISI>://WOS:A1989CE83100011

[111] A. Teverovsky, "Guidelines for Selection, Screening and Qualification of Low-Voltage Commercial Multilayer Ceramic Capacitors for Space Programs," NASA/GSFC, Greenbelt, MD 2012, http://nepp.nasa.gov/

[112] J. I. C. Andersson, E. Varescon, and M. Kiviniemi.) Imaging Detects Cracks in Multilayer Ceramic Capacitors. *Power Electronics Europe* issue 5, pp. 24-27, 2017 Available: http://www.power-mag.com/pdf/feature_pdf/1506960397_ABB_Feature.pdf

[113] S. Hull, "Nondestructive detection of cracks in ceramics using vicinal illumination," in *25th International Symposium for Testing and Failure Analysis, ISTFA*, Santa Clara, CA, 1999, pp. 217-223.

[114] K. O. Sridhar Canumalla, Pedro Ramirez. *Acoustic Microscopy of Tightly Closed Delaminations in Multilayer Ceramic Chip Capacitors*. Available: https://www.researchgate.net/profile/Sridhar_Canumalla/publication/253547181_Acoustic_Microscopy_of_Tightly_Closed_Delaminations_in_Multilayer_Ceramic_Chip_Capacitors/links/55ca51b708aebc967dfbe183/Acoustic-Microscopy-of-Tightly-Closed-Delaminations-in-Multilayer-Ceramic-Chip-Capacitors.pdf

[115] M. Tarr. (2007). *Failure mechanisms in ceramic capacitors*. Available: http://www.ami.ac.uk/courses/topics/0179_fmcc/index.html

[116] R. Chittick, E. Gray, J. Alexander, M. Drake, and E. Bush, "Non-destructive screening for low-voltage failure in multilayer ceramic capacitors," in *The 3rd Capacitor and Resistor Technology Symposium, CARTS'83*, Phoenix, AZ, 1983, pp. 61-69.

[117] B. Wunderle, T. Braun, D. May, and A. Mazloum, "Non-destructive failure analysis and modeling of encapsulated miniature SMD ceramic chip capacitors under thermal and mechanical loading," in *13th International Workshop on Thermal Investigation of ICs and Systems, THERMINIC 2007.*, 2007, pp. 104 - 109.

[118] M. H. Azarian, "Detection of Cracked Multi-Layer Ceramic Capacitors on Printed Circuit Board Assemblies," presented at the IMAPS Chesapeake Chapter Summer Technical Symposium, JHU APL, Laurel, 2014.

[119] A. Teverovsky, "Absorption Voltages and Insulation Resistance in Ceramic Capacitors with Cracks," *IEEE Transactions on Dielectrics and Electrical Insulation,* vol. 21, pp. 2020-2027, 2014

[120] R. G. Leisure and F. A. Willis, "Resonant ultrasound spectroscopy," *Journal of Physics-Condensed Matter,* vol. 9, pp. 6001-6029, Jul 1997 <Go to ISI>://WOS:A1997XL95400002

[121] S. A. Kim, W. L. Johnson, G. S. White, R. Roberts, and A. S. M. International, *Ultrasonic Detection of Defects in Multi layered Ceramic Capacitors for Active Implantable Medical Devices*, 2013.

[122] W. L. Johnson, S. A. Kim, G. S. White, J. Herzberger, and Ieee, "Nonlinear resonant acoustic detection of cracks in multilayer ceramic capacitors," in *2014 Ieee International Ultrasonics Symposium*, New York, 2014, pp. 248-251. <Go to ISI>://WOS:000352792500063

[123] W. L. Johnson, S. A. Kim, G. S. White, J. Herzberger, K. L. Peterson, and P. R. Heyliger, "Time-domain Analysis of Resonant Acoustic Nonlinearity Arising from Cracks in Multilayer Ceramic Capacitors," in *42nd Annual Review of Progress in Quantitative Nondestructive Evaluation: Incorporating the 6th European-American Workshop on Reliability of Nde*, 2016. <Go to ISI>://WOS:000371907800065

[124] N. H. Chan and B. S. Rawal, "An electrically-excited acoustic emission test technique for screening multilayer ceramic capacitors," in *Electronics Components Conference, 1988., Proceedings of the 38th*, 1988, pp. 502-506.

[125] S. Levikari, T. J. Kärkkäinen, C. Andersson, J. Tamminen, and P. Silventoinen, "Acoustic Phenomena in Damaged Ceramic Capacitors," *IEEE Transactions on Industrial Electronics,* vol. 65, pp. 570-577, 2018

[126] D. S. Erdahl and I. C. Ume, "Online–Offline Laser Ultrasonic Quality Inspection Tool for Multilayer Ceramic Capacitors," *IEEE Transactions on advanced packaging,* vol. 27, pp. 647-653, 2004

[127] D. S. Erdahl and I. C. Ume, "Online-offline laser ultrasonic quality inspection tool for multilayer ceramic capacitors - Part II," *Ieee Transactions on Advanced Packaging,* vol. 28, pp. 264-272, May 2005 <Go to ISI>://WOS:000229003700014

[128] A. Teverovsky, "Evaluation of case size 0603 BME ceramic capacitors," in *Components for Military and Space Electronics, CMSE'15*, Los Angeles, CA, 2015, p. 6.2. https://nepp.nasa.gov/files/26562/2015-562-Teverovsky-Final-NEPPweb-Pres-CMSE-BME-TN22758.pdf

[129] IPC-7711C/7721C, 2017, Rework, Modification and Repair of Electronic Assemblies, https://products.ihserc.com/tmp_stamp/607629926/VWHIUFAAAAAAAAAA.pdf?sess=607629926&prod=SPECS4

[130] IPC-J-STD-001G, 2017, Requirements for Soldered Electrical and Electronic Assemblies,

[131] NASA-STD-8739.2, 2011, WORKMANSHIP STANDARD FOR SURFACE MOUNT TECHNOLOGY,

[132] ECSS-Q-ST-70-38C, 2008, Space product assurance. High-reliability soldering for surface-mount and mixed technology., http://esmat.esa.int/ecss-q-st-70-38c.pdf

[133] ECSS-Q-ST-70-38C, 2017, High-reliability soldering for surface-mount and mixed technology, https://escies.org/download/webDocumentFile?id=66008

[134] Johansen_Technology, "SOLDERING APPLICATION NOTE FOR CERAMIC CHIP COMPONENTS," 2011

[135] ATC-AT#001-119. (2007). *Recommended attachment techniques for ATC multilayer chip capacitors*. Available: www.atceramics.com

[136] A. Teverovsky, "Terminal Solder Dip Testing for Chip Ceramic and Tantalum Capacitors," in *International Conference on Soldering & Reliability (ICSR)* Ontario, Canada, 2012, pp. 163-173.

[137] NEPAG, 2016, NASA Parts Selection List, NASA Parts Levels, https://nepp.nasa.gov/npsl/npsl_UsePolicy.htm